Mareike Seelinger

DNA damage tolerance in human cells mediated by the APIM-containing proteins REV3L, HLTF, and SHPRH

Doctoral Thesis

Mareike Seelinger

NTNU
Norwegian University of
Science and Technology
Faculty of Medicine and Health Sciences
Department of Clinical and Molecular Medicine

◉ **NTNU**
Norwegian University of
Science and Technology

◉ NTNU

◉ **NTNU**
Norwegian University of
Science and Technology

Mareike Seelinger

DNA damage tolerance in human cells mediated by the APIM-containing proteins REV3L, HLTF, and SHPRH

Thesis for the degree of Philosophiae Doctor

Trondheim, 27.3.2020

Norwegian University of Science and Technology
Faculty of Medicine and Health Sciences
Department of Clinical and Molecular Medicine

NTNU
Norwegian University of
Science and Technology

Studier av DNA skade toleranse i humane celler med fokus på de tre APIM inneholdende proteinene REV3L, HLTF og SHPRH

Vårt arvemateriale, DNA, finnes i alle celler og blir kontinuerlig skadet av prosesser i cellen og forskjellige stoffer vi blir utsatt for. DNA må derfor kontinuerlig repareres. Dersom skadene ikke blir reparert før cellene skal kopiere sitt DNA, vil disse skadene blokkere DNA kopieringen og dette kan føre til brudd i vårt DNA, mutasjoner og/eller celledød. Cellene våre har derfor utviklet et system for å håndtere DNA skader (DNA skade toleranse, DDT) under DNA kopieringen for å forhindre dette. DDT mekanismene kalles «Translesion Synthesis» (TLS) og «Template Switch», og blir mellom annet regulert av modifisering, en ubiquitinering, av det essensielle human proteinet Proliferating Cell Nuclear Antigen (PCNA). PCNA binder polymeraser og andre proteiner som er involvert i de forskjellige DDT mekanismene.

REV3L, HLTF og SHPRH er tre proteiner med forskjellige oppgaver i DDT som alle har en PCNA bindings sekvens, APIM, som ble oppdaget ved NTNU i 2009. REV3L er en sub-enhet av TLS polymerasen ζ (POLζ), og i artikkel 1 viser vi at POLζ binder til PCNA gjennom APIM og at dette er viktig for POLζ sin funksjon i DDT. APIM-peptider blokkerer APIM-proteiners mulighet til å binde PCNA, og vi viser i artikkel 1 at behandling av celler med APIM-peptider reduserer cellenes evne til å mutere.

I artikkel 2 viser vi at APIM i HLTF og SHPRH er funksjonelt PCNA bindende sekvenser, og at APIM i HLTF er viktig for at dette proteinet skal motvirke mutasjoner ved DDT. Videre fant vi at binding mellom SHPRH og PCNA via APIM er viktig for SHPRH stabilitet og cellulær lokalisering

I artikkel 3 undersøkte vi nærme funksjonen av HLTF og SHPRH i celler som ble behandlet med ulike typer DNA skadende cellegifter. Vi fant at HLTF og SHPRH både virker sammen og har egne spesifikke egenskaper i valg av ulike DDT mekanismer. Videre fant vi en ny rolle for SHPRH for regulering av den kjente sjekkpunkt kinasen CHK2.

Samlet viser resultatene i avhandlingen at REV3L, HLTF og SHPRH har viktige funksjoner i håndtering av ulike DNA skader og at APIM – PCNA interaksjonene for disse proteinene er viktig for deres funksjon.

Table of contents

Acknowledgements

The work presented in this thesis was carried out at the Department of Clinical and Molecular Medicine, Faculty of Medicine and Health Sciences, Norwegian University of Science and Technology (NTNU). I am thankful for the support from NTNU and the Joint Research Committee between St. Olavs and the Faculty of Medicine and Health Science (NTNU).

My deep gratitude goes to my supervisor Professor Marit Otterlei who gave me the opportunity to take a PhD and guided me through this period. Thank you for your positive attitude, enthusiasm and great scientific input that kept me engaged with my research in a positive way. Thank you also for giving me the time that I needed to come back to work after parental leaves. My appreciation extends to my co-supervisor Per Arne Aas for kindly answering every question that came up in the lab and thank you also for feedback on articles and this thesis.

I also want to thank all my colleagues. Special thanks to Siri, Synnøve, Caroline, Anala, Camilla and Karine for all the non-work-related talks and a great atmosphere in the office. Thanks for cheering me up when I again had "one last experiment" to do.

Thanks to my family, all friends and neighbors for great times off work and for sometimes asking and sometimes not asking how it is going with the PhD ;) Importantly, I want to thank everyone who helped us during the busy periods of the last months, especially Stefan, Silke, Rüdiger and Gudrun.

Special thanks to Daniel, for all the jokes, even in stressful times (I appreciate those, even if it is sometimes hard to show ;), and for always supporting me. And finally, big hugs to our three girls, the PhD period was probably not easier, but much more fun with you!

Trondheim, March 2020

Mareike Seelinger

List of papers

Paper 1:

APIM-mediated REV3L-PCNA interaction important for error free TLS over UV-induced DNA lesions in human cells

Synnøve Brandt Ræder, Anala Nepal*, Karine Øian Bjørås*, <u>Mareike Seelinger</u>*, Rønnaug Steen Kolve, Aina Nedal, Rebekka Müller and Marit Otterlei

*Equal contribution

International Journal of Molecular Sciences 2018, doi:10.3390/ijms20010100

Paper 2:

Roles of HLTF and SHPRH in DNA damage tolerance depend on direct interactions with PCNA

<u>Mareike Seelinger</u> and Marit Otterlei

Manuscript submitted

Paper 3:

The human RAD5 homologs, HLTF and SHPRH, have distinct functions in DNA damage tolerance dependent on the DNA lesion type

<u>Mareike Seelinger</u>, Caroline Krogh Søgaard and Marit Otterlei

Manuscript

Abbreviations

6-4PP	(6-4)photoproduct
APC/C	Anaphase-promoting complex/cyclosome
APE1	AP-endonuclease 1
ATM	Serine-protein kinase Ataxia Telangiectasia mutated
ATR	Ataxia Telangiectasia and Rad3-related protein
ATRIP	ATR interacting protein
BIR	Break-induced replication
BRCA2	Breast cancer type 2 susceptibility protein
CDC25A	M-phase inducer phosphatase 1
CDC45	Cell division cycle 45
CDK	Cyclin-dependent kinase
CHK	Checkpoint kinase
CMG	CDC45-MCM-GINS
CPD	Pyrimidine dimers
DDR	DNA damage response
DDT	DNA damage tolerance
DKK	DBF4-dependent kinase
D-loop	Displacement loop
DNA2	DNA replication helicase/nuclease 2
DSB	DNA double strand break
dsDNA	Double-stranded DNA
EFP	Interferon-inducible ubiquitin-protein isopeptide E3
EME1	Crossover junction endonuclease
FA	Fanconi Anemia
FAN1	Fanconi-associated nuclease 1
FANC	FA complementation group
FBH1	F-box DNA helicase 1

GINS	Go ichi ni san complex
hABH	Human AlkB homologues
HIRAN	HIP116 Rad5p N-terminal
HIV-1	Human immunodeficiency virus 1
HLTF	Helicase-like transcription factor
HR	Homologous recombination
HU	Hydroxyurea
ICL	Interstrand crosslink
IGF-1R	Insulin-like growth factor-1 receptor
ISG-15	Interferon-stimulated gene 15
MCM2-7	Minichromosome maintenance DNA helicase complex
MGMT	O^6-methylguanine-DNA methyltransferase
MHF	FANCM-associated histone fold protein 1
MMC	Mitomycin c
MMR	Mismatch repair
MMS	Methyl methanesulfonate
MPG	Methyl purine DNA glycosylase
MRE11	Meiotic recombination 11 homolog 1
MUS81	Structure-specific endonuclease subunit
N1-meA	N1-methyladenine
N3-meA	N3-methyladenine
N3-meC	N3-methylcytosine
N3-meG	N3-methylguanine
N7-meA	N7-methyladenine
N7-meG	N7-methylguanine
NBS1	Nijmegen Breakage Syndrome protein 1
NER	Nucleotide excision repair
NHEJ	Non-Homologous End Joining
O6-meG	O6-methylguanine

P21	Cyclin-dependent kinase inhibitor 1
P53	Cellular tumor antigen p53
PARI	PCNA-associated recombination inhibitor
PARP1	Poly(ADP-ribose) polymerase 1
PCD	Predicted unstructured region
PCNA	Proliferating cell nuclear antigen
PIP-box	PCNA interacting peptide-box
POL	Polymerase
pre-RC	Pre-recognition complex
PrimPOL	Primase-polymerase
PTM	Posttranslational modification
RAD18	E3 ubiquitin-protein ligase
RAD6	Ubiquitin-conjugating enzyme E2
REV3L	POLζ catalytic subunit
REV7	POLζ accessory subunit
RFC	Replication factor c
RIF-1	Replication timing regulatory factor 1
RIR	REV1-interacting region
RNF8	Ring finger protein 8
RPA	Replication protein A
rRNA	Ribosomal RNA
SHPRH	SNF2 histone-linker PHD and RING finger domain-containing helicase
SLX1	Structure-specific endonuclease subunit
ssDNA	Single-stranded DNA
SUMO	Small ubiquitin-like modifier
TF	Transcription factor
TLS	Translesion synthesis
TS	Template switch
UNG	Uracil-DNA glycosylase

USP	Ubiquitin specific peptidase
USP7	Ubiquitin carboxyl-terminal hydrolase 7
UV	Ultraviolet
WRN	Werner syndrome ATP-dependent helicase
XP	Xeroderma Pigmentosum
XPF	Xeroderma pigmentosum group F-complementing protein
XPV	Xeroderma Pigmentosum Variant

Amino acid abbreviations

A	Alanine		M	Methionine
D	Aspartate		Q	Glutamine
E	Glutamate		R	Arginine
F	Phenylalanine		S	Serine
G	Glycine		T	Threonine
H	Histidine		V	Valine
I	Isoleucine		W	Tryptophan
K	Lysine		Y	Tyrosine
L	Leucine			

Base abbreviations

A	Adenine
C	Cytosine
G	Guanine
T	Thymine

1   Introduction

DNA is continuously exposed to a variety of exogenous and endogenous DNA damaging agents. Depending on the DNA lesion, cells have evolved different DNA damage response (DDR) pathways. Still, some DNA lesions are not repaired prior to replication and cause replication stress. DNA lesions on the template strand during replication cannot be accommodated by the high-fidelity replicative DNA polymerases POLδ and POLε and accordingly stall upstream of the impediment. Prolonged replication fork arrest can cause replication fork collapse and DNA double strand breaks (DSBs) and hence threatens chromosome stability. To maintain the genome, it is necessary to minimize errors passed to daughter cells. This is illustrated by failure or delay of correct DNA replication which is associated with developmental disorders, premature aging, neurological disorders, and cancer (Cooper, Tait et al. 2014). Special mechanisms, the DNA damage tolerance (DDT) pathways have developed to handle DNA damage in actively replicating cells.

DDT, sometimes referred to as post-replication repair, is conserved from bacteria and is in humans commonly divided into translesion synthesis (TLS), which enables DNA lesion bypass by error-prone TLS polymerases, and two error-free DDT pathways: template switch in presence of fork reversal (TS by fork reversal) and template switch by homologous recombination (TS by HR). The TS pathways use the newly synthesized sister chromatid as a template (Pilzecker, Buoninfante et al. 2019). The choice of the DDT pathway is at least partly regulated by posttranslational modifications (PTMs) on proliferating cell nuclear antigen (PCNA) (reviewed in (Slade 2018)). Although the knowledge of DDT has increased dramatically during the last decades, DDT is still not fully understood. This work focuses on the role of three DDT proteins, namely the POLζ catalytic subunit REV3L, the SNF2 histone-linker PHD and RING finger domain-containing helicase (SHPRH) and the helicase-like transcription factor (HLTF), all containing an AlkB homologue 2 PCNA-interacting motif (APIM) as PCNA interacting motif. This introduction aims to describe the DDT pathways, DDT activation and DDT regulation with focus on these three proteins and the role of PCNA.

1.1   PCNA

One main regulative protein in DDT is PCNA, a homotrimer with head-to-tail aligned subunits. PCNA is described as the "heart of the replication fork" or the "maestro of the replication". Besides its role in DNA synthesis, PCNA is involved in the coordination of DDR, cell cycle control, gene transcription, epigenomic maintenance and sister-chromatid cohesion (Mailand, Gibbs-Seymour et al. 2013). In addition to these canonical roles, PCNA is involved in the regulation of apoptosis (Yin, Xie et al. 2015), immune responses (Rosental, Brusilovsky et al. 2011), and cellular signaling (Olaisen, Muller et al. 2015, Olaisen, Kvitvang et al. 2018, Sogaard, Nepal et al. 2019). Thus, PCNA is a "hub"-protein and most cellular processes in response to stress imply PCNA. PCNA is the binding platform for several TLS polymerases, involved in the polymerase switch form replicative to TLS polymerases in presence of replication stress. The regulation of DDT was first thought to be mainly regulated by PTMs on PCNA, i.e. PCNA monoubiquitination inducing TLS and polyubiquitination inducing TS (Ghosal and Chen 2013). However, TLS also occurs in absence of PCNA ubiquitination (Hendel, Krijger et al. 2011). It is not completely resolved how important PCNA polyubiquitination is for the occurrence of the error-free pathways, but at least some fork remodeling enzymes are dependent on PCNA polyubiquitination.

So far two PCNA binding-motifs have been discovered, PCNA interacting peptide-box (PIP-box) (Warbrick 1998) and APIM (Gilljam, Feyzi et al. 2009), sharing the same binding site on PCNA (Muller, Misund et al. 2013, Sebesta, Cooper et al. 2017). Whether PIP-box-containing proteins or APIM-containing proteins interact with PCNA, is at least partly regulated by PTMs on PCNA (Gilljam, Feyzi et al. 2009, Ciccia, Nimonkar et al. 2012, Choe and Moldovan 2017). In presence of cellular stress an APIM-containing peptide was shown to inhibit interactions of APIM-containing proteins with PCNA. This impairs cellular stress responses, including TLS, because many proteins involved in cellular stress contain APIM (Muller, Misund et al. 2013, Gederaas, Sogaard et al. 2014, Raeder, Nepal et al. 2018, Sogaard, Blindheim et al. 2018, Sogaard, Moestue et al. 2018, Sogaard, Nepal et al. 2019). The APIM consensus (K/R)-(F/Y/W)-(L/I/V/A)-(L/I/V/A)-(K/R) (Gilljam, Feyzi et al. 2009) is present in ~300 proteins (Olaisen, Kvitvang et al. 2018), including REV3L, HLTF and SHPRH. In Paper 1 and 2 in this thesis we suggest that APIM in REV3L, HLTF and SHPRH are functional PCNA-interacting motifs.

1.2 Human REV3L

Human REV3L is a 3130 amino acids (aa) large protein, containing APIM in the predicted unstructured region (PCD) (aa 1240–1244), which is not present in yeast Rev3 (Gilljam, Feyzi et al. 2009). REV3L is the catalytic subunit of B-family TLS polymerase POLζ. The POLζ complex consists of three additional subunits: the accessory subunit REV7, P50 and P66 (Baranovskiy, Lada et al. 2012, Makarova and Burgers 2015). P50 and P66 are also subunits of the replicative polymerase POLδ (Baranovskiy, Lada et al. 2012). REV7 is a HORMA (Hop1, Rev7, Mad2) protein, forming a homodimer. Both homodimer subunits can simultaneously bind to REV3L (Korzhnev, Neculai et al. 2016). In yeast, Rev7 stimulates the catalytic activity of Rev3 by 20-30 fold (Nelson, Lawrence et al. 1996). The assembling of all four subunits is important to obtain the highest catalytic activity of human POLζ (Makarova, Stodola et al. 2012). Alterations in REV3L expression levels are associated with chromosome instability and carcinogenesis (Wittschieben, Reshmi et al. 2006, Lange, Takata et al. 2011), and REV3L deletion is incompatible with embryonic mouse viability (Esposito, Godindagger et al. 2000, Wittschieben, Shivji et al. 2000, Van Sloun, Varlet et al. 2002). This illustrates the importance of REV3L for genetic stability. In yeast, Polζ is responsible for nearly all spontaneous mutagenesis (reviewed in (Northam, Robinson et al. 2010)), while human POLζ is vital for cell proliferation and genomic stability, also in absence of induced DNA damage (Lange, Wittschieben et al. 2012). In addition to TLS, REV3L is involved in somatic hypermutation (SHM), normal replication, in HR-dependent DSB and interstrand crosslink (ICL) repair (Zan, Komori et al. 2001, Sharma and Canman 2012, Sharma, Hicks et al. 2012), as well as in replication of "fragile-site" regions. In the latter, REV3L acts independently of REV7 (Bhat, Andersen et al. 2013). *De novo* mutations in REV3L are associated with a neurological disorder called Möbius Syndrome (Tomas-Roca, Tsaalbi-Shtylik et al. 2015), and a tumor suppressor role of POLζ is suggested in lung cancers (Brondello, Pillaire et al. 2008, Zhang, Chen et al. 2013).

In DDT, POLζ is involved in TLS at the stalled fork and in TLS in postreplicative single-stranded DNA (ssDNA) gaps (Prakash, Johnson et al. 2005, Jansen, Tsaalbi-Shtylik et al. 2009, Quinet, Carvajal-Maldonado et al. 2017) (Figure 1). The TLS polymerase activity of POLζ is discussed in 1.6.2.
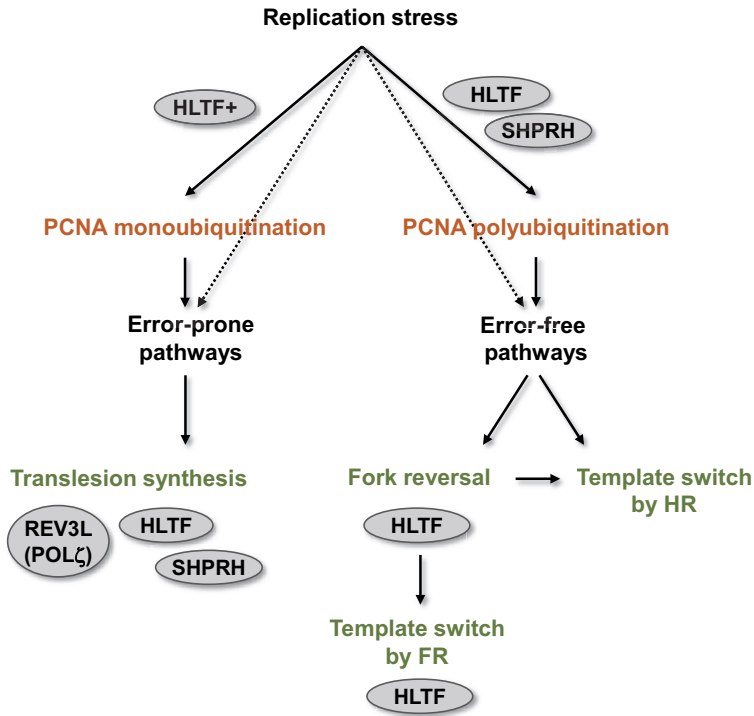
Figure 1. Overview over REV3L, HLTF and SHPRH involvement in DDT pathways and DDT regulation.
Regulation of DDT by PTMs on PCNA is depicted in orange, DDT pathways are depicted in green. Involvement of REV3L, HLTF and SHPRH is illustrated in gray circles.

1.3   The RAD5 homologs HLTF and SHPRH

Yeast Rad5 is a multi-domain protein (Unk, Hajdu et al. 2010) containing an E3 RING-finger ligase domain, SNF2 helicase domain and a HIP116 Rad5p N-terminal (HIRAN) domain. Human cells have two RAD5 homologs, namely HLTF and SHPRH. HLTF is the homolog with the largest sequence and domain homology with yeast Rad5 (Motegi, Liaw et al. 2008) and was initially identified for its DNA binding and transcriptional activity (Ding, Descheemaeker et al. 1996). Both human RAD5 homologs contain an APIM sequence located at their C-terminus within the helicase domain of the proteins, KFIVK (amino acid (aa) 959-963) in HLTF and RFLIK (aa 1631-1635) in SHPRH (Gilljam, Feyzi et al. 2009) as illustrated in Figure 2.
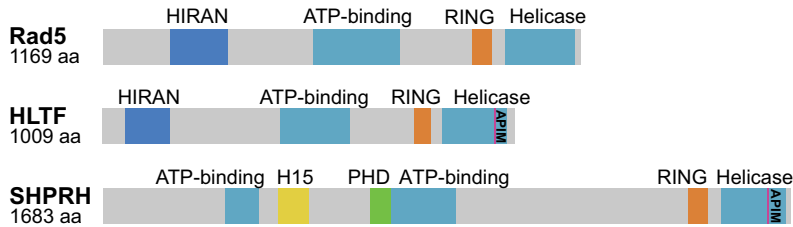
4

Figure 2. Protein domain structure of yeast Rad5, human HLTF and human SHPRH. Adapted from (Chang and Cimprich 2009).

Both HLTF and SHPRH contain a RING domain. The RING domain in HLTF is involved in polyubiquitination of PCNA (Motegi, Liaw et al. 2008, Unk, Hajdu et al. 2008). However, both proteins are important for maintaining genomic stability by stimulating error-free DDT via PCNA polyubiquitination (Motegi, Sood et al. 2006, Unk, Hajdu et al. 2006, Motegi, Liaw et al. 2008, Unk, Hajdu et al. 2008, Chang and Cimprich 2009, Unk, Hajdu et al. 2010) and for the selection of the DDT pathway (Lin, Zeman et al. 2011). HLTF is involved in fork reversal via its HIRAN domain (Achar, Balogh et al. 2015, Chavez, Greer et al. 2018), suggested to facilitate displacement loop (D-loop) formation in TS by fork reversal (Burkovics, Sebesta et al. 2014) and to stimulate PCNA monoubiquitination and TLS (Lin, Zeman et al. 2011) as illustrated in Figure 1. SHPRH is less studied than HLTF. Unlike Rad5 and HLTF, SHPRH contains histone H1 and H5 linker sequences and a PHD domain. PHD domains are commonly found in chromatin remodeling proteins and bind preferentially methylated H3K4; however, this has not been shown for the PHD domain in SHPRH yet (Machado, Pustovalova et al. 2013). Besides its role in DDT, SHPRH promotes ribosomal RNA (rRNA) transcription (Lee, An et al. 2017). Recently, a truncated form of SHPRH with the size of 146 amino acids, encoded by a circularRNA of SHPRH, was suggested as a tumor suppressor protein in human glioblastoma by protecting full-length SHPRH from degradation (Zhang, Huang et al. 2018). This truncated form of SHPRH also contains APIM.

SHPRH and especially HLTF are suggested to be tumor suppressor proteins because loss of function or dysregulation were observed in cancers (Kim, Chung et al. 2006, Capouillez, Noel et al. 2011, Zhang, Huang et al. 2018, Bryant, Sunjevaric et al. 2019). HLTF is often epigenetically silenced by promotor hypermethylation in colon cancers (~ 40 %) (Moinova, Chen et al. 2002), and HLTF or SHPRH depletion increases the chance of chromosome abnormalities in presence of cellular stress (Motegi, Sood et al. 2006, Motegi, Liaw et al. 2008).

Recently, a germline loss-of-function mutation in HLTF was associated with myelodysplastic syndromes, a disorder of hematopoietic stem cells. Loss of HLTF resulted in a higher amount of DNA damage and this was suggested to be caused by decreased PCNA polyubiquitination (Takaoka, Kawazu et al. 2019). HLTF degradation is associated with human immunodeficiency virus 1 (HIV-1) infection and this is assumed as a strategy for the virus to antagonize DDT in these cells (Lahouassa, Blondot et al. 2016).

1.4   Replication stress

Several factors can induce replication stress, including reduction of nucleotide pools, ribonucleotides in the template, physical obstacles to replicative polymerases like DNA lesions, DNA-protein complexes, DNA-RNA hybrids or difficult to replicate regions (reviewed in (Zeman and Cimprich 2014)). DNA lesions can, for example, be caused endogenously by reactive oxygen species, spontaneous deamination and lipid peroxidation (De Bont and van Larebeke 2004) or exogenously by ultraviolet (UV) radiation or by genotoxic chemical compounds such as the alkylating and crosslinking agents methyl methanesulfonate (MMS), cisplatin or mitomycin c (MMC). Impediments provoking replicative polymerase stalling cause replication stress. The activation of DDT is then required to avoid replication fork collapse and genomic instability. The risk of cancer strongly correlates with the proliferation rate of a certain tissue, because most of the mutations in unperturbed cells occur during replication (Tomasetti and Vogelstein 2015).

1.4.1   UV, MMS, MMC and cisplatin generated DNA lesions

In this thesis UV, MMS, cisplatin and MMC were used to generate different types of DNA lesions resulting in replication stress, if not repaired prior to replication. The following chapter discusses the spectra of DNA lesions caused by these agents and specific DDR pathways to handle these lesions outside S-phase.

UV radiation mainly forms cyclobutene pyrimidine dimers (CPDs) (~80 %) and (6-4)photoproducts (6-4PPs) (Pfeifer 1997, Yoon, Lee et al. 2000). The latter is rapidly repaired by nucleotide excision repair (NER). CPDs are less efficiently repaired by NER, because they cause a minor distortion of the DNA helix than 6-4PPs (Kemp and Sancar 2012, Hu, Adar et al. 2015). Therefore, CPDs are more frequently an obstacle during replication. POLη, a TLS polymerase, is important in bypassing CPDs during replication, because it can e.g. bypass thymine-thymine (TT)-CPD dimers correctly by inserting adenine-adenine (AA) (Cordonnier, Lehmann et al. 1999). The importance of POLη is further illustrated by the Xeroderma Pigmentosum Variant (XPV) syndrome, which is caused by POLη deficiency and associated with hypersensitivity to sunlight and a ~1000 times increase in skin cancer (Kraemer, Lee et al. 1987, Kraemer, Lee et al. 1994, Inui, Oh et al. 2008).

MMS produces N7-methylguanine (N7-MeG) adducts (~83 %), N3-methyladenine (N3-MeA) (10.4 %), N1-methyladenine (N1-MeA) (3.8 %), and N7-methyladenine (N7-MeA) (1.8 %), and less than 1 % of N3-methylguanine (N3-MeG), O6-methylguanine (O6-MeG), N3-methylcytosine (N3-MeC) in double-stranded DNA (dsDNA), and cytosine-diester (reviewed in (Drablos, Feyzi et al. 2004). In ssDNA the amount of N3-MeC is estimated to be around 10 %. N7-MeG, N3-MeA and N3-MeG are repaired by the methyl purine DNA glycosylase (MPG, also called AAG) during base excision repair (BER) (reviewed in (Krokan and Bjoras 2013)). N3-MeA is unstable and quickly converted into abasic sites (Plosky, Frank et al. 2008). N3-MeA was initially thought to be a "replication blocking lesion", but later Y-family TLS polymerases have been shown to be able to bypass this lesion during replication (Johnson, Yu et al. 2007, Plosky, Frank et al. 2008). N1-MeA and N3-MeC are repaired by human AlkB homologue 2 (hABH2) and hABH3 by direct repair via oxidative demethylation, with a preference for dsDNA and ssDNA, respectively (Aas, Otterlei et al. 2003, Falnes, Bjoras et al. 2004). For N7-MeA no repair mechanism has been described so far. There is some evidence that alkylated bases can serve as substrate for NER, but this is less well established (Huang, Hsu et al. 1994, Guo, Hanawalt et al. 2013). O6-MeG is repaired by direct repair catalyzed by the O^6-methylguanine-DNA methyltransferase (MGMT) (Tubbs, Pegg et al. 2007).

MMC is a mono- and bifunctional alkylating agent widely used in cancer treatment. MMC induces mainly monoadducts, preferentially at Guanines (G), and a low amount (~ 4 %) of intrastrand crosslinks at GpG-sites (leading to DNA bending). Both lesions are usually repaired by NER. Furthermore, MMC induces interstrand crosslinks (ICLs) at CpG-sites which are

repaired by ICL repair. This is a complex repair mechanism requiring cooperation of multiple DNA repair pathways like NER, TLS, Fanconi Anemia (FA) and HR (Bizanek, McGuinness et al. 1992, Tomasz 1995, Williams, Gottesman et al. 2013, Marteijn, Lans et al. 2014). The fraction of ICLs (~14 %) is the main contributor to physiological challenges after MMC treatment (Warren, Maccubbin et al. 1998, Scharer 2005).

Another widely used drug in chemotherapy, cisplatin, is activated by a process called aquation and readily forms covalent bonds with purines in the DNA, resulting in the formation of 1-2-intrastrand crosslinks at GpG and ApG (> 95 %) (Kartalou and Essigmann 2001). Cisplatin also generates a small amount of ICLs (2-5 %). Cisplatin ICLs cause a larger distortion of the DNA than ICLs formed by MMC (reviewed in (Hashimoto, Anai et al. 2016)). During replication ICLs are repaired by ICL repair with the involvement of TLS polymerases. POLζ for instance is involved in bypass of both MMC and cisplatin ICLs (Hicks, Chute et al. 2010). DNA lesions and repair pathways are summarized in Table 1.

Table 1. DNA lesions spectrum and corresponding DDR pathways induced by certain DNA damaging agents.

Agent	DNA lesion	Repair mechanism
UV	CPDs	NER
	6-4PP	NER
MMS	N7-MeG	BER (MPG glycosylase)
	N3-MeA	BER (MPG glycosylase)
	N1-MeA	Direct repair (hABH2)
	N7-MeA	unknown
	N3-MeG	BER (MPG glycosylase)
	O6-MeG	MGMT
	N3-MeC	Direct repair (hABH2 or hABH3)
MMC	Monoadducts at Guanines	NER
	Intrastrand crosslinks	NER
	ICLs	Cooperation of NER, TLS, FA and HR
Cisplatin	Intrastrand crosslinks	NER
	ICLs	Cooperation of NER, TLS, FA and HR

DNA damage response pathways in absence of replication

NER and BER repair lesions outside of actively replicating regions. NER is a highly conserved pathway evolved to remove bulky lesions that cause distortions to the DNA double helix (e.g. adducts, photolesions or intrastrand crosslinks). NER can be performed during transcription and is then called transcription coupled NER. In this process DNA damage on the transcribed strand is detected due to stalling of the RNA polymerase. Lesions throughout the genome can be repaired by global genome NER, which acts independent of transcription. NER is a multistep repair pathway involving the action of several so-called XP-proteins. These perform a dual incision step and mediate removal of a 22-30 nucleotide fragment followed by gap filling and ligation. Defect in one of the XP-proteins causes Xeroderma Pigmentosum (XP), a syndrome characterized by hypersensitivity to sunlight, illustrating the importance of this pathway for repairing UV-induced DNA lesions (reviewed in (Marteijn, Lans et al. 2014)). BER is the main repair pathway for small base lesions, such as DNA lesions arising from oxidation, deamination or alkylation. These are endogenous lesions frequently occurring in each cell every day. The specificity step in BER is the excision of the DNA base by one of the 11 known DNA glycosylases. This results in an apurinic/apyrimidinic site (AP-site) which is cleaved and a single nucleotide is inserted before ligation (reviewed in (Krokan and Bjoras 2013)).

ICLs are a challenge for the cell´s DNA repair and tolerance systems. ICLs are highly cytotoxic, because they block unwinding of the DNA strands by the CMG[1] helicase and cause replicative polymerase stalling. In addition, ICLs block DNA transcription. The bypass or repair of ICLs require an interplay between several repair pathways. These include unhooking of the crosslink followed by an interplay between NER and TLS to remove the adduct from the DNA and to complete DNA replication. ICL repair differs in G1- and S-phase; however, the detailed mechanism is not fully understood yet. During G0- and G1-phase of the cell cycle, ICL repair seems to be independent of HR. Recognition, the first incision step, and unhooking of the ICL, are three steps that are facilitated by NER proteins, generating an intrastrand dinucleotide adduct. After the first incision, the ssDNA gap is filled by NER/TLS, i.e. the unhooked ICL is bypassed by a polymerase. Especially POLκ, POLζ and REV1 are suggested as important polymerases after the first incision step. The unhooked ICL is then removed through a second

---

[1] cell division cycle 45 (CDC45) - minichromosome maintenance DNA helicase complex (MCM) - go ichi ni san complex (GINS)

incision by NER proteins and the gap is filled by POLδ like in normal NER (reviewed in (Hashimoto, Anai et al. 2016)). Furthermore, POLη and POLι might have a role in lesion bypass during ICL repair, and the amount of duplex surrounding the ICL (position of unhooking the ICL) seems to affect the bypass and efficiency of TLS polymerases (reviewed in (Roy and Scharer 2016)). Interestingly, even in absence of DNA replication, ICL repair requires PCNA monoubiquitination, probably for the recruitment of TLS polymerases (Williams, Gottesman et al. 2012).

ICLs can also be processed by BER in concert with mismatch repair (MMR) proteins. In case of a cisplatin ICL, the cytosine is believed to be flipped away from the helix, becoming a substrate for deamination, converting cytosine to uracil. Uracil-DNA glycosylase (UNG) can excise the base, leaving an AP-site in the DNA, which is incised by AP-endonuclease 1 (APE1) and the gap is filled by POLβ. DNA synthesis by POLβ in ICL repair often leads to mismatches (reviewed in (Kothandapani and Patrick 2013)). These mismatches, especially after processing cisplatin ICLs, are recognized by MMR. MMR consists of recognition proteins MSH2-MSH6, MSHK2-MSH3, which recruit downstream proteins, including MLH1-PMS2, exonuclease 1 (EXO1), POLδ and DNA ligase. The absence of MMR proteins is suggested as a trigger for cisplatin resistance (Jiricny 2006, Sawant, Kothandapani et al. 2015). There is evidence that MSH2-MSH6 can directly sense distorting ICLs outside replication and process them by recruiting downstream MMR proteins (Kato, Kawasoe et al. 2017). The repair of less distorting ICLs seems to be dependent on replication (Raschle, Knipscheer et al. 2008, Kato, Kawasoe et al. 2017). ICL repair in replicating cells is described in 1.7.

1.4.2 Stalled replication forks

Replicative polymerases (POLε and POLδ) cannot accommodate bulky lesions. Most lesions, except ICLs, allow progression of the CMG helicase, but induce an uncoupling of the CMG-helicase (DNA unwinding) from the replicative polymerase (DNA synthesis) on the leading strand. This results in extended ssDNA stretches and can activate the intra-S checkpoint (Byun, Pacek et al. 2005). Lagging strand lesions only become an obstacle for replication fork progression if the damage impairs unwinding by the helicase, but usually DNA replication continues as scheduled with the next Okazaki fragment (reviewed in (Marians 2018)). The

resulting ssDNA is quickly coated with replication protein A (RPA), protecting the ssDNA stretches (Zellweger, Dalcher et al. 2015). However, cellular RPA pools are limited, and exhaustion of the RPA pool may result in unprotected replication forks that are unable to complete DNA replication (Toledo, Altmeyer et al. 2013). Long RPA-coated ssDNA stretches upstream of stalled polymerases are a signal for intra-S checkpoint activation, but they also directly recruit proteins that prevent exhaustion of the RPA pool and replication fork collapse. For example, RPA can be a signal for i) primase-polymerase (PrimPOL) recruitment (Guilliam, Brissett et al. 2017), ii) recruitment of the fork remodeler SMARCAL1[2] (Ciccia, Bredemeyer et al. 2009), iii) recruitment of the E3 ubiquitin-protein ligase (RAD18) which together with ubiquitin-conjugating enzyme E2 (RAD6) ubiquitinates PCNA (Davies, Huttner et al. 2008), iv) recruitment of cellular tumor antigen p53 (P53) which facilitates lesion bypass and fork regression with help of POLι, HLTF and Zinc Finger RANBP2-Type Containing 3 (ZRANB3) (Hampp, Kiessling et al. 2016) and v) recruitment of the DNA repair protein RAD51, a protein which is involved in replication fork stabilization and fork reversal. In addition, RAD51 prevents excessive PrimPOL-mediated elongation of nascent DNA (Hashimoto, Ray Chaudhuri et al. 2010, Vallerga, Mansilla et al. 2015, Zellweger, Dalcher et al. 2015), as illustrated in Figure 3. In total, RPA seems to be signal for both checkpoint activation and the activation of DDT (reviewed in (Leung, Baxley et al. 2018)).

1.4.3 Replication fork stabilization

The regulation of nuclease activity plays a key role in replication fork restart. Nucleases, like the DNA replication helicase/nuclease 2 (DNA2), help to degrade nascent DNA which seems to be important for an efficient replication fork restart after fork reversal (Thangavel, Berti et al. 2015). However, stalled replication forks need to be protected from unwanted degradation, predominantly by EXO1 and meiotic recombination 11 homolog 1 (MRE11) (Lemacon, Jackson et al. 2017). This protection is performed by RAD51-ssDNA filaments, formed by RAD51 in concert with the breast cancer type 2 susceptibility protein (BRCA2), comparable to RAD51´s function in canonical homologous recombination (HR) (Kolinjivadi, Sannino et al. 2017, Spirek, Mlcouskova et al. 2018). These filaments are assembled in response to Ataxia

---

[2] SWI/SNF related, matrix associated, actin dependent regulator of chromatin, subfamily A like 1

Telangiectasia and Rad3-related protein (ATR)-mediated phosphorylation of RPA. Phosphorylated RPA recruits BRCA2 to stalled replication forks. BRCA2 then stimulates RAD51 filament formation on ssDNA and inhibits replication fork degradation by repressing MRE11 nuclease activity (Schlacher, Christ et al. 2011), as illustrated in Figure 3. BRCA1 and FA complementation group D2 (FANCD2) are additional proteins involved in repression of MRE11 nuclease activity (reviewed in (Liao, Ji et al. 2018)). In absence of BRCA2, which is mutated in familial breast cancers, MRE11 degrades the regressed arm of the replication fork and triggers Structure-Specific Endonuclease Subunit (MUS81)-dependent fork rescue (described in 1.6.3) (Lemacon, Jackson et al. 2017). The importance of BRCA2 is illustrated by uncontrolled fork degradation through MRE11 in BRCA2-deficient mouse embryonic fibroblasts stem cells, resulting in cell lethality (Ray Chaudhuri, Callen et al. 2016).
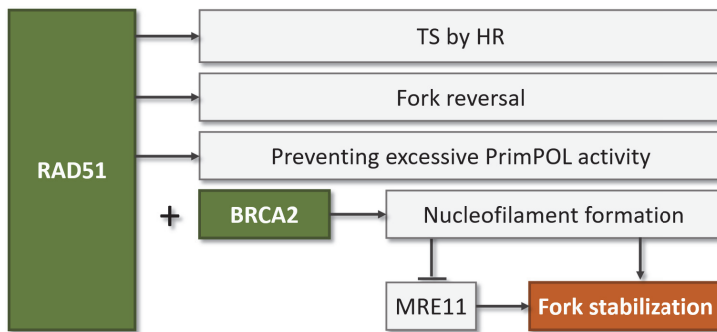

Figure 3. Fork stabilization by RAD51 and BRCA2. RAD51 and BRCA2 mediate RAD51 filament formation which stabilizes ssDNA and prevents MRE11-dependent nascent strand degradation. Additional processes at a stalled replication fork involving RAD51 are also depicted.

1.4.4 Origin firing

Origins are licensed by the minichromosome maintenance DNA helicase (MCM2-7) complex and the formation of the pre-recognition complex (pre-RC) in G1-phase of the cell cycle. Licensing is completed by cell division cycle 45 (CDC45) and go ichi ni san complex (GINS), attaching to the MCM2-7 complex and thus forming the CMG-helicase (Ilves, Petojevic et al. 2010). DBF4-dependent kinase (DDK) and cyclin-dependent kinase (CDK) are activated for transition from G1- to S-phase, where POLε and POLδ associate with the CMG-helicase for replication of the leading and lagging strand, respectively.
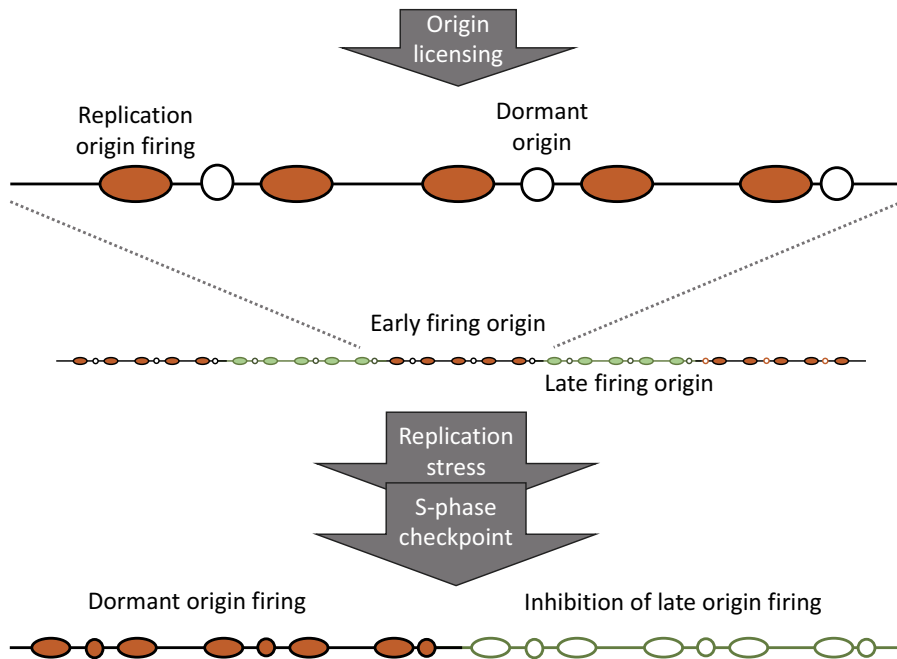
Figure 4. Changes in origin firing in presence of replication stress. Not all licensed origins are activated during replication. Dormant origins can be activated by the intra-S checkpoint in presence of replication stress. Late firing origins are inhibited by the intra-S checkpoint. Based on (Alver, Chadha et al. 2014, Boos and Ferreira 2019).

Origin activation/firing is tightly regulated to ensure replication of the entire genome and to avoid re-replication. Dormant origins are origins that can be activated if replication from nearby origins is compromised (reviewed in (Courtot, Hoffmann et al. 2018)). Only 10 % of the in G1-phase licensed replication origins initiate replication in S-phase, the rest remains dormant and is replicated passively by an incoming replication fork (Ge and Blow 2010, McIntosh and Blow 2012). The intra-S checkpoint is important for regulation of origin firing in S-phase (Petermann, Woodcock et al. 2010). Dormant origins are not essential for S-phase progression in the absence of replication stress (Woodward, Gohler et al. 2006), but MCM2-7 dependent dormant origin firing suppresses replication fork stalling in S-phase, prevents S-phase arrest and increases cell survival in presence of replication stress (Ibarra, Schwob et al. 2008, Kawabata, Luebben et al. 2011). Furthermore, licensing by MCM2-7 after checkpoint-kinase 1 (CHK1) activation decreases the distance between replication origins and provides "normal" replication fork progression even in presence of replication stress (Ge and Blow 2010). ATR-deficient cells exhibit unscheduled global origin firing resulting in excessive ssDNA stretches. Excessive ssDNA causes exhaustion of nuclear RPA pools and in consequence nucleus-wide breakage of

stalled replication forks. Notably, this fork breakage occurs with a delay, indicating that replication forks can be protected independent of ATR activation for some time (Toledo, Altmeyer et al. 2013). Dormant origin firing seems to be important for genome maintenance, as illustrated by mice with reduced MCM2 or MCM4 expression levels causing an early onset of cancer (Pruitt, Bailey et al. 2007, Shima, Alcaraz et al. 2007). It is assumed that global/late origins are inhibited, whereas local/dormant origins are activated upon replication stress (reviewed in (Yekezare, Gomez-Gonzalez et al. 2013)). A simplified model of activation and repression of origin firing during S-phase is illustrated in Figure 4.

1.4.5   Intra-S checkpoint

The intra-S checkpoint, also referred to as replication checkpoint or ATR/CHK1 checkpoint, can be activated by accumulation of ssDNA resulting from blocked DNA synthesis (Zellweger, Dalcher et al. 2015). Activation of the intra-S checkpoint in response to replication stress decreases the sensitivity of cells towards several replication stalling agents such as ionizing radiation, cisplatin, MMS and UV (Cliby, Roberts et al. 1998). In addition, ATR is activated in the absence of exogenously induced DNA damage in order to control origin firing (reviewed in (Iyer and Rhind 2017)). Replication stress dependent RPA-coated ssDNA is recognized by the ATR interacting protein (ATRIP) which in turn recruits and activates ATR (Ball, Myers et al. 2005). Many more proteins are involved in full checkpoint activation, including several proteins with a role in DDT, which illustrates the complexity of the intra-S checkpoint. These are e.g. Claspin, the Timeless-Tipin complex (Kemp, Akan et al. 2010) and BRCA1 (Yarden, Metsuyanim et al. 2012), three proteins which are also known to trigger PCNA monoubiquitination (see 1.5). Poly(ADP-ribose) polymerase 1 (PARP1) is also required for full activation of the checkpoint by rapidly binding to CHK1 at unresected stalled replication forks (Min, Bruhn et al. 2013). In addition, PARP1 fulfills an important role in replication fork reversal (see 1.6.3.1).

Consequences of the intra-S checkpoint activation

The intra-S checkpoint predominantly inhibits new origin firing and activates dormant origin firing, as illustrated in Figure 5.
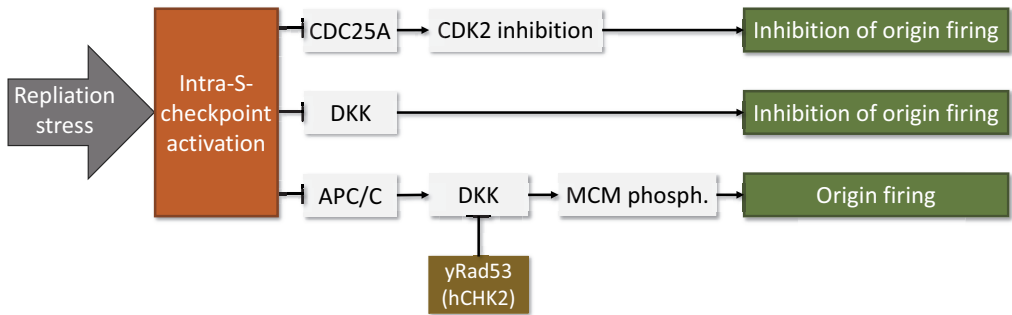
Figure 5. Simplified consequences of intra-S checkpoint activation. Activation of the intra-S checkpoint results in phosphorylation of effector proteins (white), resulting in activation of origin firing or inhibition of origin firing.

New origin firing is inhibited by phosphorylation of the M-phase inducer phosphatase 1 (CDC25A), a protein of the CDC45 family of phosphatases, through CHK1 (and CHK2 upon IR treatment) (Sorensen, Syljuasen et al. 2003). CDC25A inhibits the cyclin dependent kinase 2 (CDK2) and prevents unscheduled and abortive mitosis by inhibiting new origin firing (Donzelli and Draetta 2003). CDC7-DBF4 kinase (DKK) is essential in replication initiation by phosphorylation of MCM2-7. During replication stress, DKK is required for full CHK1 activation (Sasi, Coquel et al. 2018). Once the checkpoint is activated it inactivates anaphase-promoting complex/cyclosome (APC/C), a ubiquitin ligase, preventing DKK degradation (Ferreira, Santocanale et al. 2000, Day, Palle et al. 2010, Yamada, Watanabe et al. 2013). It is assumed that DKK first initiates intra-S checkpoint activation, and then the activated checkpoint inhibits DKK-dependent late origin firing (Sasi, Coquel et al. 2018). Recently, CHK1 deficiency in unperturbed cells resulted in reduced replication fork elongation, excess origin firing and increased DNA damage levels (Gonzalez Besteiro, Calzetta et al. 2019). In yeast, Rad53 (CHK2 in humans) was found to block origin firing through phosphorylation of Dbf4 (Zegerman and Diffley 2010). Furthermore, yeast Rad53 mutants contained an accumulation of reversed forks, abnormal replication intermediates and larger ssDNA regions at the replication fork (Lopes, Foiani et al. 2006).

Replication slowdown can be orchestrated by inhibition of origin firing or reduction of replication fork speed. In response to MMS, replication locally slowed down independent of checkpoint activation, and globally by a reduction of origin firing dependent on checkpoint activation (Iyer and Rhind 2017). However, the general S-phase duration is not increased during replication stress due to a fluctuating CDK2 activity that regulates the DNA synthesis rate

(Daigh, Liu et al. 2018). Thus, replication fork slowing is a checkpoint-independent and local effect caused by a replication fork encountering a damaged template (Iyer and Rhind 2017). In Paper 3 we suggest that the reduced CHK2 activation in human cells lacking SHPRH might be an explanation for the observed lower MMS sensitivity and unperturbed replication in these cells.

Regulation of DDT proteins by the intra-S checkpoint

The intra-S checkpoint directly regulates the activity of several important DDT proteins, for instance Bloom´s helicase (BLM), SMARCAL1 or POLη. BLM is a RECQ helicase which is deficient in Bloom´s syndrome, a disease associated with genetic instability, short stature and cancer. BLM mediates fork reversal and D-loop resolution (Larsen and Hickson 2013). FANCD2 is an essential regulator of BLM during replication stress. BLM is phosphorylated by ATR and cooperates with FANCD2 to inhibit new origin firing and to promote replication fork restart (Davies, North et al. 2007, Chaudhury, Sareen et al. 2013). SMARCAL1, a fork remodeling enzyme, illustrates the importance of checkpoint regulation in response to stalled replication forks. SMARCAL1 is activated by RPA coated ssDNA, independent of checkpoint activation (Ciccia, Bredemeyer et al. 2009, Betous, Mason et al. 2012). However, checkpoint activation leads to an inactivation/phosphorylation of SMARCAL1 by ATR. This regulation is suggested to prevent aberrant fork processing and fork collapse after efficient fork reversal activity (Couch, Bansbach et al. 2013). Furthermore, activation of the intra-S checkpoint regulates the stability of POLη. POLη phosphorylation by CDK2 persists from S- until G2/M-phase and stabilizes the protein. After lesion bypass, POLη is dephosphorylated and degraded (Bertoletti, Cea et al. 2017).

However, intra-S checkpoint activation does not directly correlate with ssDNA formation at the replication fork, the amount of fork uncoupling, the amount of postreplicative gaps or the amount of reversed replication forks (Zellweger, Dalcher et al. 2015). Activation of the intra-S checkpoint and DDT are believed to be parallel and partly independent pathways (Leung, Baxley et al. 2018). Recently, activation of the intra-S checkpoint after accumulation of ssDNA at stalled forks versus accumulation of ssDNA in postreplicative gaps (TS by HR), were described as two different checkpoint responses, yet, with similar outcomes. Interestingly, the activation of the checkpoint response in late S-phase (TS by HR) seems to be slower and does not inhibit late origin firing (reviewed in (Galanti and Pfander 2018)).

16

1.5   Regulation of DDT by posttranslational modifications on PCNA

Multiple proteins are involved in regulating DDT, but how TLS, fork reversal and TS by HR exactly are coordinated is not clear. PTMs on PCNA play a role in activating several pathways to rescue stalled replication forks, as illustrated in Figure 6.

1.5.1   PCNA ubiquitination

Ubiquitin, a 8.6 kDa protein with a C-terminal glycine, can be conjugated to a lysine side chain of another protein. Ubiquitination of proteins requires the presence of ubiquitin ligases to catalyze the reaction. It was initially discovered as a modification causing proteasome-mediated degradation. However, ubiquitination also regulates DDT: TLS is activated by monoubiquitinated PCNA, whereas fork reversal and TS by HR are activated by polyubiquitinated PCNA.

PCNA can be monoubiquitinated at K164 by the RAD6-RAD18 E2-E3 ubiquitin ligase complex in response to RPA-coated ssDNA in presence of replication stress. K164 is located on the back side of PCNA, opposite to the binding sites of polymerases. This allows recruitment and binding of ubiquitin-binding proteins without inhibiting replication (reviewed in (Slade 2018)). PCNA can also be ubiquitinated by other ubiquitin ligases, e.g. by ring finger protein 8 (RNF8) (Zhang, Chea et al. 2008). In addition, numerous proteins stimulate PCNA ubiquitination, including HLTF by its RING domain (Lin, Zeman et al. 2011), proteins involved in intra-S checkpoint response such as FANCD2, RAD51 (independent of BRCA2) (Chen, Bosques et al. 2016), CHK1, cyclin-dependent kinase inhibitor 1 (P21), P53, Claspin, Timeless, Nijmegen Breakage Syndrome protein 1 (NBS1) (reviewed in (Slade 2018)), BRCA1 (Tian, Sharma et al. 2013), and the TLS polymerases POLη, POLϰ and REV1 (reviewed in (Kanao and Masutani 2017)). Recently, AKT (also called Protein Kinase B) was identified as a regulator of PCNA ubiquitination as AKT inhibition inhibited recruitment of TLS polymerases to DNA damage sites and impaired PCNA ubiquitination (Villafanez, Garcia et al. 2019).

Following ssDNA formation in presence of replication stress, PCNA is rapidly monoubiquitinated. This stimulates the interaction between PCNA and TLS polymerases.

PCNA monoubiquitination increases the activity and processivity of TLS polymerases with POLη exhibiting the highest affinity to monoubiquitinated PCNA (reviewed in (Slade 2018)). TLS was initially suggested to be dependent on PCNA monoubiquitination (Hoege, Pfander et al. 2002, Kannouche, Wing et al. 2004). Although, it was shown later that TLS also occurs in absence of PCNA monoubiquitination, albeit with lower efficacy (Hendel, Krijger et al. 2011). However, PCNA monoubiquitination seems to be required for Gap-filling TLS (described briefly in 1.6.2.1) (reviewed in (Hedglin and Benkovic 2017)). Because PCNA is a homotrimer, it can be triple monoubiquitinated at K164. This triple monoubiquitination is catalyzed by RAD18 and suggested to activate a POLη-independent TLS pathway; although, this remains to be fully characterized (Kanao, Masuda et al. 2015). PCNA, in addition, can be ubiquitinated at several other lysins, e.g. K242 and K117, but their exact role in DDT, if any, is not clear (Leung, Baxley et al. 2018). An important repressive regulator of PCNA ubiquitination is the ubiquitin-specific protease (USP1). Upon UV irradiation, USP1 is cleaved by its own protease activity, significantly decreasing USP1 levels and allowing PCNA to be monoubiquitinated (Hedglin and Benkovic 2017).

In yeast, PCNA polyubiquitination occurs stepwise at Lysine 164 (K164) after previous monoubiquitination of PCNA by Rad6 and Rad18. The same was observed in human cells, where PCNA is polyubiquitinated by HLTF and SHPRH, in concert with the E2 ubiquitin conjugating enzyme MMS2-UBC13, similar to Rad5/Mms2-Ubc13 in yeast (reviewed in (Kanao and Masutani 2017)). In addition to HLTF and SHPRH, the existence of a third E3 ubiquitin ligase has been suggested, since PCNA polyubiquitination was observed in HLTF and SHPRH double knockout mouse cells (Krijger, Lee et al. 2011). After previous monoubiquitination or triple monoubiquitination, stepwise PCNA polyubiquitination is mediated in the absence of RAD6 and RAD18 (Masuda, Mitsuyuki et al. 2018).

However, *in vitro* experiments suggest that PCNA is predominantly polyubiquitinated by another mechanism starting with a HLTF-dependent K63-linked ubiquitin-chain formation on MMS2-UBC13. This ubiquitin-chain is then transferred "en bloc" to RAD6 and further to PCNA. The latter step is mediated with the help of RAD18 (Masuda, Suzuki et al. 2012) (see Figure 6). This way, TS can occur without previous monoubiquitination of PCNA. The ligase activity of HLTF for the ubiquitin-chain formation is stimulated by HLTF's HIRAN domain binding to dsDNA at stalled primer ends. The same study also reported a HLTF dependent coupling between PCNA mono-and polyubiquitination. PCNA can be polyubiquitinated by

HLTF after previous monoubiquitination with the help of HLTF. However, the occurrence of PCNA polyubiquitination in absence of HLTF requires previous PCNA monoubiquitination at all three trimers. Interestingly, HLTF´s binding to PCNA, likely via APIM, causes a reduction in ubiquitin-chain formation (Masuda, Mitsuyuki et al. 2018).
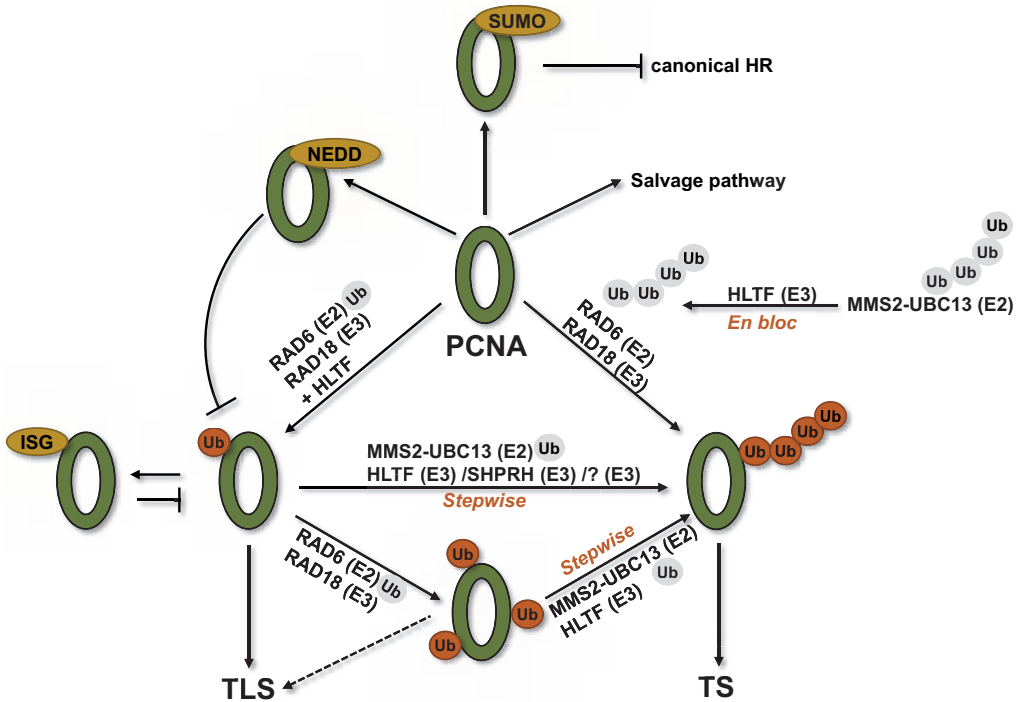

Figure 6. Regulation of DDT by PTMs on PCNA. PTMs on PCNA (green) known to be involved in DDT regulation are depicted; ubiquitination (Ub) on PCNA in orange, ubiquitination on ligases that ubiquitinate PCNA in gray. SUMOylation (SUMO), NEDDylation (NEDD) and ISGylation (ISG) are illustrated in yellow. Involvement of HLTF and SHPRH at certain ubiquitination steps is shown.

ZRANB3, a fork reversal protein (see 1.6.3), is identified as a reader of PCNA polyubiquitination. PCNA polyubiquitination enhances ZRANB3´s affinity to PCNA (Ciccia, Nimonkar et al. 2012, Vujanovic, Krietsch et al. 2017). Recently, POLκ interaction with K48-linked polyubiquitinated PCNA was shown to be important for replication fork restart after hydroxyurea (HU) treatment (Tonzi, Yin et al. 2018). Although, the general impact of PCNA polyubiquitination is not clear and under discussion. MMS2 deficient cells, for instance, obtain an increased amount of mutations in presence of UV-induced replication stress (Li, Xiao et al. 2002). A similar effect was observed in HLTF deficient cells (Lin, Zeman et al. 2011). Another

study, however, did not find any requirement of PCNA polyubiquitination for DDT after UV induced replication stress (Gervai, Galicza et al. 2017). Thus, PCNA polyubiquitination might not always be required, but at least for fork reversal by ZRANB3 it is important and several studies strongly indicate that presence of PCNA polyubiquitination activates error-free DDT (reviewed in (Leung, Baxley et al. 2018)).

Interestingly, phosphorylation of PCNA by the insulin-like growth factor-1 receptor (IGF-1R) labels PCNA for mono- and polyubiquitination and is also important for handling replication stress by the DDT pathways. IGF-1R was also suggested to stimulate the binding of HLTF and SHPRH to PCNA (Waraky, Lin et al. 2017).

1.5.2 Other posttranslational modifications on PCNA with roles in DDT

In addition to ubiquitination, SUMOylation, NEDDylation and ISGylation of PCNA have an impact on DDT.

Human PCNA can be modified by a small ubiquitin-like modifier (SUMO) at K164 (Tsutakawa, Yan et al. 2015). SUMOylated yeast PCNA binds two distinct proteins, antirecombinase Srs2 and ubiquitin ligase Rad18 (Parker and Ulrich 2012). Srs2 prevents HR during S-phase by disrupting Rad51 nucleoprotein filaments (Pfander, Moldovan et al. 2005). In human cells, the PCNA-associated recombination inhibitor (PARI) interacts with SUMOylated PCNA and fulfills the role of controlling the occurrence of HR events in S-phase (Moldovan, Dejsuphong et al. 2012, Burkovics, Dome et al. 2016). SUMOylation of human PCNA is limited to S-phase, occurs both in presence and absence of replication stress, and does not inhibit TS by HR (Hoege, Pfander et al. 2002, Branzei, Vanoli et al. 2008). Instead, SUMOylated human PCNA seems to stimulate TS with the involvement of HR proteins. This discrepancy between negatively regulating HR events and positively regulating HR-like events (TS by HR), is believed to be at least partly caused by distinct functions of HR proteins in DSB repair and TS by HR (Mohiuddin, Evans et al. 2018). In yeast, it is reported that PCNA can be ubiquitinated and SUMOylated at the same time (Parker and Ulrich 2012).

NEDD8 is the ubiquitin-like protein with the highest similarity to ubiquitin (Kamitani, Kito et al. 1997), and it is, similarly to ubiquitin, conjugated to K164 on PCNA by the RAD18 E3 ligase. NEDDylation of PCNA antagonizes PCNA ubiquitination as well as POLη recruitment and foci formation in response to exogenously induced oxidative stress (Guan, Yu et al. 2018).

Interferon-stimulated gene 15 (ISG-15) is also a ubiquitin-like protein (Haas, Ahrens et al. 1987). It is conjugated to K164 and K168 on PCNA. The interferon-inducible ubiquitin-protein isopeptide E3 (EFP) ligase can bind to monoubiquitinated PCNA and facilitates ISGylation of PCNA. ISGylation is a late response to UV, resulting in recruitment of USP10 to deubiquitinate PCNA, which in consequence terminates TLS (Park, Yang et al. 2014).

In absence of PTMs on PCNA, another HR-like pathway (Salvage pathway), was suggested to be induced in G2/M as a backup pathway for DDT (Branzei and Szakal 2016) (see 1.6.3.3).

1.6   DDT mechanisms

TLS, fork reversal and TS by HR are referred to as DDT mechanisms. In presence of replication stress, these mechanisms are activated to increase the chance of continuous replication and genome integrity. Impediments for the replication fork can either be processed at the replication fork or in postreplicative gaps after repriming. DDT mechanisms can be error-free or error-prone, depending on the activated mechanism and the type of obstacle on the template DNA. After error-free DDT, the bypassed lesion on the template strand can later be repaired, for instance by MMR or NER. It is not clear, how exactly the choice between the different DDT mechanisms is made is not clear, but it is thought to be dependent on the type of DNA lesion and the degree of replication stress (Masuda, Mitsuyuki et al. 2018)).

1.6.1   Repriming upon replication stress

DNA synthesis on the lagging strand is naturally discontinuous and includes scheduled repriming (synthesis of RNA primers) for the next Okazaki fragment by the primase subunit of POLα. Repriming thus prevents excessive uncoupling of the CMG helicase from DNA

synthesis when the replicative polymerase encounters a lesion on the lagging strand. On the leading strand a replication stalling lesion results in an uncoupling event and long RPA-coated ssDNA stretches. Here, repriming downstream of the lesion is suggested as a replication fork restart mechanism, leaving small ssDNA gaps opposite of the lesion (Elvers, Johansson et al. 2011). Repriming on the leading strand is facilitated by the replicative primase in *Escherichia coli* and *Saccharomyces cerevisiae* (Heller and Marians 2006, Lopes, Foiani et al. 2006). Yet, in human cells, PrimPOL, a member of the Archaeo-Eukaryotic Primase family, containing both primase and TLS polymerase activity, is responsible for repriming and reinitiating DNA synthesis on the leading strand (Iyer, Koonin et al. 2005, Mouron, Rodriguez-Acebes et al. 2013, Guilliam and Doherty 2017). Unlike most of the other polymerases PrimPOL does not interact with PCNA (Guilliam, Jozwiakowski et al. 2015). PrimPOL downregulation results in a decreased fork rate independent of dormant origin firing (Rodriguez-Acebes, Mouron et al. 2018) and is important for replication, also in unperturbed cells, by preventing excessive replication fork stalling and mutations (Bailey, Bianchi et al. 2019). A model of repriming by PrimPOL in presence of a leading strand lesion resulting in a postreplicative gap, a process also called "lesion skipping", is illustrated in Figure 7.
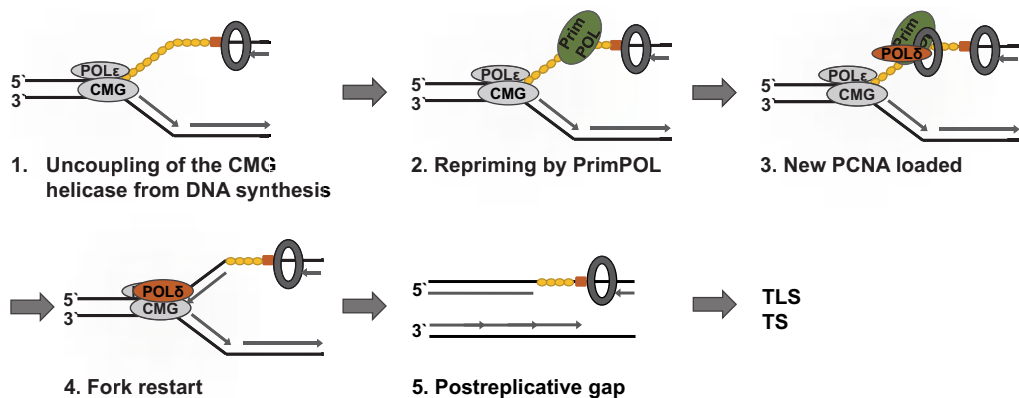

Figure 7. Model for repriming on the leading strand by PrimPOL. 1. A lesion on the leading strand, that cannot be accommodated by POLε, results in uncoupling of the CMG helicase from DNA synthesis. The CMG helicase continues unwinding, resulting in long stretches of RPA-coated ssDNA (yellow). POLε has high affinity to the CMG helicase, but low affinity to PCNA (gray circle), and is therefore suggested to stay bound to the CMG helicase. 2. PCNA stays at the lesion. PrimPOL (green) binds downstream of the lesion on the leading strand and synthesizes a new primer. 3. Replicative POLδ (orange) bound to a new PCNA molecule extends the primer until (4.) catching up with the CMG helicase. The replication fork is re-established and POLδ is replaced by POLε. 5. The remaining postreplicative gap can be processed by TLS or TS. Adapted from (Hedglin and Benkovic 2017).

22

1.6.2   Translesion synthesis

TLS has been extensively studied during the last decades and two models, TLS "on the fly" and Gap-filling TLS, have been proposed. TLS "on the fly" implies lesion bypass at the ongoing replication fork, whereas Gap-filling TLS occurs after repriming in postreplicative gaps (Hedglin and Benkovic 2017). In both models the replicative polymerase is exchanged by an inserter TLS polymerase (polymerase switch), which can replicate over bulky lesions followed by the same or another TLS polymerase as an extender polymerase (Quinet, Lerner et al. 2018). Due to the nature of TLS polymerases, which have more spacious catalytic sites and lack proofreading (exonuclease) activities, TLS is often error-prone (Makarova, Stodola et al. 2012, Yang, Gao et al. 2018).

1.6.2.1 TLS model

In the TLS "on the fly" model, bypass of the lesion occurs before the replication fork is restarted/recoupled (Figure 8A). The replicative polymerase is replaced by a TLS polymerase replicating until reaching an undamaged template. Then, POLδ replicates the leading strand until it catches up with the stalled CMG helicase, where it is replaced by POLε. With this event, DNA synthesis and unwinding are re-coupled, and the replication fork can continue. In the model of Gap-filling TLS, bypass of the lesion occurs after the replication fork has been restarted by a repriming event. The lesion, now in a postreplicative ssDNA gap on the leading strand, is bypassed by a TLS polymerase, replicating from the aborted primer until reaching the undamaged template. Then the TLS polymerase is replaced by POLδ, which synthesizes the rest of the DNA in the ssDNA gap. On the lagging strand, repriming is performed by POLα-primase (not by PrimPOL), starting a new Okazaki fragment (Figure 8 B and C). The ssDNA gap with the lesion is left upstream. TLS polymerases then replicate over the lesion, followed by POLδ extension until the postreplicative gap is filled (reviewed in (Hedglin and Benkovic 2017)).
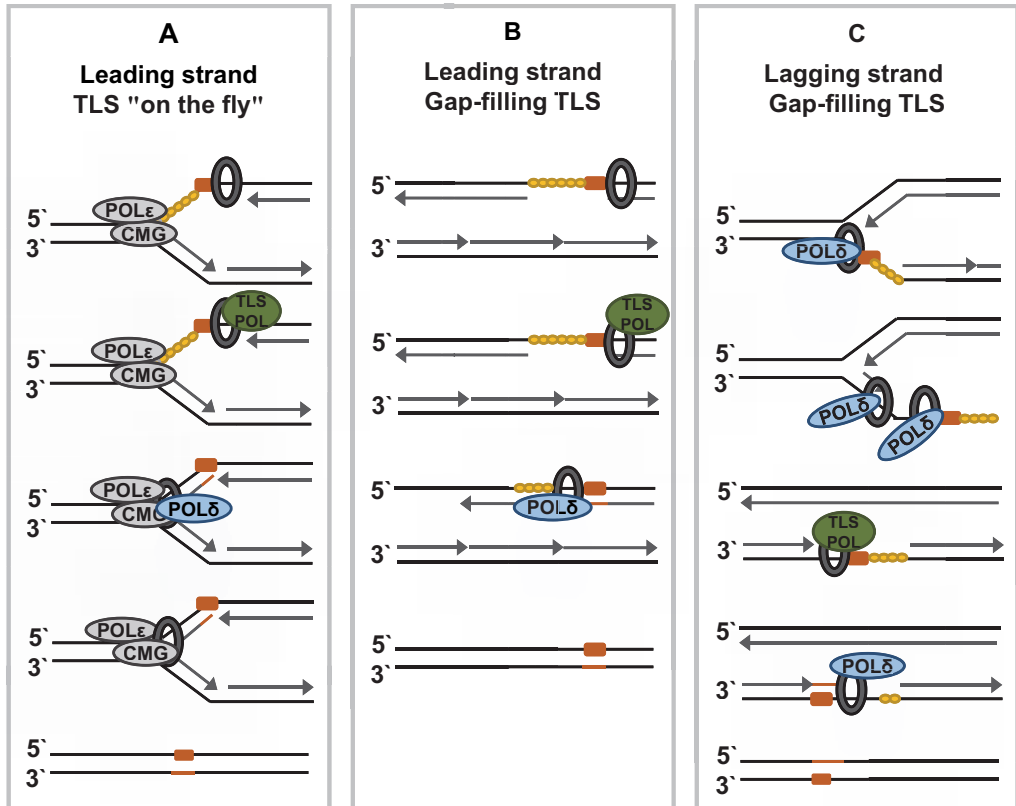
Figure 8. Model for TLS "on the fly" and Gap-filling TLS. (A) Leading strand TLS "on the fly". Bypass by a TLS polymerase occurs before the replication fork is restarted by POLδ, recoupling DNA synthesis with the CMG helicase. (B) Leading strand Gap-filling TLS. Bypass by a TLS polymerase after repriming and by PrimPOL. (C) Lagging strand Gap-filling TLS. Bypass by a TLS polymerase after scheduled repriming by POLα-primase. PCNA is depicted as a gray circle, RPA in yellow, POLδ in blue, TLS polymerases in green, POLε and CMG helicase in gray. Adapted from (Hedglin and Benkovic 2017).

1.6.2.2 TLS polymerases

Polymerases involved in TLS are mainly the Y-family polymerases POLη, POLι, POLκ and REV1, and the B-family polymerase POLζ. In addition, two A-family polymerases, POLθ and POLν, and three X-family polymerases, POLβ, POLλ and POLμ, exhibit bypass polymerase activities. Lately, PrimPOL has been added to the list of TLS polymerases. TLS polymerases lack exonuclease activities and have more relaxed active sites. This results in lower fidelity but allows TLS polymerases to accommodate bulky distorted bases (reviewed in (Vaisman and Woodgate 2017)). In addition, TLS polymerases have lower processivity than replicative polymerases, but they often replicate accurately over specific types of lesions. Still, TLS

polymerases often cause mutations with potentially deleterious consequences. Therefore, recruitment of TLS polymerases and regulation of their activity must be strictly regulated. The type of TLS polymerase used at specific lesions probably depends on several factors, including cell type, damage load or location of the lesion/obstacle in the chromosome. Because of their mutagenic properties, TLS polymerases are involved in somatic hypermutation of immunoglobulins. In addition, TLS polymerases are important for replication over fragile sites and more complex DNA structures (reviewed in (Quinet, Lerner et al. 2018)).

POLζ, unlike replicative B-family polymerases, lacks a 3´-5´ exonuclease activity (Nelson, Lawrence et al. 1996, Sharma and Canman 2012). POLζ is more efficient in extending from a primer at a mismatch (misincorporation frequency of 10^{-1} to 10^{-2}) than in inserting nucleotides opposite a lesion (misincorporation frequency of 10^{-4} to 10^{-5}); however, it can do both (Johnson, Washington et al. 2000, Prakash, Johnson et al. 2005). POLζ, but not REV1, is important for Gap-filling TLS, and TLS "on the fly" over UV-induced TT- 6-4PPs is mediated by POLζ in a mainly error-free manner (Jansen, Tsaalbi-Shtylik et al. 2009, Yoon, Prakash et al. 2010, Quinet, Martins et al. 2016). On the other hand, replication over TT-CPDs by POLζ is often error-prone (Yoon, Prakash et al. 2009). In presence of cisplatin-induced pt-GG, POLζ can extend the primer after previous nucleotide insertion by POLη (Lee, Gregory et al. 2014). Lately, POLκ has been described as an accurate extender of POLη in this case (Jha and Ling 2018). However, POLζ seems to be important for the bypass of both, cisplatin and MMC derived intrastrand crosslinks (Hicks, Chute et al. 2010). POLζ forms a complex with REV1 and multiple other TLS proteins (illustrated in Figure 9).

The formation of the Polζ-Rev1 complex increases the mismatch extension activity of Polζ in yeast (Acharya, Johnson et al. 2006). In human cells, POLζ-REV1 interaction prevents REV1 from degradation, because the REV7 subunit stabilizes REV1 and prevents it from polyubiquitination by APC (Chun, Kok et al. 2013). The dimerization of REV7 is important for the function of the REV1-POLζ complex in TLS (Rizzo, Vassel et al. 2018). Furthermore, REV7 binds the transcription factor TFII-I, which is required for efficient TLS over UV lesions. This binding is dependent on the simultaneous interaction of one of the APIMs in TFII-I with PCNA. Thus, TFII-I binding to PCNA bridges POLζ and PCNA. Therefore, TFII-I was suggested to cause a polymerase switch from POLη/ι/κ to POLζ, because it specifically interacts with the POLζ subunit REV7 but not with POLη or POLι (Fattah, Hara et al. 2014).
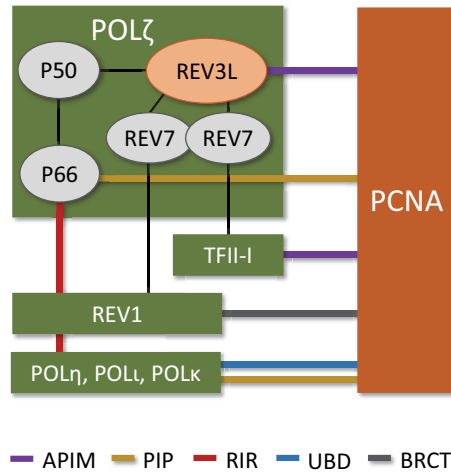
Figure 9. Simplified schematic view of POLζ subunits binding to REV1, TFII-I, and PCNA. POLζ can bind to PCNA via the PIP box of its P66 subunit (Ducoux, Urbach et al. 2001) and via APIM of REV3L (Paper 1). The REV7 subunit of POLζ can in addition bind to the C-terminal domain of REV1, and RIR of P66 can simultaneously bind to C-terminal domain of REV1, forming a POLζ-REV1 complex. In addition, REV1 contains a N-terminal BRCT domain which can interact with PCNA (Pustovalova, Maciejewski et al. 2013), resulting in a POLζ-REV1-PCNA complex. TFII-I can further bind to REV7 (Fattah, Hara et al. 2014).

REV1 is a Y-family polymerase and its polymerase activity primarily inserts C opposite of AP-sites (Nelson, Lawrence et al. 1996). However, the main role of REV1 in TLS is probably to serve as a scaffold protein for other TLS polymerases (Quinet, Martins et al. 2016). Besides REV1, three additional Y-family polymerases are involved in TLS, namely POLη, POLκ and POLι. They all contain a REV1-interacting region (RIR), enabling them to bind to the C-terminal domain (CTD) of REV1 (reviewed in (Vaisman and Woodgate 2017)). In addition, they can bind to PCNA via non-canonical PIP-boxes (Hishiki, Hashimoto et al. 2009). **POLη,** the first purified and most studied TLS polymerase, is encoded by the Xeroderma Pigmentosum Variant (XPV) gene. *XPV* deficiency is associated with defective replication of UV-induced lesions (Masutani, Kusumoto et al. 1999), because POLη bypasses TT-CPDs in an error-free manner (Johnson, Prakash et al. 1999). Among TLS polymerases, POLη exhibits a unique non-catalytic function in bridging RAD18 and PCNA and thereby stimulating PCNA monoubiquitination after UV irradiation (Durando, Tateishi et al. 2013). PCNA monoubiquitination is not essential for POLη in TLS, but it increases the affinity of POLη to PCNA (Sabbioneda, Gourdin et al. 2008, Hendel, Krijger et al. 2011, Krijger, van den Berk et al. 2011). **POLκ** and POLζ, probably in concert with POLθ, serve as an error-prone backup for POLη in replication over UV-induced TT-CPDs (Ziv, Geacintov et al. 2009, Yoon, McArthur

et al. 2019). TLS by POLκ often results in single-base deletions (Wolfle, Washington et al. 2003), but POLκ efficiently extends from mismatched primers (Washington, Johnson et al. 2002), and it is the most faithful polymerase for bypassing benzopyrene-derived N2-guanine adducts (Prakash, Johnson et al. 2005). Recently, POLκ, but neither of the other Y-family polymerases nor POLζ, has been shown to be important for replication fork restart after HU treatment. This activity of POLκ was dependent on FANCD2 and the interaction of POLκ with polyubiquitinated PCNA (Tonzi, Yin et al. 2018). **POLι** can also serve as a backup for POLη, e.g. in XPV cells; however, it is generally very mutagenic (Tissier, McDonald et al. 2000, Wang, Woodgate et al. 2007). The A-family polymerase, **POLθ**, participates in TLS as an inserter polymerase for bypassing TT-CPDs as an alternate route for bypass by POLκ and POLζ. Furthermore, POLθ is an extender polymerase across 6-4PPs as an alternate route to the error-free bypass by POLζ (Yoon, McArthur et al. 2019). Other so-called TLS polymerases seem to have minor roles in TLS.

POLδ can bypass some DNA lesions during replication, e.g. weakly blocking adducts in an error-prone manner (Fazlieva, Spittle et al. 2009); however, it usually rapidly dissociates from the DNA upon replication fork stalling (Hedglin, Pandey et al. 2016).

1.6.2.3 Polymerase switch during TLS

Two models for polymerase switch during TLS, involving POLζ, have been proposed. i) The binding of POLζ to the hub protein REV1 could be the basis for an exchange of TLS polymerases (from the inserter polymerase to the extender polymerase). In this model the inserter Y-family polymerase binds to REV1 via RIR. Competitive binding of RIR in this Y-family polymerase with the RIR of the POLζ subunit P66 to REV1 causes the exchange of the inserter to the extender polymerase (Pustovalova, Magalhaes et al. 2016). ii) The polymerase switch from replicative POLδ to POLζ could be mediated via the two shared subunits, P50 and P66. This model is based on studies in yeast, showing that mutations in the accessory subunits of Polδ affect mutagenesis similar to mutations in Polζ (Baranovskiy, Babayeva et al. 2008). Hence, the POLδ subunit P125 is suggested to dissociate from the DNA upon POLδ stalling, while the P50 and P66 subunits remain bound to PCNA and recruit POLζ. POLζ can then bypass the lesion on its own or in concert with a Y-family polymerase. Afterwards POLζ is replaced by POLδ (Baranovskiy, Lada et al. 2012). So far, these models have not been verified *in vivo*.

Two models have also been proposed for the binding of TLS polymerases to the polymerase scaffold protein PCNA. i) In the so-called Piggyback model, TLS polymerases and the replicative polymerase bind to PCNA simultaneously. Replicative POLδ binds to the front side of PCNA via its PIP-box, facing towards the direction of DNA synthesis. TLS polymerases bind via their ubiquitin binding domains to the back side of PCNA, the side of monoubiquitination. This model is based on observations showing that POLη travels with the replication fork and is able to stimulate PCNA monoubiquitination, thereby increasing its own affinity to PCNA. Upon encountering a lesion, POLδ dissociates and the Y-family TLS polymerase can bypass the lesion. ii) The so-called Toolbelt model is based on PCNA being a homotrimer, allowing binding of up to three TLS polymerases simultaneously. The most appropriate TLS polymerase could be selected by turning PCNA, depending on the lesion and on nucleotide incorporation kinetics of the TLS polymerase. Hence, once POLδ encounters the lesion, it dissociates, PCNA is ubiquitinated and TLS polymerases can bind to PCNA (reviewed in (Slade 2018)). Since the residence time of TLS polymerases is less than 1 second, dynamically rapid exchange of polymerases at the replication fork is suggested until the most appropriate polymerase is identified and bypasses the lesion (Sabbioneda, Gourdin et al. 2008).

Besides PTMs on PCNA, also PTMs on TLS polymerases regulate the activity of the polymerases and their affinity to PCNA. POLη e.g. can be ubiquitinated, phosphorylated and SUMOylated. Monoubiquitination of POLη blocks its binding to other ubiquitylated proteins and impedes its PCNA interaction (Jung, Hakem et al. 2011), while polyubiquitination of POLη causes its proteasomal degradation (Jung, Qian et al. 2012). POLη can be phosphorylated at several sites; however, this PTM on POLη occurs first in late S/G2, after the bulk of DNA is replicated, and persists until G2/M. Phosphorylation of POLη appears to be mediated in a checkpoint dependent manner and seems to be important for its stability and for postreplicative gapfilling after S-phase completion (Bertoletti, Cea et al. 2017). SUMOylation of POLη is suggested to be important for preventing under-replicated DNA, also in the absence of externally induced replication stress (Despras, Sittewelle et al. 2016). POLκ and POLι ubiquitination or SUMOylation are suggested to be involved in regulating their polymerase activities (reviewed in (Slade 2018)). Thus, PTMs on TLS polymerases are likely to be involved in the polymerase switch in TLS as well.

1.6.2.4 RAD5 homologs in TLS

Both RAD5 homologs are involved in TLS; HLTF by recruiting POLη after UV induced DNA damage and SHPRH by recruiting POLκ after methyl methanesulfonate (MMS) induced DNA damage (Lin, Zeman et al. 2011). Interestingly, yeast Rad5 is also involved in TLS via interaction with Rev1 after PCNA monoubiquitination. Disruption of this interaction results in decreased UV-induced mutagenesis (Xu, Lin et al. 2016), suggesting a role for Rad5 in the recruitment of TLS polymerases.

1.6.3   Homology-directed DDT

If a replication fork stalls and cannot be rescued by a converging replication fork, the stalled fork must be restarted in order to prevent fork collapse. Homology-directed DDT, also known as TS pathways, can, besides TLS, rescue replication forks. TS pathways use the sister chromatid as a template. The two TS pathways, TS by fork reversal and TS by HR in postreplicative gaps, are both dependent on unwinding/separating the nascent strands from the template and on annealing of the nascent strands (Pilzecker, Buoninfante et al. 2019). In human cells, fork reversal is suggested to be the predominant mechanism to rescue replication forks, whereas in yeast reversed replication forks are observed only after deficiency in checkpoint activation or repriming (Sogo, Lopes et al. 2002, Fumasoni, Zwicky et al. 2015, Zellweger, Dalcher et al. 2015). Fork reversal can be induced by mild treatments, suggesting that it occurs frequently and is a global response to different types of replication stress (Zellweger, Dalcher et al. 2015, Vujanovic, Krietsch et al. 2017). Although not directly proven, a reversed fork is believed to be used for lesion bypass by TS, but can have other outcomes as well, as discussed below. The term "fork reversal" is used for the formation of the chickenfoot structure, and "fork restoration" for the conversion of the chickenfoot structure back to a functional replication fork. In literature these processes are not clearly defined and additional terms like fork regression and fork remodeling are inconstantly used, often for both processes.

1.6.3.1 Replication fork reversal

Fork reversal is a mechanism where the parental strands in the lesion containing region are reannealed and the newly synthesized daughter strands are unpaired from the templates and annealed (Neelsen and Lopes 2015). This results in a "chickenfoot" intermediate, which can be visualized by electron microscopy, and which is suggested to be dependent on PCNA polyubiquitination (Vujanovic, Krietsch et al. 2017). HLTF, as a translocase, can remove proteins from stalled replication forks, providing access for fork reversal enzymes (Achar, Balogh et al. 2011). In addition to the F-box DNA helicase 1 (FBH1), three proteins of the SNF2 family of DNA translocases, HLTF, ZRANB3, and SMARCAL1, have been reported to facilitate fork reversal *in vivo* in human cells (Fugger, Mistrik et al. 2015, Taglialatela, Alvarez et al. 2017). Figure 10 illustrates fork reversal/chickenfoot structure formation in presence of replication stress. Due to different preferences of binding partners of HLTF, ZRANB3, and SMARCAL1, they are suggested to catalyze fork reversal depending on the different conditions at the stalled replication fork. However, an interplay between these proteins has also been suggested, e.g. HLTF could facilitate PCNA polyubiquitination, leading to recruitment ZRANB3, which has a high affinity to polyubiquitinated PCNA (Vujanovic, Krietsch et al. 2017). Additionally, nucleases at the reversed fork could change the structure, conveying the 3´end of the leading strand close to the fork junction, forming a substrate for HLTF (Chavez, Greer et al. 2018). Several other proteins can reverse replication forks *in vitro*, among them are the RECQ helicases Werner syndrome ATP-dependent helicase (WRN) and BLM (reviewed in (Neelsen and Lopes 2015)), the HR protein RAD54 (Bugreev, Rossi et al. 2011) and FANCM, a member of the FA core complex (Gari, Decaillet et al. 2008). However, their function *in vivo* remains to be determined.

Fork reversal is a RAD51-regulated global response to replication-blocking impediments and can be activated independent of checkpoint activation. Thus, RAD51 is an important fork reversal protein and was shown to be required for fork reversal in response to several genotoxic agents (Zellweger, Dalcher et al. 2015). In addition, RAD51's function in the RAD51-BRCA2-axis is important for stabilizing reversed forks. Lately, another HR protein, RAD52, has been identified to protect the reversed arms of the chickenfoot structure by counteracting excessive SMARCAL1 and MRE11 activity (Malacaria, Pugliese et al. 2019).
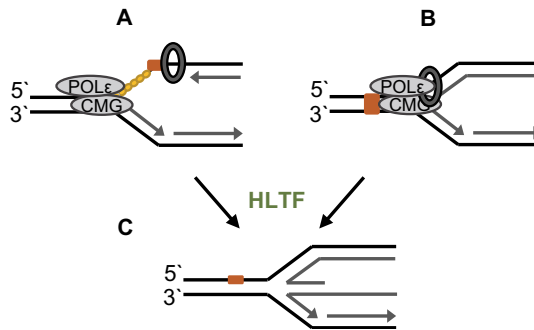
Figure 10. Chickenfoot structure formation / replication fork reversal. (A) Lesion on the leading strand that impedes DNA synthesis by the replicative polymerase (B) ICL that blocks both the replicative polymerase and the CMG helicase. (C) Chickenfoot structure / reversed replication fork, mediated for instance by HLTF.

Fork reversal causes accumulation of ssDNA, and the intra-S checkpoint, which is stimulated by RPA-coated ssDNA, is often activated at some point during replication fork reversal or TS (Liao, Ji et al. 2018). Defects in fork reversal proteins are linked to impaired replication fork slow down and associated with cancer or developmental defects (Friedrich, Lee et al. 2010, Ray Chaudhuri, Hashimoto et al. 2012, Santangelo, Gigante et al. 2014, de Voer, Hahn et al. 2015, Zellweger, Dalcher et al. 2015). EM studies suggest that 500-4,000 reversed forks may exist per cell after treatment with fork stalling agents; however, only some cells contained activated S-phase checkpoints (Zellweger, Dalcher et al. 2015).

1.6.3.2 Processing reversed replication forks

The reversed fork can be handled by at least four mechanisms including processing by nucleases, stabilization by RAD51, branch migration by RECQ1 and resection by WRN and DNA2 (illustrated in Figure 11).

1. Excessive nuclease cleavage of reversed replication forks (e.g. by the crossover junction endonuclease MUS81) can cause DSBs at the fork. These can be repaired by POLδ-dependent break-induced replication (BIR), thus rescuing the replication fork (Lemacon, Jackson et al. 2017). This HR-like mechanism is dependent on RAD51 and RAD52 (Davis and Symington 2004, Sotiriou, Kamileri et al. 2016, Malacaria, Pugliese et al. 2019). BIR can process a one-ended DSB that occurs during replication via several cycles of D-loop formation and reinvasion, followed by resolution or dissolution of the D-loop (Smith, Llorente et al. 2007). However, BIR is slow (4h), suggested to be highly error-prone and leading to loss of heterozygosity (Deem,

Keszthelyi et al. 2011). Therefore, BIR is suggested as a backup mechanism, if, for instance, replication fork restart by DNA2 (cleaves flaps and is involved in 5´end resection of DSBs) dependent resection, fails (Thangavel, Berti et al. 2015). The serine-protein kinase Ataxia Telangiectasia Mutated (ATM)/CHK2 checkpoint seems to be activated prior to BIR (Malkova, Naylor et al. 2005).

2. The reversed fork is stabilized by RAD51 filaments, which prevent nascent DNA degradation under prolonged replication stress (Schlacher, Christ et al. 2011, Zellweger, Dalcher et al. 2015). In the absence of RAD51 filaments, as observed in BRCA1/2-deficient cells, fork stability can be restored by deletion of fork reversal enzymes (Taglialatela, Alvarez et al. 2017).

3. Branch migration and replication fork restart by the RECQ1 DNA helicase, is a "TS by fork reversal" mechanism observed in human cells (Berti, Ray Chaudhuri et al. 2013). RECQ1 limits the activity of DNA2 and thereby prevents excessive strand degradation (Thangavel, Berti et al. 2015). Interestingly, RECQ1 interacts with PARP1, which in turn inhibits the helicase activity of RECQ1. PARP1 is therefore suggested as an early protein acting at stalled replication forks, causing replication fork slowdown, and thus allowing DNA lesions to be repaired prior to replication fork restoration and restart by RECQ1. PARP1 inhibition consequently does not result in replication fork slowdown, but in an increase in DSBs formation (Berti, Ray Chaudhuri et al. 2013).

4. Reversed forks can be processed by a DNA2- and WRN (a RECQ helicase with exonuclease activity)-depending mechanism. This includes resection of reversed replication forks and induction of "TS by fork reversal". Lately, the replication timing regulatory factor 1 (RIF1), was shown to be important for limiting DNA2- and WRN-dependent unscheduled resection of reversed replication forks and for preventing genome instability (Garzon, Ursich et al. 2019). Branch migration and restart of resected replication forks can be mediated by SMARCAL1, which preferentially interacts with a 3´ssDNA-tail coated with RPA (Betous, Couch et al. 2013). Replication fork restart by SMARCAL1 prevents MUS81-dependent DSB formation, indicating that branch migration is the first choice of replication fork restart after resection (Betous, Mason et al. 2012). In addition, *in vitro* it was shown that HLTF can form D-loops at stalled replication forks, independent of RAD51 (Burkovics, Sebesta et al. 2014). Further, in Rad5 overexpressing yeast cells, processing of the reversed replication fork in a HR-like mechanism by the HIRAN domain of Rad5 was recently shown. This was independent of

Rad5´s role in PCNA polyubiquitination (Bryant, Sunjevaric et al. 2019). D-loops can be dissolved for instance by BLM (a RECQ helicase with dissolvase functions) or converted into a Holliday junction, which can also be cleaved by MUS81, inducing BIR (Sidorova, Kehrli et al. 2013, Prado 2018). Thus, HR proteins are important for maintaining genome integrity in the presence of replication stress (reviewed in (Ait Saada, Lambert et al. 2018)).
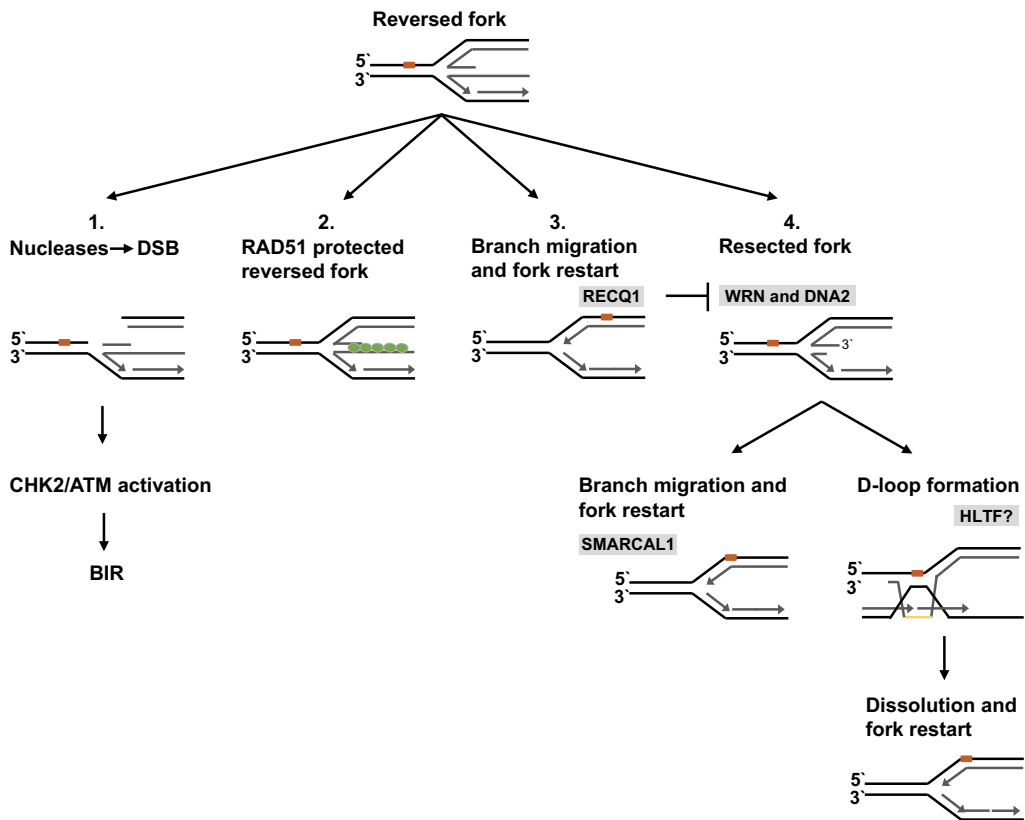
Figure 11. Models for processing reversed replication forks. 1. DSB formation by nucleases leading to checkpoint activation and repair by BIR. 2. Fork protection by RAD51 filaments. 3. Branch migration and restart by RECQ1. 4. Fork resection by WRN and DNA2 followed by branch migration and fork restart by SMARCAL1 or D-loop formation and fork restart.

In addition, HLTF, ZRANB3 and SMARCAL1 are all able to restore replication forks *in vitro* (Betous, Couch et al. 2013, Chavez, Greer et al. 2018); however, it seems that SMARCAL1 can restore both leading and lagging gapped forks, whereas HLTF and ZRANB3 prefer fork restoration of forks with lagging gapped forks (Chavez, Greer et al. 2018). These properties might be regulated by RPA bound to the reversed fork, because SMARCAL1 is stimulated by

RPA bound to the leading strand (Bhat, Betous et al. 2015), whereas HLTF and ZRANB3 are inhibited by RPA (Betous, Couch et al. 2013, Chavez, Greer et al. 2018). To summarize, the protective effects of the chickenfoot structure are mainly avoiding replication fork collapse and promoting fork restart (reviewed in (Liao, Ji et al. 2018)).

1.6.3.3 Template switch by homologous recombination in postreplicative gaps

In human cells, TS by HR in postreplicative gaps plays a minor role compared fork reversal, while it is a frequently occurring mechanism in yeast (Fumasoni, Zwicky et al. 2015).
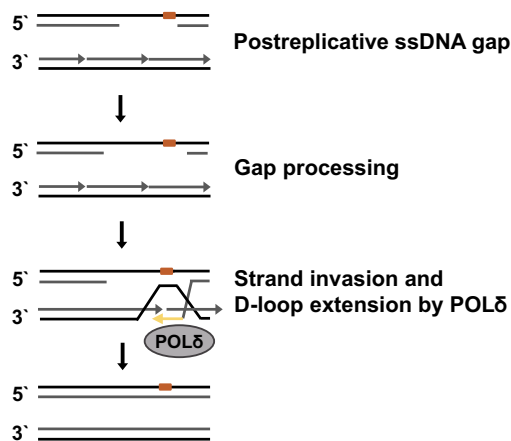

Figure 12. TS by HR in postreplicative gaps. The first step of strand invasion is mediated by Exo1 and Mre11 nucleases that enlarge the ssDNA gaps (reviewed in (Galanti and Pfander 2018)). Strand invasion requires several HR proteins, forming a D-loop, which is extended by POLδ. The sister-chromatid junction is dissolved into mainly non-crossover products (Giannattasio, Zwicky et al. 2014). Adapted from (Prado 2018).

Evidence of a HR-like mechanism, filling in postreplicative gaps in a DDT manner, therefore first came from yeast (Prakash 1981). The model of TS by HR, as illustrated in Figure 12, involves several HR proteins, resulting in D-loop formation. POLδ extends the D-loop by using the intact sister chromatid as template. POLε and TLS polymerases are believed to be dispensable for TS by HR (Vanoli, Fumasoni et al. 2010). In addition to TS by HR, another HR-like pathway, called the Salvage pathway, has been described for postreplicative gap-filling, possibly as a backup for TS by HR. So far, TS by HR has not been verified in human cells; however, it likely plays a minor role in human cells, because TLS seems to be the predominant mechanism for postreplicative gap-filling in human cells (see 1.6.2.1) (reviewed in (Prado 2018)).

1.7   ICL repair in S-phase

ICLs were first assumed to absolutely block the CMG helicase and DNA synthesis, because they covalently bind the two DNA strands. However, it has later been shown that DNA synthesis can resume past an ICL, leaving behind crosslinked parental strands (Huang, Liu et al. 2013). This mechanism is different from lesion bypass by TLS polymerases or repriming. Still, ICLs seem to be predominantly repaired during replication. Three models of ICL repair in S-phase have been suggested (reviewed in (Datta and Brosh 2019)), as illustrated in Figure 13.

1. A replication fork encountering an ICL can be rescued by a converging replication fork. One CMG helicase is removed from the DNA to allow replication of the leading strand until up to 1 nucleotide from the ICL. Activation of the FA pathway by monoubiquitination of the FANCI-FANCD2 complex leads to recruitment of endonucleases for incision and unhooking of the ICL. Endonucleases suggested to be able to facilitate this step are the Xeroderma Pigmentosum group F-complementing protein (XPF), MUS81 together with the crossover junction endonuclease EME1, the structure-specific endonuclease subunit SLX1, and the Fanconi-associated nuclease 1 (FAN1). Following a double incision causing a DSB in one of the sister chromatids, the unhooked ICL is bypassed by TLS polymerases. The DSB is then repaired by HR and the unhooked ICL is removed by NER. Furthermore, MMR protein complexes are involved in ICL recognition, unhooking and HR-mediated repair of the processed ICL-induced DSBs (reviewed in (Datta and Brosh 2019)).

2. The "Fork traverse" model was first described by Seidman and colleagues (Huang, Liu et al. 2013). In this model, the ICL is, like lesions after repriming by PrimPOL, left behind and repaired later. The FANCM/FANCM-associated histone fold protein 1 (MHF) complex promotes replication traverse over the ICL without unwinding, independent of FA core proteins, but with requirement of the BLM helicase (Ling, Huang et al. 2016). It is not quite clear how the replisome is re-established. This model seems to be the predominant pathway for handling ICLs during replication in human cells (Huang, Liu et al. 2013). The ICL could then be processed postreplicatively, probably through incision by nucleases, bypass by TLS polymerases and involvement of HR and NER. However, the exact steps are not known.

3. ICL repair after fork reversal by one of the converging replication forks. After CMG helicase unloading, the replication fork which has not been reversed, is incised by endonucleases. The ICL is unhooked and processed as described in 1. (reviewed in (Datta and Brosh 2019)).
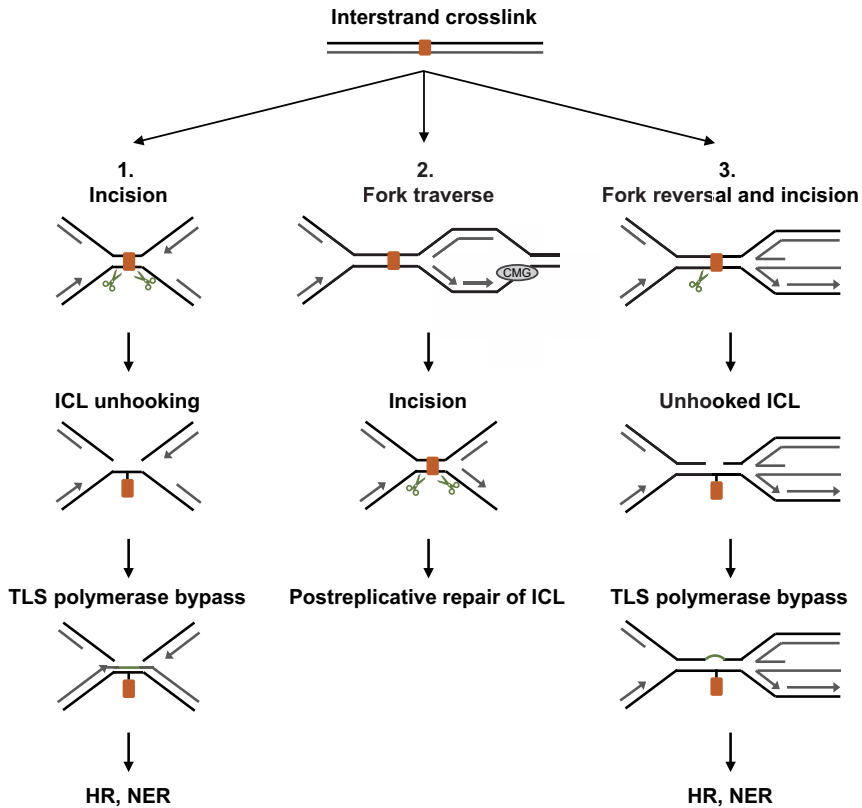
Figure 13. ICL repair during replication. 1. A replication fork encountering an ICL can be rescued by a converging replication fork. 2. The "Replication traverse" model. 3. ICL repair after fork reversal of one of the converging replication forks (reviewed in (Datta and Brosh 2019)).

Multiple proteins must be coordinated in order to handle an ICL during replication. All three models include formation of a DSB, which is repaired by HR (Niedernhofer, Odijk et al. 2004, Hanada, Budzowska et al. 2006). In addition to HR proteins, FA and NER proteins are important for ICL repair. This is illustrated by hypersensitivity to ICLs in cells from FA patients with a mutation in one of the 19 FA genes (reviewed in (Datta and Brosh 2019)) and by the hypersensitivity of NER and HR mutants in yeast (reviewed in (Hashimoto, Anai et al. 2016)). TLS polymerases that are able to bypass ICLs are POLκ, POLη, POLν, POLι, POLζ and REV1

(Roy and Scharer 2016), with REV1, POLζ and POLη being the most important ones (Shen, Jun et al. 2006, Zhao, Biertumpfel et al. 2012). PCNA is monoubiquitinated in the presence of ICLs both in S- and G1-phase, and PCNA monoubiquitination, but not polyubiquitination, is required for ICL repair (McHugh and Sarkar 2006, Inoue, Kikuchi et al. 2014). HLTF and the fork protecting protein FANCJ seem to regulate each other's activity. HLTF depletion increases sensitivity towards MMC in FANCJ ko cells. Thus, HLTF may play a role in replication-coupled ICL repair (Peng, Cong et al. 2018). Our data presented in Paper 3 indicate that both the RAD5 homologs play a role in ICL repair.

2   Aims of the study

DDT is important for gene stability as well as chemotherapy resistance. Therefore, DDT might be a possible drug target for cancer treatment. Our group has developed an APIM-containing cell penetrating peptide (APIM-peptide) which blocks the APIM-protein binding-site on PCNA. In presence of cellular stress, APIM-proteins have a higher affinity to PCNA than PIP-box proteins and APIM proteins are therefore more affected by these peptides. The APIM-peptide is currently under development for use in cancer therapy. The functionality of APIM motifs and the way these proteins are involved in the management of replication stress, are important for understanding the mode of action of the APIM-peptide.

We therefore aimed to gain further insight into the functionality of three APIM containing proteins (REV3L, HLTF and SHPRH) in DDT and to further verify the general role of HLTF and SHPRH in DDT.

1. REV3L is the catalytic subunit of POLζ. The aim of Paper 1 was to examine if APIM in REV3L is a functional motif and if it is important for POLζ´s role in TLS. We also wanted to examine the impact of inhibiting APIM-protein - PCNA interactions on mutagenesis.
2. The human RAD5 homologs HLTF and SHPRH both contain APIM. In Paper 2 we aimed to investigate the functionality and importance of APIM in these two proteins in DDT.
3. The aim of Paper 3 was to further clarify the role of HLTF and SHPRH in response to different replication fork stalling agents and how HLTF and SHPRH contribute to DDT regulation.

3 Summary of papers

Paper 1: International Journal of Molecular Sciences 2018, Int J Mol Sci 20(1)

APIM-mediated REV3L-PCNA interaction important for error free TLS over UV-induced DNA lesions in human cells

DDT pathways help cells to cope with replication stress and are particularly important for the survival of cancer cells. The catalytic subunit of POLζ, REV3L contains a potential PCNA-interacting motif (APIM), and we investigated the importance of direct binding of REV3L to PCNA during TLS.

By using confocal microscopy, we found an enhanced nuclear fraction of overexpressed REV3L after MMC or Leptomycin B treatment, indicating that REV3L levels in the nucleus are actively and tightly regulated. When we co-overexpressed REV3L and a REV3L-APIM-mutant (F1241A) together with PCNA, both full-length proteins colocalized with PCNA in replication foci. However, overexpressed APIM-peptides, containing a mutation in APIM (K**A**VLK), did not colocalize with PCNA, while the wildtype APIM-peptide did. Furthermore, overexpressed APIM-peptides decreased full-length REV3L colocalization with PCNA. The decrease was more pronounced for REV3L-F1241A than for wildtype full-length REV3L. This suggests that the mutation of APIM reduces the affinity of REV3L to PCNA and that APIM in REV3L is a functional PCNA binding motif.

Mutagenesis assays performed in cells overexpressing REV3L indicated a reduction in mutation frequency and a shift in the mutation spectra of UV-irradiated reporter plasmids compared to REV3L F1241A overexpression. This indicates that APIM in REV3L is important for error-free POLζ functions in bypassing UV-lesions.

A cell penetrating APIM-peptide, previously shown to inhibit the interaction of APIM-proteins to PCNA, decreased the UV-induced mutation frequency in several human cell lines. However, APIM-peptide treatment had a smaller impact on the mutation frequency in a cell line carrying a one amino acid deletion upstream of APIM (ΔA1237). These results suggest that the effect of APIM-peptide treatment was at least partly due to inhibition of POLζ-mediated TLS.

In total, our study shows that APIM in REV3L is a functional PCNA-interacting motif and that POLζ´s role in TLS over UV-lesions can be inhibited by APIM-peptides targeting PCNA.

Paper 2: Manuscript submitted

Roles of HLTF and SHPRH in DNA damage tolerance depend on direct interactions with PCNA

In order prevent genome instability under replicative stress, cells have evolved DDT mechanisms which are at least partly regulated by mono- and polyubiquitination of PCNA. HLTF and SHPRH are homologs of yeast Rad5, known to ubiquitinate PCNA, and likely to be involved in both TLS and TS. HLTF, in addition, is involved in fork reversal. Both proteins contain APIM, and here we investigated the functionality of APIM in HLTF and SHPRH.

Wildtype and APIM-mutant versions of HLTF and SHPRH full-length proteins colocalized with PCNA in foci resembling replication foci when co-expressed with PCNA. However, overexpression of APIM-peptides, containing the APIM sequence found in HLTF and SHPRH, resulted in colocalization with overexpressed PCNA, while overexpression of the corresponding APIM-mutant (F to A)-peptides did not. In addition, we found a larger fraction of the APIM-mutant versions of the full-length proteins (HLTF F960A, SHPRH F1632A) in the cytosol, compared to wildtype proteins. This suggests that both RAD5 proteins contain a functional APIM.

Furthermore, foci intensity in the presence of APIM-peptide overexpression was more reduced for HLTF F960A-YFP than for HLTF-YFP, suggesting that APIM in HLTF is important to remain in foci. The increased nuclear abundancy of HLTF after Leptomycin B (nuclear export blocker) treatment suggests an actively regulated nuclear HLTF level.

In addition to the observed elevated levels of overexpressed SHPRH F1632A-YFP in cytosol, treatment of SHPRH-overexpressing cells with an APIM-peptide increased cytosolic SHPRH levels. These results suggest that APIM in SHPRH is important for the nuclear localization of SHPRH. Pulldown-experiments illustrate the importance of APIM in both proteins for their direct interaction with PCNA, because intact APIM in both HLTF and SHPRH was required for maximal pulldown of PCNA in presence of DNA damage.

Plasmid-based mutagenesis assays showed an increased mutation frequency after HLTF F960A overexpression compared to overexpressed wildtype protein, suggesting that the direct interaction between HLTF and PCNA is important for error-free bypass/repair. SHPRH overexpression increased the mutation frequency, whereas SHPRH F1632A did not, suggesting that TLS is stimulated by SHPRH in an APIM-dependent manner. Both RAD5 proteins reduced

the fraction of mutations on the transcribed strand compared to the non-transcribed strand, and we observed differences in the mutation spectra after overexpressing wildtype proteins compared to the APIM-mutant versions of the proteins.

This study shows that APIM in HLTF is important for error-free bypass of UV-lesions and APIM in SHPRH is important for nuclear localization and/or stability of SHPRH. In total, we suggest that APIM in both, HLTF and SHPRH, is a functional PCNA-interacting motif.

Paper 3: Manuscript

The human RAD5 homologs, HLTF and SHPRH, have distinct functions in DNA damage tolerance dependent on the DNA lesion type

HLTF and SHPRH are both involved in DDT; however, little is known about their cooperation in response to replication stress. In this study we investigated the consequences of knocking out these two RAD5 homologs in presence of different DNA lesions.

After exposure of human HLTF knockout (ko), SHPRH ko, and HLTF/SHPRH double knockout (dko) cells to MMC, cisplatin, MMS or UV, the cell lines had different sensitivities to the different drugs. HLTF/SHPRH dko cells were less sensitive than the control cells and the single ko cells in response to UV, cisplatin and MMS. Thus, cells lacking both RAD5 homologs seem to exhibit increased DNA repair and/or lesion bypass mechanisms in response to intrastrand crosslinks, monoadducts, alkylated bases and CPDs. However, in response to MMC, a drug that induces more ICLs, all ko cells were more sensitive than the control cells, but the dko cells were least sensitive. This indicates an importance of both RAD5 homologs for repair of ICLs during replication.

Mutagenesis assays were conducted by using UV- or MMS-damaged SupF reporter plasmids. In the HLTF/SHPRH dko cells we measured a reduced mutation frequency over UV-lesions, but no change in mutation frequency over MMS-lesions compared to control cells. In addition, the mutation spectra in plasmids from dko cells differed from the single ko cell lines in response to both UV and MMS. This suggests an interconnection of HLTF and SHPRH and reveals alterations in DDT when both HLTF and SHPRH are deficient, compared to single ko.

While SHPRH ko did not significantly affect the mutation frequency, the absence of HLTF increased the mutation frequency after both UV- and MMS-induced DNA lesions. This indicates an involvement of HLTF in error-free bypass or repair of UV- and MMS-lesions. Furthermore, we observed a higher fraction of HLTF ko cells in S-phase 24 h after MMS treatment, indicating that HLTF affects cell cycle progression.

Interestingly, we could not detect a change in mutation frequency after MMS-induced DNA damage in cells lacking SHPRH, even though these cells grew faster after MMS treatment in viability assays. This phenotype could possibly be explained by the observed reduced phosphorylation of CHK2, MCM2 S139, which can modulate the cell cycle checkpoint and origin firing. In addition, we found increased levels of deletions in the isolated plasmids from

dko cells and reduced levels of γH2AX in SHPRH ko and HLTF/SHPRH dko cells upon MMS treatment.

Our study suggests that the RAD5 homologs HLTF and SHPRH exhibit distinctive functions in DDT, but also reveal a mutual functional dependency, dependent on the type of DNA lesion.

4 Discussion

4.1 DDT contributing to drug resistance

Development of resistance to chemotherapeutic drugs is a challenge in cancer therapy. Cisplatin is one of the most effective anticancer drugs used in treatment of a variety of solid tumors. However, resistance development is a major limitation for the use of this drug in the clinic today. Several mechanisms can contribute to cisplatin resistance, including decrease in drug uptake, increase in drug efflux, detoxification and tolerance of cisplatin-induced DNA lesions. In the case of drug resistance by increased tolerance of DNA lesions, TLS polymerases are suggested to play a major role. POLη is upregulated upon cisplatin treatment and shown to be important for progression of the replication fork and POLζ upregulation is associated with cisplatin resistance in cervical cancer (reviewed in (Rocha, Silva et al. 2018). TLS polymerases contribute directly to the emergence of therapeutic resistance by promoting resistance-causing mutations (Xie, Doles et al. 2010). REV3L has been suggested as a promising drug target, because REV3L downregulation could sensitize tumors that were intrinsically resistant to cisplatin in a xenograft mouse model of non-small cell lung cancer (Doles, Oliver et al. 2010). In addition, REV3L depletion could generally suppress cancer cell growth (Doles, Oliver et al. 2010, Knobel, Kotov et al. 2011) and sensitize cervical cancers to cisplatin (Yang, Shi et al. 2015).

Targeting DDT via PCNA

PCNA, a central protein also in DDT, can be targeted by APIM-peptides (Gilljam, Feyzi et al. 2009, Ciccia, Nimonkar et al. 2012, Gilljam, Muller et al. 2012, Bacquin, Pouvelle et al. 2013, Fattah, Hara et al. 2014, Olaisen, Muller et al. 2015, Raeder, Nepal et al. 2018), reducing the interaction of APIM containing proteins with PCNA. Since APIM is found in more than 300 proteins (https://tare.medisin.ntnu.no/pcna/index.php), the APIM-peptide has a potential impact on multiple pathways. Until now functional APIM proteins have been verified in seven proteins involved in DDT: i) REV3L, the catalytic domain of POLζ (Paper 1), ii and iii) the two human RAD5 homologs, HLTF and SHPRH, involved in TLS, fork reversal and TS (Paper 2), iv) the transcription factor TFII-I required for TLS (Fattah, Hara et al. 2014), v) ZRANB3

involved in restart and reversal of the replication fork (Ciccia, Nimonkar et al. 2012), vi) RAD51B involved in RAD51 foci formation (Date, Katsura et al. 2006, Gilljam, Feyzi et al. 2009), and vii) FBH1 involved in both HR and DDT (Bacquin, Pouvelle et al. 2013). In addition, FANCC, a member of the FA core complex required for the recruitment of REV1 to damage sites, also contains APIM, but this APIM sequence has not yet been verified to be a functional motif (Gilljam, Feyzi et al. 2009). The APIM-peptide can therefore potentially impair each of the above-mentioned proteins in DDT and thereby be a tool to combat mutagenesis and drug resistance.

It has been shown that APIM peptides increase the efficacy of cisplatin in cisplatin resistant bladder cancer cells (Sogaard, Blindheim et al. 2018). In Paper 1 we showed that APIM-peptide treatment in HEK293 cells reduces the mutation frequency by ~70 %, while the mutation frequency in the isogenic REV3L deficient cell line (ΔA1237) was only reduced by 30 %. This suggests that mutagenesis by POLζ can be inhibited by the APIM-peptide, but that other DDT proteins also contribute to this effect. In Paper 2 we found that APIM-peptide treatment triggered nuclear export of SHPRH, suggesting an impact on the general functionality of SHPRH if its direct binding to PCNA is impaired. Altogether, these results suggest that the APIM-peptide can affect DDT and drug sensitivity via inhibition of multiple DDT proteins.

Fork reversal is a main mechanism for handling DNA lesions induced by chemotherapy. Reversed forks can be degraded by nucleases, but this can be prevented by BRCA2-dependent RAD51 filaments bound to ssDNA at reversed replication forks. In BRCA2-deficient cells insufficient replication fork protection therefore causes degradation of reversed forks by nucleases and causes hypersensitivity to replication-stalling agents (reviewed in (Liao, Ji et al. 2018)). However, silencing of fork reversal mediators like HLTF, SMARCAL1 and ZRANB3, two of which contain APIM, in BRCA2-deficient cells increases fork protection and decreases genomic instability (reviewed in (Bhat and Cortez 2018)). Thus, awareness of persistent mutations in cancer cells is vital when combining drugs, for instance drugs causing replication fork stalling. Thus, the APIM-peptide in combination with replication stalling agents might not be ideal in BRAC1/2 deficient cells, because the APIM-peptide possibly reduces fork reversal.

Stress-related function of PCNA and affinity differences of PCNA interacting motifs

APIM- and PIP-box motifs bind to the same hydrophobic pocket on PCNA (Muller, Misund et al. 2013, Sebesta, Cooper et al. 2017). However, overexpression of the APIM-peptide in HeLa and U2OS cells does not affect proliferation (Gilljam, Feyzi et al. 2009), while overexpression of the PIP-box-peptide inhibits proliferation in the same cells (Warbrick 2006). Additionally, binding of APIM to PCNA seems to be regulated by PTMs on PCNA, as illustrated by experiments pulling down a sub-fraction of PCNA when using an APIM-peptide fused to YFP as bait (Gilljam, Feyzi et al. 2009). PCNA is known to be modified upon cellular stress (Choe and Moldovan 2017, Kanao and Masutani 2017) and most APIM-containing proteins are stress-related proteins, suggesting a special role of APIM-PCNA interactions during cellular stress (Gilljam, Feyzi et al. 2009, Muller, Misund et al. 2013, Gederaas, Sogaard et al. 2014, Sogaard, Blindheim et al. 2018, Sogaard, Moestue et al. 2018, Sogaard, Nepal et al. 2019).

The PIP-box **Q**TS**M**TD**FY** in p21^{Cip1} (also known as CDK-interacting protein 1) is the PIP-box with highest affinity to PCNA (Warbrick 1998, Slade 2018). The interaction site on PCNA for the PIP-box in ZRANB3 (**Q**$_1$HD**I**$_4$RS**F**$_7$**F**$_8$) can be divided into the "Q-pocket" and the "Socket". The Q-pocket binds the Q-residue at position 1. The "Socket" binds the hydrophobic residue at position 4 and the aromatic residues at position 7 and 8 of the PIP-box (Hishiki, Hashimoto et al. 2009). See Figure 14 for alignment of PIP-box and APIM amino acids sequences. Crystallization of PCNA together with a peptide containing the APIM in ZRANB3 (RFLVK) illustrates the importance of F, L and K of APIM for binding to PCNA. Interestingly, in addition to APIM in ZRANB3, two residues upstream of APIM (S and I in **S**D**I**T-R**FL**V**K**) are also involved in binding to PCNA. The S-residue binds to the Q-pocket and the amino acids FLK bind to the Socket, similar to Q and IFF of the PIP-box (Hara, Uchida et al. 2018). Interactions with the Q-pocket are often absent or reduced in non-canonical PIP-boxes, where Q in position 1 is replaced by another amino acid. This likely explains some of the lower affinities that have been observed for TLS polymerases containing non-canonical PIP-boxes compared to replicative polymerases with a canonical PIP-box (Hishiki, Hashimoto et al. 2009). In line with this, the Q-pocket interaction of APIM in ZRANB3 is less important for the binding to PCNA than the Socket (Hara, Uchida et al. 2018); however, upstream amino acids in APIM could influence the affinity to PCNA, similar to what has been observed for amino acids downstream of the APIM sequences (Prestel et al, 2019, Fu et al, 2015).

The one amino acid deletion upstream of APIM in REV3L, as in the REV3L ΔA1237 deletion cell line (Paper 1), resulted in reduced nuclear localization when overexpressed as a YFP fusion protein. In addition, we observed clear changes in the mutation spectra in this cell line. Interestingly, this deletion causes a switch of the amino acid that potentially binds to the Q-pocked (from G to S) (Figure 14). This amino acid switch could be responsible for a lower affinity to PCNA, and thereby lead to the observed lower abundance of REV3L ΔA1237 in the nucleus. Reduced affinities for PCNA followed by reduced nuclear levels were also observed for HLTF and SHPRH when the second amino acid of APIM was mutated to A (Paper 2).

Q-pocket   **Socket**

P21 PIP-box	**Q**	T	S	**M**	T	D	**F**	**Y**		
ZRANB3 PIP-box	Q	H	D	I	R	S	F	F		
ZRANB3 APIM	S		D	I	T	R	**F**	**L**	V	**K**
REV3L APIM	G		A	E	V	K	F	V	L	K
REV3L ΔA1237 APIM	S		G	E	V	K	F	V	L	K
HLTF APIM	V		I	I	T	K	F	I	V	K
SHPRH APIM	T		I	V	H	R	F	L	I	K
APIM-peptide				M	D	R	W	L	V	K

☐ PIP-box
☐ APIM
☐ Amino acid shift

Figure 14. Q-pocket and Socket of different PIP-box and APIM sequences. Amino acid sequences of several PIP-box or APIM containing proteins in the Q-pocket and the Socket are aligned. In addition, the APIM sequence of the cell penetrating peptide (APIM-peptide) (Muller et al, 2013) is depicted. PIP box is depicted in green, APIM in blue. The amino acid shift in the Q-pocket after A1247 deletion in REV3L is depicted in yellow.

Involvement of HLTF and SHPRH in multiple repair pathways

HLTF/SHPRH dko cells were less sensitive to cisplatin, MMS and UV compared to the control cells. Lack of SHPRH seem to cause a reduced sensitivity to MMS, but we did not detect increased TLS in these cells. MMS is an agent causing several DNA lesions that are mainly repaired by BER (reviewed in (Wyatt and Pittman 2006)). Because SHPRH ko cells grew unperturbed after MMS exposure, our results could indicate an involvement of SHPRH in modulation of BER. Excessive levels of BER intermediates, i.e. strand breaks, can potentially be toxic and/or mutagenic. Furthermore, the results indicate that, in absence of SHPRH, MMS lesions are processed efficiently in a way that does not increase mutations on the reporter

plasmid or in the levels of chromosomal DNA breaks, apoptosis or cell cycle arrest, compared to single HLTF ko cells. However, we detected less CHK2 phosphorylation in both cell lines lacking SHPRH (Paper 3). This led to the hypothesis that the absence of SHPRH might increase origin firing via reducing CHK2 phosphorylation. A role of yeast Rad53 (CHK2 in human) in inhibition of origin firing has been suggested previously (Cordon-Preciado, Ufano et al. 2006, Lopes, Foiani et al. 2006, Zegerman and Diffley 2010). One study associated reduced levels of DNA breaks with an increase in origin firing in a P53 ko cell line (Benedict, van Harn et al. 2018). We detected reduced levels of γH2AX in the SHPRH single and double ko cell lines; however, we repeatedly gained a reduced yield of replicated plasmids from SupF assays in the HLTF/SHPRH dko cells. Furthermore, increases in deletions (1 bp, and >20 bp) were detected in plasmids isolated from the SHPRH ko and HLTF/SHPRH dko cells, respectively. This could be an indication of increased levels of collapsed replication forks, strand breaks or repair by BIR/HR or Non-Homologous End Joining (NHEJ) in these cells. However, the observed differences in the reporter plasmids might not directly reflect the changes in the chromosome in these cell lines when treated with UV or MMS. Still, our results suggest that a lack of SHPRH strongly modulates repair/tolerance pathways.

In addition, 3meC lesions are generally more abundant in ssDNA (10 %), e.g. during replication, than in dsDNA (<1%) (Drablos, Feyzi et al. 2004). Since we damaged the plasmids prior to transfection, these plasmids were damaged as dsDNA. In contrast, in the viability assays, replicating cells (contain more ssDNA) were treated with MMS. Thus, the fraction of dsDNA and ssDNA is likely different in plasmids compared to genomic DNA. We therefore expect that the MMS damaged SupF plasmids probably carry a slightly different MMS lesion spectrum than genomic DNA in MMS treated cells. Further, the mutation frequency in the reporter plasmids might not reflect the mutation frequency in the genomic DNA. 3meC lesions can be repaired by hABH2 (Aas, Otterlei et al. 2003, Falnes, Bjoras et al. 2004) or bypassed by TLS polymerases (Furrer and van Loon 2014), and, as discussed in Paper 3, HLTF may influence repair of bypass of 3meC.

HLTF and/or SHPRH may affect multiple replication-associated repair mechanisms in addition to BER, including NER, direct repair by ABH2 and MMR. Modulation of any of these could explain some of the sensitivity and mutation pattern phenotypes observed in the different ko cells. However, this remains to be examined.

HLTF^{-/-} mouse cells downregulate the transcriptional activity of RAD52, leading to a G2/M arrest and apoptosis upon replication stress. The reduced RAD52 level represses the canonical HR activity and genomic stability (Helmer, Foreman et al. 2013). RAD52 deficiency is also reported to increase nascent strand degradation and excessive fork reversal (Malacaria, Pugliese et al. 2019). We could not detect G2/M arrest in the HLTF ko cells after MMS treatment; however, these cells had a slower proliferation rate and were more sensitive to cisplatin, UV and MMS induced DNA damage than parental cells, SHPRH ko and dko cells (Paper 3). We observed an increased mutation frequency in HLTF ko cells after both UV- and MMS-induced DNA lesions (Paper 3). This increased mutation frequency could be caused by both, RAD52 downregulation in the HLTF ko cells and lack of stimulation of TLS.

4.2   HLTF and SHPRH are multi-domain proteins

HLTF and SHPRH are multi-domain proteins and thus multiple, also unknown functions of HTLF or SHPRH could contribute to the observed phenotypes. For example, the ubiquitin ligase activity of SHPRH could regulate degradation of different types of proteins, including proteins involved in inhibition of origin firing and/or proteins activating checkpoints, leading to increased origin firing and reduced checkpoint activations in SHPRH ko cells. HLTF also contains a ubiquitin ligase activity that could affect multiple pathways, and, in addition, HLTF is a known transcription factor. Recently, ubiquitin signaling pathways have been shown to be involved in the regulation of origin firing (Coulombe, Nassar et al. 2019).

HLTF activity and stability is increased by interaction with the ubiquitin carboxyl-terminal hydrolase 7 (USP7). USP7 deubiquitinates HLTF and increases the half-life of HLTF in the presence of replication stress (Qing, Han et al. 2011). SHPRH, could potentially also be involved in regulating the stability of HLTF, or visa versa. This could explain the inter-dependent functions of HLTF and SHPRH observed in Paper 3, and, possibly the changes in mutation frequency after overexpression of either of these proteins (Paper 2).

4.3   Limitations of methods

Our results obtained from the plasmid based SupF assay cannot directly be compared with DDT mechanisms during replication of chromosomal DNA. For example, replication forks constitute large complexes of proteins, including chromatin remodeling proteins dynamically interacting with each other. How and when TLS polymerases interact with each other, with PCNA, or other proteins at the replication fork is still not exactly resolved, but the proximity to DNA is important for their function in DDT. The relative abundance of different proteins in these complexes are probably closely regulated, because overexpression of one of the TLS proteins affects DTT, as seen in Paper 1 and Paper 2. Such an imbalance of proteins at the replication fork might not be identical during replication of plasmid and chromosomal DNA. We observed less mutations in cells overexpressing REV3L than in the control cells (Paper 1). Still, APIM-peptide treatment reduced mutation frequency in wildtype cells by 70 % and only 30 % in the REV3L impaired cell line (REV3L Δ A1237), indicating that REV3L is inhibited by the APIM-peptide. Overexpression of REV3L might dysregulate the complex formation of REV7, REV1 and PCNA (Martin and Wood 2019), possibly followed by a dysregulation of POLζ as an inserter or extender polymerase. In contrast, APIM-peptide treatment in our study targets endogenous POLζ levels.

In support of closely regulated nuclear levels of TLS proteins, we showed that the nuclear levels of REV3L (Paper 1) and HLTF (Paper 2) are regulated by nuclear export. PCNA interactions are likely important for this regulation as the APIM-mutant versions of all these proteins were more cytosolic. In addition, the fraction of SHPRH in the cytosol was increased after treatment with the APIM-peptide (Paper 2). HLTF is found to be both overexpressed and reduced in cancer. Overexpression of Rad5 in *Saccharomyces cerevisiae* results in cisplatin sensitivity and increased aberrant TS by HR, illustrated by the formation of crossover products independent of upstream DDT proteins (Bryant, Sunjevaric et al. 2019). In line with this, both TLS polymerase deficiency and overexpression of TLS polymerases are linked to several cancer types and associated with TLS dysregulation (Yang, Gao et al. 2018). Our results illustrate the importance of balanced DDT protein levels at the replication fork.

Our experiments are less informative regarding TS by HR, because plasmid-based assays seem to cause extensive replication fork uncoupling in presence of replication stress, and HR requires

both parental strands in the proximity of the replication fork (Pages, Mazon et al. 2012). Thus, our results likely underscore the occurrence of TS by HR or TS by fork reversal and in consequence the involvement of REV3L, HLTF and/or SHPRH in these DDT mechanisms. Nevertheless, the SupF assay is useful to analyze the range of mutations induced by a certain DNA damaging agent and to gain insights into the contribution of certain proteins in inducing mutations compared to an intern control.

4.4   Suggestions for further experiments

To investigate the hypothesis of increased origin firing in SHPRH ko cells, MMS sensitivity assays could be performed after knockdown (e.g. siRNA) of MCM2/MCM4. These proteins are important for origin licensing. It has been shown that a 50 % reduction of MCM2, MCM3 or MCM5 proteins is sufficient to allow normal origin firing but inhibits dormant origin firing upon replicative stress (Ge, Jackson et al. 2007, Ibarra, Schwob et al. 2008). Therefore, it could be tested if the sensitivity to MMS increases upon MCM2/MCM4 reduction.

In addition, we could examine the expression of proteins involved in origin licensing/firing in the HLTF ko, SHPRH ko and HLTF/SHPRH dko cell lines, e.g. CDC45 or DBF4. CDC45 is rate limiting for the firing of replication origins, and, in yeast, DBF4 phosphorylation is shown to be mediated by Rad53 (CHK2 homolog), resulting in inhibition of origin firing (Zegerman and Diffley 2010).

To investigate if a lack of PrimPOL activity is responsible for the increase in mutations in plasmids from HLTF ko cells, the amount of ssDNA stretches in the ko cell lines could be examined by performing a modified fiber analysis protocol (Quinet, Carvajal-Maldonado et al. 2017). This would give insight into ssDNA gap-formation/PrimPOL-induction in these cells.

To test if HLTF is involved in direct repair by ABH2, the level of 3meC could be measured by mass spectrometry in MMS treated HLTF ko, ABH2 ko and HLTF/ABH2 dko cells (Rosic, Amouroux et al. 2018).

The mutation frequency in MMC damaged plasmids compared to cisplatin damaged plasmids could be investigated to get insight into the contribution of HLTF and SHPRH in ICL repair compared to repair of interstrand and monoadducts in presence of replication.

Finally, we could examine if our results can be verified in one additional cell line, e.g. by knocking out HLTF and/or SHPRH in the diploid cell line HEK293.

5 Conclusion

This work gives insight into the importance of the three DDT proteins REV3L, HLTF and SHPRH and the functionality of their APIM sequences. The overall results of the three papers show important functions of all three proteins in handling DNA lesions during replication and indicate that their affinity to PCNA via APIM is important for the function of these proteins in DDT. HLTF and SHPRH possessed distinct functions in DDT, HLTF contributes to error-free DDT in response to UV and MMS, and SHPRH is possibly involved in cell cycle control and dormant origin firing. However, the two proteins also seem to be interconnected, as HLTF/SHPRH dko cells exhibited a reduced sensitivity to cisplatin-induced replication stress and strongly reduced the mutation frequency in presence of UV-lesions, compared to both single ko cell lines. The exact roles of HLTF and SHPRH in DDT in presence of different DNA lesions require further investigation. In total this work identified three drug targets that can likely be inhibited by APIM-peptides. These results are important for understanding the mode of action of the APIM-peptide, which is currently in clinical phase I.

References

Aas, P. A., M. Otterlei, P. O. Falnes, C. B. Vagbo, F. Skorpen, M. Akbari, O. Sundheim, M. Bjoras, G. Slupphaug, E. Seeberg and H. E. Krokan (2003). "Human and bacterial oxidative demethylases repair alkylation damage in both RNA and DNA." Nature **421**(6925): 859-863.

Achar, Y. J., D. Balogh and L. Haracska (2011). "Coordinated protein and DNA remodeling by human HLTF on stalled replication fork." Proc Natl Acad Sci U S A **108**(34): 14073-14078.

Achar, Y. J., D. Balogh, D. Neculai, S. Juhasz, M. Morocz, H. Gali, S. Dhe-Paganon, C. Venclovas and L. Haracska (2015). "Human HLTF mediates postreplication repair by its HIRAN domain-dependent replication fork remodelling." Nucleic Acids Res **43**(21): 10277-10291.

Acharya, N., R. E. Johnson, S. Prakash and L. Prakash (2006). "Complex formation with Rev1 enhances the proficiency of Saccharomyces cerevisiae DNA polymerase zeta for mismatch extension and for extension opposite from DNA lesions." Mol Cell Biol **26**(24): 9555-9563.

Ait Saada, A., S. A. E. Lambert and A. M. Carr (2018). "Preserving replication fork integrity and competence via the homologous recombination pathway." DNA Repair (Amst) **71**: 135-147.

Alver, R. C., G. S. Chadha and J. J. Blow (2014). "The contribution of dormant origins to genome stability: from cell biology to human genetics." DNA Repair (Amst) **19**: 182-189.

Bacquin, A., C. Pouvelle, N. Siaud, M. Perderiset, S. Salome-Desnoulez, C. Tellier-Lebegue, B. Lopez, J. B. Charbonnier and P. L. Kannouche (2013). "The helicase FBH1 is tightly regulated by PCNA via CRL4(Cdt2)-mediated proteolysis in human cells." Nucleic Acids Res **41**(13): 6501-6513.

Bailey, L. J., J. Bianchi and A. J. Doherty (2019). "PrimPol is required for the maintenance of efficient nuclear and mitochondrial DNA replication in human cells." Nucleic Acids Res **47**(8): 4026-4038.

Ball, H. L., J. S. Myers and D. Cortez (2005). "ATRIP binding to replication protein A-single-stranded DNA promotes ATR-ATRIP localization but is dispensable for Chk1 phosphorylation." Mol Biol Cell **16**(5): 2372-2381.

Baranovskiy, A. G., N. D. Babayeva, V. G. Liston, I. B. Rogozin, E. V. Koonin, Y. I. Pavlov, D. G. Vassylyev and T. H. Tahirov (2008). "X-ray structure of the complex of regulatory subunits of human DNA polymerase delta." Cell Cycle **7**(19): 3026-3036.

Baranovskiy, A. G., A. G. Lada, H. M. Siebler, Y. Zhang, Y. I. Pavlov and T. H. Tahirov (2012). "DNA polymerase delta and zeta switch by sharing accessory subunits of DNA polymerase delta." J Biol Chem **287**(21): 17281-17287.

Benedict, B., T. van Harn, M. Dekker, S. Hermsen, A. Kucukosmanoglu, W. Pieters, E. Delzenne-Goette, J. C. Dorsman, E. Petermann, F. Foijer and H. Te Riele (2018). "Loss

of p53 suppresses replication-stress-induced DNA breakage in G1/S checkpoint deficient cells." Elife **7**.

Berti, M., A. Ray Chaudhuri, S. Thangavel, S. Gomathinayagam, S. Kenig, M. Vujanovic, F. Odreman, T. Glatter, S. Graziano, R. Mendoza-Maldonado, F. Marino, B. Lucic, V. Biasin, M. Gstaiger, R. Aebersold, J. M. Sidorova, R. J. Monnat, Jr., M. Lopes and A. Vindigni (2013). "Human RECQ1 promotes restart of replication forks reversed by DNA topoisomerase I inhibition." Nat Struct Mol Biol **20**(3): 347-354.

Bertoletti, F., V. Cea, C. C. Liang, T. Lanati, A. Maffia, M. D. M. Avarello, L. Cipolla, A. R. Lehmann, M. A. Cohn and S. Sabbioneda (2017). "Phosphorylation regulates human poleta stability and damage bypass throughout the cell cycle." Nucleic Acids Res **45**(16): 9441-9454.

Betous, R., F. B. Couch, A. C. Mason, B. F. Eichman, M. Manosas and D. Cortez (2013). "Substrate-selective repair and restart of replication forks by DNA translocases." Cell Rep **3**(6): 1958-1969.

Betous, R., A. C. Mason, R. P. Rambo, C. E. Bansbach, A. Badu-Nkansah, B. M. Sirbu, B. F. Eichman and D. Cortez (2012). "SMARCAL1 catalyzes fork regression and Holliday junction migration to maintain genome stability during DNA replication." Genes Dev **26**(2): 151-162.

Bhat, A., P. L. Andersen, Z. Qin and W. Xiao (2013). "Rev3, the catalytic subunit of Polzeta, is required for maintaining fragile site stability in human cells." Nucleic Acids Res **41**(4): 2328-2339.

Bhat, K. P., R. Betous and D. Cortez (2015). "High-affinity DNA-binding domains of replication protein A (RPA) direct SMARCAL1-dependent replication fork remodeling." J Biol Chem **290**(7): 4110-4117.

Bhat, K. P. and D. Cortez (2018). "RPA and RAD51: fork reversal, fork protection, and genome stability." Nat Struct Mol Biol **25**(6): 446-453.

Bizanek, R., B. F. McGuinness, K. Nakanishi and M. Tomasz (1992). "Isolation and structure of an intrastrand cross-link adduct of mitomycin C and DNA." Biochemistry **31**(12): 3084-3091.

Boos, D. and P. Ferreira (2019). "Origin Firing Regulations to Control Genome Replication Timing." Genes (Basel) **10**(3).

Branzei, D. and B. Szakal (2016). "DNA damage tolerance by recombination: Molecular pathways and DNA structures." DNA Repair (Amst) **44**: 68-75.

Branzei, D., F. Vanoli and M. Foiani (2008). "SUMOylation regulates Rad18-mediated template switch." Nature **456**(7224): 915-920.

Brondello, J. M., M. J. Pillaire, C. Rodriguez, P. A. Gourraud, J. Selves, C. Cazaux and J. Piette (2008). "Novel evidences for a tumor suppressor role of Rev3, the catalytic subunit of Pol zeta." Oncogene **27**(47): 6093-6101.

Bryant, E. E., I. Sunjevaric, L. Berchowitz, R. Rothstein and R. J. D. Reid (2019). "Rad5 dysregulation drives hyperactive recombination at replication forks resulting in cisplatin sensitivity and genome instability." Nucleic Acids Res **47**(17): 9144-9159.

Bugreev, D. V., M. J. Rossi and A. V. Mazin (2011). "Cooperation of RAD51 and RAD54 in regression of a model replication fork." Nucleic Acids Res **39**(6): 2153-2164.

Burkovics, P., L. Dome, S. Juhasz, V. Altmannova, M. Sebesta, M. Pacesa, K. Fugger, C. S. Sorensen, M. Y. Lee, L. Haracska and L. Krejci (2016). "The PCNA-associated protein PARI negatively regulates homologous recombination via the inhibition of DNA repair synthesis." Nucleic Acids Res **44**(7): 3176-3189.

Burkovics, P., M. Sebesta, D. Balogh, L. Haracska and L. Krejci (2014). "Strand invasion by HLTF as a mechanism for template switch in fork rescue." Nucleic Acids Res **42**(3): 1711-1720.

Byun, T. S., M. Pacek, M. C. Yee, J. C. Walter and K. A. Cimprich (2005). "Functional uncoupling of MCM helicase and DNA polymerase activities activates the ATR-dependent checkpoint." Genes Dev **19**(9): 1040-1052.

Capouillez, A., J. C. Noel, M. Arafa, V. Arcolia, M. Mouallif, S. Guenin, P. Delvenne, A. Belayew and S. Saussez (2011). "Expression of the helicase-like transcription factor and its variants during carcinogenesis of the uterine cervix: implications for tumour progression." Histopathology **58**(6): 984-988.

Chang, D. J. and K. A. Cimprich (2009). "DNA damage tolerance: when it's OK to make mistakes." Nat Chem Biol **5**(2): 82-90.

Chaudhury, I., A. Sareen, M. Raghunandan and A. Sobeck (2013). "FANCD2 regulates BLM complex functions independently of FANCI to promote replication fork recovery." Nucleic Acids Res **41**(13): 6444-6459.

Chavez, D. A., B. H. Greer and B. F. Eichman (2018). "The HIRAN domain of helicase-like transcription factor positions the DNA translocase motor to drive efficient DNA fork regression." J Biol Chem **293**(22): 8484-8494.

Chen, X., L. Bosques, P. Sung and G. M. Kupfer (2016). "A novel role for non-ubiquitinated FANCD2 in response to hydroxyurea-induced DNA damage." Oncogene **35**(1): 22-34.

Choe, K. N. and G. L. Moldovan (2017). "Forging Ahead through Darkness: PCNA, Still the Principal Conductor at the Replication Fork." Mol Cell **65**(3): 380-392.

Chun, A. C., K. H. Kok and D. Y. Jin (2013). "REV7 is required for anaphase-promoting complex-dependent ubiquitination and degradation of translesion DNA polymerase REV1." Cell Cycle **12**(2): 365-378.

Ciccia, A., A. L. Bredemeyer, M. E. Sowa, M. E. Terret, P. V. Jallepalli, J. W. Harper and S. J. Elledge (2009). "The SIOD disorder protein SMARCAL1 is an RPA-interacting protein involved in replication fork restart." Genes Dev **23**(20): 2415-2425.

Ciccia, A., A. V. Nimonkar, Y. Hu, I. Hajdu, Y. J. Achar, L. Izhar, S. A. Petit, B. Adamson, J. C. Yoon, S. C. Kowalczykowski, D. M. Livingston, L. Haracska and S. J. Elledge (2012). "Polyubiquitinated PCNA recruits the ZRANB3 translocase to maintain genomic integrity after replication stress." Mol Cell **47**(3): 396-409.

Cliby, W. A., C. J. Roberts, K. A. Cimprich, C. M. Stringer, J. R. Lamb, S. L. Schreiber and S. H. Friend (1998). "Overexpression of a kinase-inactive ATR protein causes sensitivity to DNA-damaging agents and defects in cell cycle checkpoints." EMBO J **17**(1): 159-169.

Cooper, C. A., T. Tait, H. Gray, G. Cimprich, R. C. Santore, J. C. McGeer, C. M. Wood and D. S. Smith (2014). "Influence of salinity and dissolved organic carbon on acute Cu toxicity to the rotifer Brachionus plicatilis." Environ Sci Technol **48**(2): 1213-1221.

Cordon-Preciado, V., S. Ufano and A. Bueno (2006). "Limiting amounts of budding yeast Rad53 S-phase checkpoint activity results in increased resistance to DNA alkylation damage." Nucleic Acids Res **34**(20): 5852-5862.

Cordonnier, A. M., A. R. Lehmann and R. P. Fuchs (1999). "Impaired translesion synthesis in xeroderma pigmentosum variant extracts." Mol Cell Biol **19**(3): 2206-2211.

Couch, F. B., C. E. Bansbach, R. Driscoll, J. W. Luzwick, G. G. Glick, R. Betous, C. M. Carroll, S. Y. Jung, J. Qin, K. A. Cimprich and D. Cortez (2013). "ATR phosphorylates SMARCAL1 to prevent replication fork collapse." Genes Dev **27**(14): 1610-1623.

Coulombe, P., J. Nassar, I. Peiffer, S. Stanojcic, Y. Sterkers, A. Delamarre, S. Bocquet and M. Mechali (2019). "The ORC ubiquitin ligase OBI1 promotes DNA replication origin firing." Nat Commun **10**(1): 2426.

Courtot, L., J. S. Hoffmann and V. Bergoglio (2018). "The Protective Role of Dormant Origins in Response to Replicative Stress." Int J Mol Sci **19**(11).

Daigh, L. H., C. Liu, M. Chung, K. A. Cimprich and T. Meyer (2018). "Stochastic Endogenous Replication Stress Causes ATR-Triggered Fluctuations in CDK2 Activity that Dynamically Adjust Global DNA Synthesis Rates." Cell Syst **7**(1): 17-27 e13.

Date, O., M. Katsura, M. Ishida, T. Yoshihara, A. Kinomura, T. Sueda and K. Miyagawa (2006). "Haploinsufficiency of RAD51B causes centrosome fragmentation and aneuploidy in human cells." Cancer Res **66**(12): 6018-6024.

Datta, A. and R. M. Brosh, Jr. (2019). "Holding All the Cards-How Fanconi Anemia Proteins Deal with Replication Stress and Preserve Genomic Stability." Genes (Basel) **10**(2).

Davies, A. A., D. Huttner, Y. Daigaku, S. Chen and H. D. Ulrich (2008). "Activation of ubiquitin-dependent DNA damage bypass is mediated by replication protein a." Mol Cell **29**(5): 625-636.

Davies, S. L., P. S. North and I. D. Hickson (2007). "Role for BLM in replication-fork restart and suppression of origin firing after replicative stress." Nat Struct Mol Biol **14**(7): 677-679.

Davis, A. P. and L. S. Symington (2004). "RAD51-dependent break-induced replication in yeast." Mol Cell Biol **24**(6): 2344-2351.

Day, T. A., K. Palle, L. R. Barkley, N. Kakusho, Y. Zou, S. Tateishi, A. Verreault, H. Masai and C. Vaziri (2010). "Phosphorylated Rad18 directs DNA polymerase eta to sites of stalled replication." J Cell Biol **191**(5): 953-966.

De Bont, R. and N. van Larebeke (2004). "Endogenous DNA damage in humans: a review of quantitative data." Mutagenesis **19**(3): 169-185.

de Voer, R. M., M. M. Hahn, A. R. Mensenkamp, A. Hoischen, C. Gilissen, A. Henkes, L. Spruijt, W. A. van Zelst-Stams, C. M. Kets, E. T. Verwiel, I. D. Nagtegaal, H. K. Schackert, A. G. van Kessel, N. Hoogerbrugge, M. J. Ligtenberg and R. P. Kuiper (2015). "Deleterious Germline BLM Mutations and the Risk for Early-onset Colorectal Cancer." Sci Rep **5**: 14060.

Deem, A., A. Keszthelyi, T. Blackgrove, A. Vayl, B. Coffey, R. Mathur, A. Chabes and A. Malkova (2011). "Break-induced replication is highly inaccurate." PLoS Biol **9**(2): e1000594.

Despras, E., M. Sittewelle, C. Pouvelle, N. Delrieu, A. M. Cordonnier and P. L. Kannouche (2016). "Rad18-dependent SUMOylation of human specialized DNA polymerase eta is required to prevent under-replicated DNA." Nat Commun **7**: 13326.

Ding, H., K. Descheemaeker, P. Marynen, L. Nelles, T. Carvalho, M. Carmo-Fonseca, D. Collen and A. Belayew (1996). "Characterization of a helicase-like transcription factor involved in the expression of the human plasminogen activator inhibitor-1 gene." DNA Cell Biol **15**(6): 429-442.

Doles, J., T. G. Oliver, E. R. Cameron, G. Hsu, T. Jacks, G. C. Walker and M. T. Hemann (2010). "Suppression of Rev3, the catalytic subunit of Pol{zeta}, sensitizes drug-resistant lung tumors to chemotherapy." Proc Natl Acad Sci U S A **107**(48): 20786-20791.

Donzelli, M. and G. F. Draetta (2003). "Regulating mammalian checkpoints through Cdc25 inactivation." EMBO Rep **4**(7): 671-677.

Drablos, F., E. Feyzi, P. A. Aas, C. B. Vaagbo, B. Kavli, M. S. Bratlie, J. Pena-Diaz, M. Otterlei, G. Slupphaug and H. E. Krokan (2004). "Alkylation damage in DNA and RNA--repair mechanisms and medical significance." DNA Repair (Amst) **3**(11): 1389-1407.

Ducoux, M., S. Urbach, G. Baldacci, U. Hubscher, S. Koundrioukoff, J. Christensen and P. Hughes (2001). "Mediation of proliferating cell nuclear antigen (PCNA)-dependent DNA replication through a conserved p21(Cip1)-like PCNA-binding motif present in the third subunit of human DNA polymerase delta." J Biol Chem **276**(52): 49258-49266.

Durando, M., S. Tateishi and C. Vaziri (2013). "A non-catalytic role of DNA polymerase eta in recruiting Rad18 and promoting PCNA monoubiquitination at stalled replication forks." Nucleic Acids Res **41**(5): 3079-3093.

Elvers, I., F. Johansson, P. Groth, K. Erixon and T. Helleday (2011). "UV stalled replication forks restart by re-priming in human fibroblasts." Nucleic Acids Res **39**(16): 7049-7057.

Esposito, G., I. Godindagger, U. Klein, M. L. Yaspo, A. Cumano and K. Rajewsky (2000). "Disruption of the Rev3l-encoded catalytic subunit of polymerase zeta in mice results in early embryonic lethality." Curr Biol **10**(19): 1221-1224.

Falnes, P. O., M. Bjoras, P. A. Aas, O. Sundheim and E. Seeberg (2004). "Substrate specificities of bacterial and human AlkB proteins." Nucleic Acids Res **32**(11): 3456-3461.

Fattah, F. J., K. Hara, K. R. Fattah, C. Yang, N. Wu, R. Warrington, D. J. Chen, P. Zhou, D. A. Boothman and H. Yu (2014). "The transcription factor TFII-I promotes DNA translesion synthesis and genomic stability." PLoS Genet **10**(6): e1004419.

Fazlieva, R., C. S. Spittle, D. Morrissey, H. Hayashi, H. Yan and Y. Matsumoto (2009). "Proofreading exonuclease activity of human DNA polymerase delta and its effects on lesion-bypass DNA synthesis." Nucleic Acids Res **37**(9): 2854-2866.

Ferreira, M. F., C. Santocanale, L. S. Drury and J. F. Diffley (2000). "Dbf4p, an essential S phase-promoting factor, is targeted for degradation by the anaphase-promoting complex." Mol Cell Biol **20**(1): 242-248.

Friedrich, K., L. Lee, D. F. Leistritz, G. Nurnberg, B. Saha, F. M. Hisama, D. K. Eyman, D. Lessel, P. Nurnberg, C. Li, F. V. M. J. Garcia, C. M. Kets, J. Schmidtke, V. T. Cruz, P. C. Van den Akker, J. Boak, D. Peter, G. Compoginis, K. Cefle, S. Ozturk, N. Lopez, T. Wessel, M. Poot, P. F. Ippel, B. Groff-Kellermann, H. Hoehn, G. M. Martin, C. Kubisch and J. Oshima (2010). "WRN mutations in Werner syndrome patients: genomic

rearrangements, unusual intronic mutations and ethnic-specific alterations." <u>Hum Genet</u> **128**(1): 103-111.

Fugger, K., M. Mistrik, K. J. Neelsen, Q. Yao, R. Zellweger, A. N. Kousholt, P. Haahr, W. K. Chu, J. Bartek, M. Lopes, I. D. Hickson and C. S. Sorensen (2015). "FBH1 Catalyzes Regression of Stalled Replication Forks." <u>Cell Rep</u> **10**(10): 1749-1757.

Fumasoni, M., K. Zwicky, F. Vanoli, M. Lopes and D. Branzei (2015). "Error-free DNA damage tolerance and sister chromatid proximity during DNA replication rely on the Polalpha/Primase/Ctf4 Complex." <u>Mol Cell</u> **57**(5): 812-823.

Furrer, A. and B. van Loon (2014). "Handling the 3-methylcytosine lesion by six human DNA polymerases members of the B-, X- and Y-families." <u>Nucleic Acids Res</u> **42**(1): 553-566.

Galanti, L. and B. Pfander (2018). "Right time, right place-DNA damage and DNA replication checkpoints collectively safeguard S phase." <u>EMBO J</u> **37**(21).

Gari, K., C. Decaillet, M. Delannoy, L. Wu and A. Constantinou (2008). "Remodeling of DNA replication structures by the branch point translocase FANCM." <u>Proc Natl Acad Sci U S A</u> **105**(42): 16107-16112.

Garzon, J., S. Ursich, M. Lopes, S. I. Hiraga and A. D. Donaldson (2019). "Human RIF1-Protein Phosphatase 1 Prevents Degradation and Breakage of Nascent DNA on Replication Stalling." <u>Cell Rep</u> **27**(9): 2558-2566 e2554.

Ge, X. Q. and J. J. Blow (2010). "Chk1 inhibits replication factory activation but allows dormant origin firing in existing factories." <u>J Cell Biol</u> **191**(7): 1285-1297.

Ge, X. Q., D. A. Jackson and J. J. Blow (2007). "Dormant origins licensed by excess Mcm2-7 are required for human cells to survive replicative stress." <u>Genes Dev</u> **21**(24): 3331-3341.

Gederaas, O. A., C. D. Sogaard, T. Viset, S. Bachke, P. Bruheim, C. J. Arum and M. Otterlei (2014). "Increased Anticancer Efficacy of Intravesical Mitomycin C Therapy when Combined with a PCNA Targeting Peptide." <u>Transl Oncol</u> **7**(6): 812-823.

Gervai, J. Z., J. Galicza, Z. Szeltner, J. Zamborszky and D. Szuts (2017). "A genetic study based on PCNA-ubiquitin fusions reveals no requirement for PCNA polyubiquitylation in DNA damage tolerance." <u>DNA Repair (Amst)</u> **54**: 46-54.

Ghosal, G. and J. Chen (2013). "DNA damage tolerance: a double-edged sword guarding the genome." <u>Transl Cancer Res</u> **2**(3): 107-129.

Giannattasio, M., K. Zwicky, C. Follonier, M. Foiani, M. Lopes and D. Branzei (2014). "Visualization of recombination-mediated damage bypass by template switching." <u>Nat Struct Mol Biol</u> **21**(10): 884-892.

Gilljam, K. M., E. Feyzi, P. A. Aas, M. M. Sousa, R. Muller, C. B. Vagbo, T. C. Catterall, N. B. Liabakk, G. Slupphaug, F. Drablos, H. E. Krokan and M. Otterlei (2009). "Identification of a novel, widespread, and functionally important PCNA-binding motif." <u>J Cell Biol</u> **186**(5): 645-654.

Gilljam, K. M., R. Muller, N. B. Liabakk and M. Otterlei (2012). "Nucleotide excision repair is associated with the replisome and its efficiency depends on a direct interaction between XPA and PCNA." <u>PLoS One</u> **7**(11): e49199.

Gonzalez Besteiro, M. A., N. L. Calzetta, S. M. Loureiro, M. Habif, R. Betous, M. J. Pillaire, A. Maffia, S. Sabbioneda, J. S. Hoffmann and V. Gottifredi (2019). "Chk1 loss creates

replication barriers that compromise cell survival independently of excess origin firing." EMBO J **38**(16): e101284.

Guan, J., S. Yu and X. Zheng (2018). "NEDDylation antagonizes ubiquitination of proliferating cell nuclear antigen and regulates the recruitment of polymerase eta in response to oxidative DNA damage." Protein Cell **9**(4): 365-379.

Guilliam, T. A., N. C. Brissett, A. Ehlinger, B. A. Keen, P. Kolesar, E. M. Taylor, L. J. Bailey, H. D. Lindsay, W. J. Chazin and A. J. Doherty (2017). "Molecular basis for PrimPol recruitment to replication forks by RPA." Nat Commun **8**: 15222.

Guilliam, T. A. and A. J. Doherty (2017). "PrimPol-Prime Time to Reprime." Genes **8**(1).

Guilliam, T. A., S. K. Jozwiakowski, A. Ehlinger, R. P. Barnes, S. G. Rudd, L. J. Bailey, J. M. Skehel, K. A. Eckert, W. J. Chazin and A. J. Doherty (2015). "Human PrimPol is a highly error-prone polymerase regulated by single-stranded DNA binding proteins." Nucleic Acids Res **43**(2): 1056-1068.

Guo, J., P. C. Hanawalt and G. Spivak (2013). "Comet-FISH with strand-specific probes reveals transcription-coupled repair of 8-oxoGuanine in human cells." Nucleic Acids Res **41**(16): 7700-7712.

Haas, A. L., P. Ahrens, P. M. Bright and H. Ankel (1987). "Interferon induces a 15-kilodalton protein exhibiting marked homology to ubiquitin." J Biol Chem **262**(23): 11315-11323.

Hampp, S., T. Kiessling, K. Buechle, S. F. Mansilla, J. Thomale, M. Rall, J. Ahn, H. Pospiech, V. Gottifredi and L. Wiesmuller (2016). "DNA damage tolerance pathway involving DNA polymerase iota and the tumor suppressor p53 regulates DNA replication fork progression." Proc Natl Acad Sci U S A **113**(30): E4311-4319.

Hanada, K., M. Budzowska, M. Modesti, A. Maas, C. Wyman, J. Essers and R. Kanaar (2006). "The structure-specific endonuclease Mus81-Eme1 promotes conversion of interstrand DNA crosslinks into double-strands breaks." EMBO J **25**(20): 4921-4932.

Hara, K., M. Uchida, R. Tagata, H. Yokoyama, Y. Ishikawa, A. Hishiki and H. Hashimoto (2018). "Structure of proliferating cell nuclear antigen (PCNA) bound to an APIM peptide reveals the universality of PCNA interaction." Acta Crystallogr F Struct Biol Commun **74**(Pt 4): 214-221.

Hashimoto, S., H. Anai and K. Hanada (2016). "Mechanisms of interstrand DNA crosslink repair and human disorders." Genes Environ **38**: 9.

Hashimoto, Y., A. Ray Chaudhuri, M. Lopes and V. Costanzo (2010). "Rad51 protects nascent DNA from Mre11-dependent degradation and promotes continuous DNA synthesis." Nat Struct Mol Biol **17**(11): 1305-1311.

Hedglin, M. and S. J. Benkovic (2017). "Eukaryotic Translesion DNA Synthesis on the Leading and Lagging Strands: Unique Detours around the Same Obstacle." Chem Rev **117**(12): 7857-7877.

Hedglin, M., B. Pandey and S. J. Benkovic (2016). "Stability of the human polymerase delta holoenzyme and its implications in lagging strand DNA synthesis." Proc Natl Acad Sci U S A **113**(13): E1777-1786.

Heller, R. C. and K. J. Marians (2006). "Replication fork reactivation downstream of a blocked nascent leading strand." Nature **439**(7076): 557-562.

Helmer, R. A., O. Foreman, J. S. Dertien, M. Panchoo, S. M. Bhakta and B. S. Chilton (2013). "Role of helicase-like transcription factor (hltf) in the G2/m transition and apoptosis in brain." PLoS One **8**(6): e66799.

Hendel, A., P. H. Krijger, N. Diamant, Z. Goren, P. Langerak, J. Kim, T. Reissner, K. Y. Lee, N. E. Geacintov, T. Carell, K. Myung, S. Tateishi, A. D'Andrea, H. Jacobs and Z. Livneh (2011). "PCNA ubiquitination is important, but not essential for translesion DNA synthesis in mammalian cells." PLoS Genet **7**(9): e1002262.

Hicks, J. K., C. L. Chute, M. T. Paulsen, R. L. Ragland, N. G. Howlett, Q. Gueranger, T. W. Glover and C. E. Canman (2010). "Differential roles for DNA polymerases eta, zeta, and REV1 in lesion bypass of intrastrand versus interstrand DNA cross-links." Mol Cell Biol **30**(5): 1217-1230.

Hishiki, A., H. Hashimoto, T. Hanafusa, K. Kamei, E. Ohashi, T. Shimizu, H. Ohmori and M. Sato (2009). "Structural basis for novel interactions between human translesion synthesis polymerases and proliferating cell nuclear antigen." J Biol Chem **284**(16): 10552-10560.

Hoege, C., B. Pfander, G. L. Moldovan, G. Pyrowolakis and S. Jentsch (2002). "RAD6-dependent DNA repair is linked to modification of PCNA by ubiquitin and SUMO." Nature **419**(6903): 135-141.

Hu, J., S. Adar, C. P. Selby, J. D. Lieb and A. Sancar (2015). "Genome-wide analysis of human global and transcription-coupled excision repair of UV damage at single-nucleotide resolution." Genes Dev **29**(9): 948-960.

Huang, J., S. Liu, M. A. Bellani, A. K. Thazhathveetil, C. Ling, J. P. de Winter, Y. Wang, W. Wang and M. M. Seidman (2013). "The DNA translocase FANCM/MHF promotes replication traverse of DNA interstrand crosslinks." Mol Cell **52**(3): 434-446.

Huang, J. C., D. S. Hsu, A. Kazantsev and A. Sancar (1994). "Substrate spectrum of human excinuclease: repair of abasic sites, methylated bases, mismatches, and bulky adducts." Proc Natl Acad Sci U S A **91**(25): 12213-12217.

Ibarra, A., E. Schwob and J. Mendez (2008). "Excess MCM proteins protect human cells from replicative stress by licensing backup origins of replication." Proc Natl Acad Sci U S A **105**(26): 8956-8961.

Ilves, I., T. Petojevic, J. J. Pesavento and M. R. Botchan (2010). "Activation of the MCM2-7 helicase by association with Cdc45 and GINS proteins." Mol Cell **37**(2): 247-258.

Inoue, A., S. Kikuchi, A. Hishiki, Y. Shao, R. Heath, B. J. Evison, M. Actis, C. E. Canman, H. Hashimoto and N. Fujii (2014). "A small molecule inhibitor of monoubiquitinated Proliferating Cell Nuclear Antigen (PCNA) inhibits repair of interstrand DNA cross-link, enhances DNA double strand break, and sensitizes cancer cells to cisplatin." J Biol Chem **289**(10): 7109-7120.

Inui, H., K. S. Oh, C. Nadem, T. Ueda, S. G. Khan, A. Metin, E. Gozukara, S. Emmert, H. Slor, D. B. Busch, C. C. Baker, J. J. DiGiovanna, D. Tamura, C. S. Seitz, A. Gratchev, W. H. Wu, K. Y. Chung, H. J. Chung, E. Azizi, R. Woodgate, T. D. Schneider and K. H. Kraemer (2008). "Xeroderma pigmentosum-variant patients from America, Europe, and Asia." J Invest Dermatol **128**(8): 2055-2068.

Iyer, D. R. and N. Rhind (2017). "The Intra-S Checkpoint Responses to DNA Damage." Genes (Basel) **8**(2).

Iyer, D. R. and N. Rhind (2017). "Replication fork slowing and stalling are distinct, checkpoint-independent consequences of replicating damaged DNA." PLoS Genet **13**(8): e1006958.

Iyer, L. M., E. V. Koonin, D. D. Leipe and L. Aravind (2005). "Origin and evolution of the archaeo-eukaryotic primase superfamily and related palm-domain proteins: structural insights and new members." Nucleic Acids Res **33**(12): 3875-3896.

Jansen, J. G., A. Tsaalbi-Shtylik, G. Hendriks, J. Verspuy, H. Gali, L. Haracska and N. de Wind (2009). "Mammalian polymerase zeta is essential for post-replication repair of UV-induced DNA lesions." DNA Repair (Amst) **8**(12): 1444-1451.

Jha, V. and H. Ling (2018). "Structural Basis for Human DNA Polymerase Kappa to Bypass Cisplatin Intrastrand Cross-Link (Pt-GG) Lesion as an Efficient and Accurate Extender." J Mol Biol **430**(11): 1577-1589.

Jiricny, J. (2006). "The multifaceted mismatch-repair system." Nat Rev Mol Cell Biol **7**(5): 335-346.

Johnson, R. E., S. Prakash and L. Prakash (1999). "Efficient bypass of a thymine-thymine dimer by yeast DNA polymerase, Poleta." Science **283**(5404): 1001-1004.

Johnson, R. E., M. T. Washington, L. Haracska, S. Prakash and L. Prakash (2000). "Eukaryotic polymerases iota and zeta act sequentially to bypass DNA lesions." Nature **406**(6799): 1015-1019.

Johnson, R. E., S. L. Yu, S. Prakash and L. Prakash (2007). "A role for yeast and human translesion synthesis DNA polymerases in promoting replication through 3-methyl adenine." Mol Cell Biol **27**(20): 7198-7205.

Jung, Y. S., A. Hakem, R. Hakem and X. Chen (2011). "Pirh2 E3 ubiquitin ligase monoubiquitinates DNA polymerase eta to suppress translesion DNA synthesis." Mol Cell Biol **31**(19): 3997-4006.

Jung, Y. S., Y. Qian and X. Chen (2012). "DNA polymerase eta is targeted by Mdm2 for polyubiquitination and proteasomal degradation in response to ultraviolet irradiation." DNA Repair (Amst) **11**(2): 177-184.

Kamitani, T., K. Kito, H. P. Nguyen and E. T. Yeh (1997). "Characterization of NEDD8, a developmentally down-regulated ubiquitin-like protein." J Biol Chem **272**(45): 28557-28562.

Kanao, R., Y. Masuda, S. Deguchi, M. Yumoto-Sugimoto, F. Hanaoka and C. Masutani (2015). "Relevance of simultaneous mono-ubiquitinations of multiple units of PCNA homo-trimers in DNA damage tolerance." PLoS One **10**(2): e0118775.

Kanao, R. and C. Masutani (2017). "Regulation of DNA damage tolerance in mammalian cells by post-translational modifications of PCNA." Mutat Res **803-805**: 82-88.

Kannouche, P. L., J. Wing and A. R. Lehmann (2004). "Interaction of human DNA polymerase eta with monoubiquitinated PCNA: a possible mechanism for the polymerase switch in response to DNA damage." Mol Cell **14**(4): 491-500.

Kartalou, M. and J. M. Essigmann (2001). "Recognition of cisplatin adducts by cellular proteins." Mutat Res **478**(1-2): 1-21.

Kato, N., Y. Kawasoe, H. Williams, E. Coates, U. Roy, Y. Shi, L. S. Beese, O. D. Scharer, H. Yan, M. E. Gottesman, T. S. Takahashi and J. Gautier (2017). "Sensing and Processing

of DNA Interstrand Crosslinks by the Mismatch Repair Pathway." <u>Cell Rep</u> **21**(5): 1375-1385.

Kawabata, T., S. W. Luebben, S. Yamaguchi, I. Ilves, I. Matise, T. Buske, M. R. Botchan and N. Shima (2011). "Stalled fork rescue via dormant replication origins in unchallenged S phase promotes proper chromosome segregation and tumor suppression." <u>Mol Cell</u> **41**(5): 543-553.

Kemp, M. G., Z. Akan, S. Yilmaz, M. Grillo, S. L. Smith-Roe, T. H. Kang, M. Cordeiro-Stone, W. K. Kaufmann, R. T. Abraham, A. Sancar and K. Unsal-Kacmaz (2010). "Tipin-replication protein A interaction mediates Chk1 phosphorylation by ATR in response to genotoxic stress." <u>J Biol Chem</u> **285**(22): 16562-16571.

Kemp, M. G. and A. Sancar (2012). "DNA excision repair: where do all the dimers go?" <u>Cell Cycle</u> **11**(16): 2997-3002.

Kim, J. J., S. W. Chung, J. H. Kim, J. W. Kim, J. S. Oh, S. Kim, S. Y. Song, J. Park and D. H. Kim (2006). "Promoter methylation of helicase-like transcription factor is associated with the early stages of gastric cancer with family history." <u>Ann Oncol</u> **17**(4): 657-662.

Knobel, P. A., I. N. Kotov, E. Felley-Bosco, R. A. Stahel and T. M. Marti (2011). "Inhibition of REV3 expression induces persistent DNA damage and growth arrest in cancer cells." <u>Neoplasia</u> **13**(10): 961-970.

Kolinjivadi, A. M., V. Sannino, A. De Antoni, K. Zadorozhny, M. Kilkenny, H. Techer, G. Baldi, R. Shen, A. Ciccia, L. Pellegrini, L. Krejci and V. Costanzo (2017). "Smarcal1-Mediated Fork Reversal Triggers Mre11-Dependent Degradation of Nascent DNA in the Absence of Brca2 and Stable Rad51 Nucleofilaments." <u>Mol Cell</u> **67**(5): 867-881 e867.

Korzhnev, D. M., D. Neculai, S. Dhe-Paganon, C. H. Arrowsmith and I. Bezsonova (2016). "Solution NMR structure of the HLTF HIRAN domain: a conserved module in SWI2/SNF2 DNA damage tolerance proteins." <u>J Biomol NMR</u> **66**(3): 209-219.

Kothandapani, A. and S. M. Patrick (2013). "Evidence for base excision repair processing of DNA interstrand crosslinks." <u>Mutat Res</u> **743-744**: 44-52.

Kraemer, K. H., M. M. Lee, A. D. Andrews and W. C. Lambert (1994). "The role of sunlight and DNA repair in melanoma and nonmelanoma skin cancer. The xeroderma pigmentosum paradigm." <u>Arch Dermatol</u> **130**(8): 1018-1021.

Kraemer, K. H., M. M. Lee and J. Scotto (1987). "Xeroderma pigmentosum. Cutaneous, ocular, and neurologic abnormalities in 830 published cases." <u>Arch Dermatol</u> **123**(2): 241-250.

Krijger, P. H., K. Y. Lee, N. Wit, P. C. van den Berk, X. Wu, H. P. Roest, A. Maas, H. Ding, J. H. Hoeijmakers, K. Myung and H. Jacobs (2011). "HLTF and SHPRH are not essential for PCNA polyubiquitination, survival and somatic hypermutation: existence of an alternative E3 ligase." <u>DNA Repair (Amst)</u> **10**(4): 438-444.

Krijger, P. H., P. C. van den Berk, N. Wit, P. Langerak, J. G. Jansen, C. A. Reynaud, N. de Wind and H. Jacobs (2011). "PCNA ubiquitination-independent activation of polymerase eta during somatic hypermutation and DNA damage tolerance." <u>DNA Repair (Amst)</u> **10**(10): 1051-1059.

Krokan, H. E. and M. Bjoras (2013). "Base excision repair." <u>Cold Spring Harb Perspect Biol</u> **5**(4): a012583.

Lahouassa, H., M. L. Blondot, L. Chauveau, G. Chougui, M. Morel, M. Leduc, F. Guillonneau, B. C. Ramirez, O. Schwartz and F. Margottin-Goguet (2016). "HIV-1 Vpr degrades the HLTF DNA translocase in T cells and macrophages." Proc Natl Acad Sci U S A **113**(19): 5311-5316.

Lange, S. S., K. Takata and R. D. Wood (2011). "DNA polymerases and cancer." Nat Rev Cancer **11**(2): 96-110.

Lange, S. S., J. P. Wittschieben and R. D. Wood (2012). "DNA polymerase zeta is required for proliferation of normal mammalian cells." Nucleic Acids Res **40**(10): 4473-4482.

Larsen, N. B. and I. D. Hickson (2013). "RecQ Helicases: Conserved Guardians of Genomic Integrity." Adv Exp Med Biol **767**: 161-184.

Lee, D., J. An, Y. U. Park, H. Liaw, R. Woodgate, J. H. Park and K. Myung (2017). "SHPRH regulates rRNA transcription by recognizing the histone code in an mTOR-dependent manner." Proc Natl Acad Sci U S A **114**(17): E3424-E3433.

Lee, Y. S., M. T. Gregory and W. Yang (2014). "Human Pol zeta purified with accessory subunits is active in translesion DNA synthesis and complements Pol eta in cisplatin bypass." Proc Natl Acad Sci U S A **111**(8): 2954-2959.

Lemacon, D., J. Jackson, A. Quinet, J. R. Brickner, S. Li, S. Yazinski, Z. You, G. Ira, L. Zou, N. Mosammaparast and A. Vindigni (2017). "MRE11 and EXO1 nucleases degrade reversed forks and elicit MUS81-dependent fork rescue in BRCA2-deficient cells." Nat Commun **8**(1): 860.

Leung, W., R. M. Baxley, G. L. Moldovan and A. K. Bielinsky (2018). "Mechanisms of DNA Damage Tolerance: Post-Translational Regulation of PCNA." Genes (Basel) **10**(1).

Li, Z., W. Xiao, J. J. McCormick and V. M. Maher (2002). "Identification of a protein essential for a major pathway used by human cells to avoid UV- induced DNA damage." Proc Natl Acad Sci U S A **99**(7): 4459-4464.

Liao, H., F. Ji, T. Helleday and S. Ying (2018). "Mechanisms for stalled replication fork stabilization: new targets for synthetic lethality strategies in cancer treatments." EMBO Rep **19**(9).

Lin, J. R., M. K. Zeman, J. Y. Chen, M. C. Yee and K. A. Cimprich (2011). "SHPRH and HLTF act in a damage-specific manner to coordinate different forms of postreplication repair and prevent mutagenesis." Mol Cell **42**(2): 237-249.

Ling, C., J. Huang, Z. Yan, Y. Li, M. Ohzeki, M. Ishiai, D. Xu, M. Takata, M. Seidman and W. Wang (2016). "Bloom syndrome complex promotes FANCM recruitment to stalled replication forks and facilitates both repair and traverse of DNA interstrand crosslinks." Cell Discov **2**: 16047.

Lopes, M., M. Foiani and J. M. Sogo (2006). "Multiple mechanisms control chromosome integrity after replication fork uncoupling and restart at irreparable UV lesions." Mol Cell **21**(1): 15-27.

Machado, L. E., Y. Pustovalova, A. C. Kile, A. Pozhidaeva, K. A. Cimprich, F. C. Almeida, I. Bezsonova and D. M. Korzhnev (2013). "PHD domain from human SHPRH." J Biomol NMR **56**(4): 393-399.

Mailand, N., I. Gibbs-Seymour and S. Bekker-Jensen (2013). "Regulation of PCNA-protein interactions for genome stability." Nat Rev Mol Cell Biol **14**(5): 269-282.

Makarova, A. V. and P. M. Burgers (2015). "Eukaryotic DNA polymerase zeta." DNA Repair (Amst) **29**: 47-55.

Makarova, A. V., J. L. Stodola and P. M. Burgers (2012). "A four-subunit DNA polymerase zeta complex containing Pol delta accessory subunits is essential for PCNA-mediated mutagenesis." Nucleic Acids Res **40**(22): 11618-11626.

Malacaria, E., G. M. Pugliese, M. Honda, V. Marabitti, F. A. Aiello, M. Spies, A. Franchitto and P. Pichierri (2019). "Rad52 prevents excessive replication fork reversal and protects from nascent strand degradation." Nat Commun **10**(1): 1412.

Malkova, A., M. L. Naylor, M. Yamaguchi, G. Ira and J. E. Haber (2005). "RAD51-dependent break-induced replication differs in kinetics and checkpoint responses from RAD51-mediated gene conversion." Mol Cell Biol **25**(3): 933-944.

Marians, K. J. (2018). "Lesion Bypass and the Reactivation of Stalled Replication Forks." Annu Rev Biochem **87**: 217-238.

Marteijn, J. A., H. Lans, W. Vermeulen and J. H. Hoeijmakers (2014). "Understanding nucleotide excision repair and its roles in cancer and ageing." Nat Rev Mol Cell Biol **15**(7): 465-481.

Martin, S. K. and R. D. Wood (2019). "DNA polymerase zeta in DNA replication and repair." Nucleic Acids Res.

Masuda, Y., S. Mitsuyuki, R. Kanao, A. Hishiki, H. Hashimoto and C. Masutani (2018). "Regulation of HLTF-mediated PCNA polyubiquitination by RFC and PCNA monoubiquitination levels determines choice of damage tolerance pathway." Nucleic Acids Res **46**(21): 11340-11356.

Masuda, Y., M. Suzuki, H. Kawai, A. Hishiki, H. Hashimoto, C. Masutani, T. Hishida, F. Suzuki and K. Kamiya (2012). "En bloc transfer of polyubiquitin chains to PCNA in vitro is mediated by two different human E2-E3 pairs." Nucleic Acids Res **40**(20): 10394-10407.

Masutani, C., R. Kusumoto, A. Yamada, N. Dohmae, M. Yokoi, M. Yuasa, M. Araki, S. Iwai, K. Takio and F. Hanaoka (1999). "The XPV (xeroderma pigmentosum variant) gene encodes human DNA polymerase eta." Nature **399**(6737): 700-704.

McHugh, P. J. and S. Sarkar (2006). "DNA interstrand cross-link repair in the cell cycle: a critical role for polymerase zeta in G1 phase." Cell Cycle **5**(10): 1044-1047.

McIntosh, D. and J. J. Blow (2012). "Dormant origins, the licensing checkpoint, and the response to replicative stresses." Cold Spring Harb Perspect Biol **4**(10).

Min, W., C. Bruhn, P. Grigaravicius, Z. W. Zhou, F. Li, A. Kruger, B. Siddeek, K. O. Greulich, O. Popp, C. Meisezahl, C. F. Calkhoven, A. Burkle, X. Xu and Z. Q. Wang (2013). "Poly(ADP-ribose) binding to Chk1 at stalled replication forks is required for S-phase checkpoint activation." Nat Commun **4**: 2993.

Mohiuddin, M., T. J. Evans, M. M. Rahman, I. S. Keka, M. Tsuda, H. Sasanuma and S. Takeda (2018). "SUMOylation of PCNA by PIAS1 and PIAS4 promotes template switch in the chicken and human B cell lines." Proc Natl Acad Sci U S A **115**(50): 12793-12798.

Moinova, H. R., W. D. Chen, L. Shen, D. Smiraglia, J. Olechnowicz, L. Ravi, L. Kasturi, L. Myeroff, C. Plass, R. Parsons, J. Minna, J. K. Willson, S. B. Green, J. P. Issa and S. D.

Markowitz (2002). "HLTF gene silencing in human colon cancer." <u>Proc Natl Acad Sci U S A</u> **99**(7): 4562-4567.

Moldovan, G. L., D. Dejsuphong, M. I. Petalcorin, K. Hofmann, S. Takeda, S. J. Boulton and A. D. D'Andrea (2012). "Inhibition of homologous recombination by the PCNA-interacting protein PARI." <u>Mol Cell</u> **45**(1): 75-86.

Motegi, A., H. J. Liaw, K. Y. Lee, H. P. Roest, A. Maas, X. Wu, H. Moinova, S. D. Markowitz, H. Ding, J. H. J. Hoeijmakers and K. Myung (2008). "Polyubiquitination of proliferating cell nuclear antigen by HLTF and SHPRH prevents genomic instability from stalled replication forks." <u>Proceedings of the National Academy of Sciences of the United States of America</u> **105**(34): 12411-12416.

Motegi, A., R. Sood, H. Moinova, S. D. Markowitz, P. P. Liu and K. Myung (2006). "Human SHPRH suppresses genomic instability through proliferating cell nuclear antigen polyubiquitination." <u>J Cell Biol</u> **175**(5): 703-708.

Mouron, S., S. Rodriguez-Acebes, M. I. Martinez-Jimenez, S. Garcia-Gomez, S. Chocron, L. Blanco and J. Mendez (2013). "Repriming of DNA synthesis at stalled replication forks by human PrimPol." <u>Nat Struct Mol Biol</u> **20**(12): 1383-1389.

Muller, R., K. Misund, T. Holien, S. Bachke, K. M. Gilljam, T. K. Vatsveen, T. B. Ro, E. Bellacchio, A. Sundan and M. Otterlei (2013). "Targeting proliferating cell nuclear antigen and its protein interactions induces apoptosis in multiple myeloma cells." <u>PLoS One</u> **8**(7): e70430.

Neelsen, K. J. and M. Lopes (2015). "Replication fork reversal in eukaryotes: from dead end to dynamic response." <u>Nat Rev Mol Cell Biol</u> **16**(4): 207-220.

Nelson, J. R., C. W. Lawrence and D. C. Hinkle (1996). "Deoxycytidyl transferase activity of yeast REV1 protein." <u>Nature</u> **382**(6593): 729-731.

Nelson, J. R., C. W. Lawrence and D. C. Hinkle (1996). "Thymine-thymine dimer bypass by yeast DNA polymerase zeta." <u>Science</u> **272**(5268): 1646-1649.

Niedernhofer, L. J., H. Odijk, M. Budzowska, E. van Drunen, A. Maas, A. F. Theil, J. de Wit, N. G. Jaspers, H. B. Beverloo, J. H. Hoeijmakers and R. Kanaar (2004). "The structure-specific endonuclease Ercc1-Xpf is required to resolve DNA interstrand cross-link-induced double-strand breaks." <u>Mol Cell Biol</u> **24**(13): 5776-5787.

Northam, M. R., H. A. Robinson, O. V. Kochenova and P. V. Shcherbakova (2010). "Participation of DNA polymerase zeta in replication of undamaged DNA in Saccharomyces cerevisiae." <u>Genetics</u> **184**(1): 27-42.

Olaisen, C., H. F. N. Kvitvang, S. Lee, E. Almaas, P. Bruheim, F. Drablos and M. Otterlei (2018). "The role of PCNA as a scaffold protein in cellular signaling is functionally conserved between yeast and humans." <u>FEBS Open Bio</u> **8**(7): 1135-1145.

Olaisen, C., R. Muller, A. Nedal and M. Otterlei (2015). "PCNA-interacting peptides reduce Akt phosphorylation and TLR-mediated cytokine secretion suggesting a role of PCNA in cellular signaling." <u>Cell Signal</u> **27**(7): 1478-1487.

Pages, V., G. Mazon, K. Naiman, G. Philippin and R. P. Fuchs (2012). "Monitoring bypass of single replication-blocking lesions by damage avoidance in the Escherichia coli chromosome." <u>Nucleic Acids Res</u> **40**(18): 9036-9043.

Park, J. M., S. W. Yang, K. R. Yu, S. H. Ka, S. W. Lee, J. H. Seol, Y. J. Jeon and C. H. Chung (2014). "Modification of PCNA by ISG15 plays a crucial role in termination of error-prone translesion DNA synthesis." Mol Cell **54**(4): 626-638.

Parker, J. L. and H. D. Ulrich (2012). "A SUMO-interacting motif activates budding yeast ubiquitin ligase Rad18 towards SUMO-modified PCNA." Nucleic Acids Res **40**(22): 11380-11388.

Peng, M., K. Cong, N. J. Panzarino, S. Nayak, J. Calvo, B. Deng, L. J. Zhu, M. Morocz, L. Hegedus, L. Haracska and S. B. Cantor (2018). "Opposing Roles of FANCJ and HLTF Protect Forks and Restrain Replication during Stress." Cell Rep **24**(12): 3251-3261.

Petermann, E., M. Woodcock and T. Helleday (2010). "Chk1 promotes replication fork progression by controlling replication initiation." Proc Natl Acad Sci U S A **107**(37): 16090-16095.

Pfander, B., G. L. Moldovan, M. Sacher, C. Hoege and S. Jentsch (2005). "SUMO-modified PCNA recruits Srs2 to prevent recombination during S phase." Nature **436**(7049): 428-433.

Pfeifer, G. P. (1997). "Formation and processing of UV photoproducts: effects of DNA sequence and chromatin environment." Photochem Photobiol **65**(2): 270-283.

Pilzecker, B., O. A. Buoninfante and H. Jacobs (2019). "DNA damage tolerance in stem cells, ageing, mutagenesis, disease and cancer therapy." Nucleic Acids Res **47**(14): 7163-7181.

Plosky, B. S., E. G. Frank, D. A. Berry, G. P. Vennall, J. P. McDonald and R. Woodgate (2008). "Eukaryotic Y-family polymerases bypass a 3-methyl-2'-deoxyadenosine analog in vitro and methyl methanesulfonate-induced DNA damage in vivo." Nucleic Acids Res **36**(7): 2152-2162.

Prado, F. (2018). "Homologous Recombination: To Fork and Beyond." Genes (Basel) **9**(12).

Prakash, L. (1981). "Characterization of postreplication repair in Saccharomyces cerevisiae and effects of rad6, rad18, rev3 and rad52 mutations." Mol Gen Genet **184**(3): 471-478.

Prakash, S., R. E. Johnson and L. Prakash (2005). "Eukaryotic translesion synthesis DNA polymerases: specificity of structure and function." Annu Rev Biochem **74**: 317-353.

Pruitt, S. C., K. J. Bailey and A. Freeland (2007). "Reduced Mcm2 expression results in severe stem/progenitor cell deficiency and cancer." Stem Cells **25**(12): 3121-3132.

Pustovalova, Y., M. W. Maciejewski and D. M. Korzhnev (2013). "NMR mapping of PCNA interaction with translesion synthesis DNA polymerase Rev1 mediated by Rev1-BRCT domain." J Mol Biol **425**(17): 3091-3105.

Pustovalova, Y., M. T. Magalhaes, S. D'Souza, A. A. Rizzo, G. Korza, G. C. Walker and D. M. Korzhnev (2016). "Interaction between the Rev1 C-Terminal Domain and the PolD3 Subunit of Polzeta Suggests a Mechanism of Polymerase Exchange upon Rev1/Polzeta-Dependent Translesion Synthesis." Biochemistry **55**(13): 2043-2053.

Qing, P., L. Han, L. Bin, L. Yan and W. X. Ping (2011). "USP7 regulates the stability and function of HLTF through deubiquitination." J Cell Biochem **112**(12): 3856-3862.

Quinet, A., D. Carvajal-Maldonado, D. Lemacon and A. Vindigni (2017). "DNA Fiber Analysis: Mind the Gap!" Methods Enzymol **591**: 55-82.

Quinet, A., L. K. Lerner, D. J. Martins and C. F. M. Menck (2018). "Filling gaps in translesion DNA synthesis in human cells." Mutat Res Genet Toxicol Environ Mutagen **836**(Pt B): 127-142.

Quinet, A., D. J. Martins, A. T. Vessoni, D. Biard, A. Sarasin, A. Stary and C. F. Menck (2016). "Translesion synthesis mechanisms depend on the nature of DNA damage in UV-irradiated human cells." Nucleic Acids Res **44**(12): 5717-5731.

Raeder, S. B., A. Nepal, K. O. Bjoras, M. Seelinger, R. S. Kolve, A. Nedal, R. Muller and M. Otterlei (2018). "APIM-Mediated REV3L(-)PCNA Interaction Important for Error Free TLS Over UV-Induced DNA Lesions in Human Cells." Int J Mol Sci **20**(1).

Raschle, M., P. Knipscheer, M. Enoiu, T. Angelov, J. Sun, J. D. Griffith, T. E. Ellenberger, O. D. Scharer and J. C. Walter (2008). "Mechanism of replication-coupled DNA interstrand crosslink repair." Cell **134**(6): 969-980.

Ray Chaudhuri, A., E. Callen, X. Ding, E. Gogola, A. A. Duarte, J. E. Lee, N. Wong, V. Lafarga, J. A. Calvo, N. J. Panzarino, S. John, A. Day, A. V. Crespo, B. Shen, L. M. Starnes, J. R. de Ruiter, J. A. Daniel, P. A. Konstantinopoulos, D. Cortez, S. B. Cantor, O. Fernandez-Capetillo, K. Ge, J. Jonkers, S. Rottenberg, S. K. Sharan and A. Nussenzweig (2016). "Replication fork stability confers chemoresistance in BRCA-deficient cells." Nature **535**(7612): 382-387.

Ray Chaudhuri, A., Y. Hashimoto, R. Herrador, K. J. Neelsen, D. Fachinetti, R. Bermejo, A. Cocito, V. Costanzo and M. Lopes (2012). "Topoisomerase I poisoning results in PARP-mediated replication fork reversal." Nat Struct Mol Biol **19**(4): 417-423.

Rizzo, A. A., F. M. Vassel, N. Chatterjee, S. D'Souza, Y. Li, B. Hao, M. T. Hemann, G. C. Walker and D. M. Korzhnev (2018). "Rev7 dimerization is important for assembly and function of the Rev1/Polzeta translesion synthesis complex." Proc Natl Acad Sci U S A **115**(35): E8191-E8200.

Rocha, C. R. R., M. M. Silva, A. Quinet, J. B. Cabral-Neto and C. F. M. Menck (2018). "DNA repair pathways and cisplatin resistance: an intimate relationship." Clinics (Sao Paulo) **73**(suppl 1): e478s.

Rodriguez-Acebes, S., S. Mouron and J. Mendez (2018). "Uncoupling fork speed and origin activity to identify the primary cause of replicative stress phenotypes." J Biol Chem **293**(33): 12855-12861.

Rosental, B., M. Brusilovsky, U. Hadad, D. Oz, M. Y. Appel, F. Afergan, R. Yossef, L. A. Rosenberg, A. Aharoni, A. Cerwenka, K. S. Campbell, A. Braiman and A. Porgador (2011). "Proliferating cell nuclear antigen is a novel inhibitory ligand for the natural cytotoxicity receptor NKp44." J Immunol **187**(11): 5693-5702.

Rosic, S., R. Amouroux, C. E. Requena, A. Gomes, M. Emperle, T. Beltran, J. K. Rane, S. Linnett, M. E. Selkirk, P. H. Schiffer, A. J. Bancroft, R. K. Grencis, A. Jeltsch, P. Hajkova and P. Sarkies (2018). "Evolutionary analysis indicates that DNA alkylation damage is a byproduct of cytosine DNA methyltransferase activity." Nat Genet **50**(3): 452-459.

Roy, U. and O. D. Scharer (2016). "Involvement of translesion synthesis DNA polymerases in DNA interstrand crosslink repair." DNA Repair (Amst) **44**: 33-41.

Sabbioneda, S., A. M. Gourdin, C. M. Green, A. Zotter, G. Giglia-Mari, A. Houtsmuller, W. Vermeulen and A. R. Lehmann (2008). "Effect of proliferating cell nuclear antigen

ubiquitination and chromatin structure on the dynamic properties of the Y-family DNA polymerases." Mol Biol Cell **19**(12): 5193-5202.

Santangelo, L., M. Gigante, G. S. Netti, S. Diella, F. Puteo, V. Carbone, G. Grandaliano, M. Giordano and L. Gesualdo (2014). "A novel SMARCAL1 mutation associated with a mild phenotype of Schimke immuno-osseous dysplasia (SIOD)." BMC Nephrol **15**: 41.

Sasi, N. K., F. Coquel, Y. L. Lin, J. P. MacKeigan, P. Pasero and M. Weinreich (2018). "DDK Has a Primary Role in Processing Stalled Replication Forks to Initiate Downstream Checkpoint Signaling." Neoplasia **20**(10): 985-995.

Sawant, A., A. Kothandapani, A. Zhitkovich, R. W. Sobol and S. M. Patrick (2015). "Role of mismatch repair proteins in the processing of cisplatin interstrand cross-links." DNA Repair (Amst) **35**: 126-136.

Scharer, O. D. (2005). "DNA interstrand crosslinks: natural and drug-induced DNA adducts that induce unique cellular responses." Chembiochem **6**(1): 27-32.

Schlacher, K., N. Christ, N. Siaud, A. Egashira, H. Wu and M. Jasin (2011). "Double-strand break repair-independent role for BRCA2 in blocking stalled replication fork degradation by MRE11." Cell **145**(4): 529-542.

Sebesta, M., C. D. O. Cooper, A. Ariza, C. J. Carnie and D. Ahel (2017). "Structural insights into the function of ZRANB3 in replication stress response." Nat Commun **8**: 15847.

Sharma, S. and C. E. Canman (2012). "REV1 and DNA polymerase zeta in DNA interstrand crosslink repair." Environ Mol Mutagen **53**(9): 725-740.

Sharma, S., J. K. Hicks, C. L. Chute, J. R. Brennan, J. Y. Ahn, T. W. Glover and C. E. Canman (2012). "REV1 and polymerase zeta facilitate homologous recombination repair." Nucleic Acids Res **40**(2): 682-691.

Shen, X., S. Jun, L. E. O'Neal, E. Sonoda, M. Bemark, J. E. Sale and L. Li (2006). "REV3 and REV1 play major roles in recombination-independent repair of DNA interstrand cross-links mediated by monoubiquitinated proliferating cell nuclear antigen (PCNA)." J Biol Chem **281**(20): 13869-13872.

Shima, N., A. Alcaraz, I. Liachko, T. R. Buske, C. A. Andrews, R. J. Munroe, S. A. Hartford, B. K. Tye and J. C. Schimenti (2007). "A viable allele of Mcm4 causes chromosome instability and mammary adenocarcinomas in mice." Nat Genet **39**(1): 93-98.

Sidorova, J. M., K. Kehrli, F. Mao and R. Monnat, Jr. (2013). "Distinct functions of human RECQ helicases WRN and BLM in replication fork recovery and progression after hydroxyurea-induced stalling." DNA Repair (Amst) **12**(2): 128-139.

Slade, D. (2018). "Maneuvers on PCNA Rings during DNA Replication and Repair." Genes (Basel) **9**(8).

Smith, C. E., B. Llorente and L. S. Symington (2007). "Template switching during break-induced replication." Nature **447**(7140): 102-105.

Sogaard, C. K., A. Blindheim, L. M. Rost, V. Petrovic, A. Nepal, S. Bachke, N. B. Liabakk, O. A. Gederaas, T. Viset, C. J. Arum, P. Bruheim and M. Otterlei (2018). ""Two hits - one stone"; increased efficacy of cisplatin-based therapies by targeting PCNA's role in both DNA repair and cellular signaling." Oncotarget **9**(65): 32448-32465.

Sogaard, C. K., S. A. Moestue, M. B. Rye, J. Kim, A. Nepal, N. B. Liabakk, S. Bachke, T. F. Bathen, M. Otterlei and D. K. Hill (2018). "APIM-peptide targeting PCNA improves the efficacy of docetaxel treatment in the TRAMP mouse model of prostate cancer." Oncotarget **9**(14): 11752-11766.

Sogaard, C. K., A. Nepal, V. Petrovic, A. Sharma, N. B. Liabakk, T. S. Steigedal and M. Otterlei (2019). "Targeting the non-canonical roles of PCNA modifies and increases the response to targeted anti-cancer therapy " Oncotarget **In press**.

Sogo, J. M., M. Lopes and M. Foiani (2002). "Fork reversal and ssDNA accumulation at stalled replication forks owing to checkpoint defects." Science **297**(5581): 599-602.

Sorensen, C. S., R. G. Syljuasen, J. Falck, T. Schroeder, L. Ronnstrand, K. K. Khanna, B. B. Zhou, J. Bartek and J. Lukas (2003). "Chk1 regulates the S phase checkpoint by coupling the physiological turnover and ionizing radiation-induced accelerated proteolysis of Cdc25A." Cancer Cell **3**(3): 247-258.

Sotiriou, S. K., I. Kamileri, N. Lugli, K. Evangelou, C. Da-Re, F. Huber, L. Padayachy, S. Tardy, N. L. Nicati, S. Barriot, F. Ochs, C. Lukas, J. Lukas, V. G. Gorgoulis, L. Scapozza and T. D. Halazonetis (2016). "Mammalian RAD52 Functions in Break-Induced Replication Repair of Collapsed DNA Replication Forks." Mol Cell **64**(6): 1127-1134.

Spirek, M., J. Mlcouskova, O. Belan, M. Gyimesi, G. M. Harami, E. Molnar, J. Novacek, M. Kovacs and L. Krejci (2018). "Human RAD51 rapidly forms intrinsically dynamic nucleoprotein filaments modulated by nucleotide binding state." Nucleic Acids Res **46**(8): 3967-3980.

Taglialatela, A., S. Alvarez, G. Leuzzi, V. Sannino, L. Ranjha, J. W. Huang, C. Madubata, R. Anand, B. Levy, R. Rabadan, P. Cejka, V. Costanzo and A. Ciccia (2017). "Restoration of Replication Fork Stability in BRCA1- and BRCA2-Deficient Cells by Inactivation of SNF2-Family Fork Remodelers." Mol Cell **68**(2): 414-430 e418.

Takaoka, K., M. Kawazu, J. Koya, A. Yoshimi, Y. Masamoto, H. Maki, T. Toya, T. Kobayashi, Y. Nannya, S. Arai, T. Ueno, H. Ueno, K. Suzuki, H. Harada, A. Manabe, Y. Hayashi, H. Mano and M. Kurokawa (2019). "A germline HLTF mutation in familial MDS induces DNA damage accumulation through impaired PCNA polyubiquitination." Leukemia **33**(7): 1773-1782.

Thangavel, S., M. Berti, M. Levikova, C. Pinto, S. Gomathinayagam, M. Vujanovic, R. Zellweger, H. Moore, E. H. Lee, E. A. Hendrickson, P. Cejka, S. Stewart, M. Lopes and A. Vindigni (2015). "DNA2 drives processing and restart of reversed replication forks in human cells." J Cell Biol **208**(5): 545-562.

Tian, F., S. Sharma, J. Zou, S. Y. Lin, B. Wang, K. Rezvani, H. Wang, J. D. Parvin, T. Ludwig, C. E. Canman and D. Zhang (2013). "BRCA1 promotes the ubiquitination of PCNA and recruitment of translesion polymerases in response to replication blockade." Proc Natl Acad Sci U S A **110**(33): 13558-13563.

Tissier, A., J. P. McDonald, E. G. Frank and R. Woodgate (2000). "poliota, a remarkably error-prone human DNA polymerase." Genes Dev **14**(13): 1642-1650.

Toledo, L. I., M. Altmeyer, M. B. Rask, C. Lukas, D. H. Larsen, L. K. Povlsen, S. Bekker-Jensen, N. Mailand, J. Bartek and J. Lukas (2013). "ATR prohibits replication catastrophe by preventing global exhaustion of RPA." Cell **155**(5): 1088-1103.

Tomas-Roca, L., A. Tsaalbi-Shtylik, J. G. Jansen, M. K. Singh, J. A. Epstein, U. Altunoglu, H. Verzijl, L. Soria, E. van Beusekom, T. Roscioli, Z. Iqbal, C. Gilissen, A. Hoischen, A. P. M. de Brouwer, C. Erasmus, D. Schubert, H. Brunner, A. Perez Aytes, F. Marin, P. Aroca, H. Kayserili, A. Carta, N. de Wind, G. W. Padberg and H. van Bokhoven (2015). "De novo mutations in PLXND1 and REV3L cause Mobius syndrome." Nat Commun **6**: 7199.

Tomasetti, C. and B. Vogelstein (2015). "Cancer etiology. Variation in cancer risk among tissues can be explained by the number of stem cell divisions." Science **347**(6217): 78-81.

Tomasz, M. (1995). "Mitomycin C: small, fast and deadly (but very selective)." Chem Biol **2**(9): 575-579.

Tonzi, P., Y. Yin, C. W. T. Lee, E. Rothenberg and T. T. Huang (2018). "Translesion polymerase kappa-dependent DNA synthesis underlies replication fork recovery." Elife **7**.

Tsutakawa, S. E., C. Yan, X. Xu, C. P. Weinacht, B. D. Freudenthal, K. Yang, Z. Zhuang, M. T. Washington, J. A. Tainer and I. Ivanov (2015). "Structurally distinct ubiquitin- and sumo-modified PCNA: implications for their distinct roles in the DNA damage response." Structure **23**(4): 724-733.

Tubbs, J. L., A. E. Pegg and J. A. Tainer (2007). "DNA binding, nucleotide flipping, and the helix-turn-helix motif in base repair by O6-alkylguanine-DNA alkyltransferase and its implications for cancer chemotherapy." DNA Repair (Amst) **6**(8): 1100-1115.

Unk, I., I. Hajdu, A. Blastyak and L. Haracska (2010). "Role of yeast Rad5 and its human orthologs, HLTF and SHPRH in DNA damage tolerance." DNA Repair (Amst) **9**(3): 257-267.

Unk, I., I. Hajdu, K. Fatyol, J. Hurwitz, J. H. Yoon, L. Prakash, S. Prakash and L. Haracska (2008). "Human HLTF functions as a ubiquitin ligase for proliferating cell nuclear antigen polyubiquitination." Proc Natl Acad Sci U S A **105**(10): 3768-3773.

Unk, I., I. Hajdu, K. Fatyol, B. Szakal, A. Blastyak, V. Bermudez, J. Hurwitz, L. Prakash, S. Prakash and L. Haracska (2006). "Human SHPRH is a ubiquitin ligase for Mms2-Ubc13-dependent polyubiquitylation of proliferating cell nuclear antigen." Proc Natl Acad Sci U S A **103**(48): 18107-18112.

Vaisman, A. and R. Woodgate (2017). "Translesion DNA polymerases in eukaryotes: what makes them tick?" Crit Rev Biochem Mol Biol **52**(3): 274-303.

Vallerga, M. B., S. F. Mansilla, M. B. Federico, A. P. Bertolin and V. Gottifredi (2015). "Rad51 recombinase prevents Mre11 nuclease-dependent degradation and excessive PrimPol-mediated elongation of nascent DNA after UV irradiation." Proc Natl Acad Sci U S A **112**(48): E6624-6633.

Van Sloun, P. P., I. Varlet, E. Sonneveld, J. J. Boei, R. J. Romeijn, J. C. Eeken and N. De Wind (2002). "Involvement of mouse Rev3 in tolerance of endogenous and exogenous DNA damage." Mol Cell Biol **22**(7): 2159-2169.

Vanoli, F., M. Fumasoni, B. Szakal, L. Maloisel and D. Branzei (2010). "Replication and recombination factors contributing to recombination-dependent bypass of DNA lesions by template switch." PLoS Genet **6**(11): e1001205.

Villafanez, F., I. A. Garcia, S. Carbajosa, M. F. Pansa, S. Mansilla, M. C. Llorens, V. Angiolini, L. Guantay, H. Jacobs, K. P. Madauss, I. Gloger, V. Gottifredi, J. L. Bocco and G. Soria (2019). "AKT inhibition impairs PCNA ubiquitylation and triggers synthetic lethality in homologous recombination-deficient cells submitted to replication stress." Oncogene **38**(22): 4310-4324.

Vujanovic, M., J. Krietsch, M. C. Raso, N. Terraneo, R. Zellweger, J. A. Schmid, A. Taglialatela, J. W. Huang, C. L. Holland, K. Zwicky, R. Herrador, H. Jacobs, D. Cortez, A. Ciccia, L. Penengo and M. Lopes (2017). "Replication Fork Slowing and Reversal upon DNA Damage Require PCNA Polyubiquitination and ZRANB3 DNA Translocase Activity." Mol Cell **67**(5): 882-890 e885.

Wang, Y., R. Woodgate, T. P. McManus, S. Mead, J. J. McCormick and V. M. Maher (2007). "Evidence that in xeroderma pigmentosum variant cells, which lack DNA polymerase eta, DNA polymerase iota causes the very high frequency and unique spectrum of UV-induced mutations." Cancer Res **67**(7): 3018-3026.

Waraky, A., Y. Lin, D. Warsito, F. Haglund, E. Aleem and O. Larsson (2017). "Nuclear insulin-like growth factor 1 receptor phosphorylates proliferating cell nuclear antigen and rescues stalled replication forks after DNA damage." J Biol Chem **292**(44): 18227-18239.

Warbrick, E. (1998). "PCNA binding through a conserved motif." Bioessays **20**(3): 195-199.

Warbrick, E. (2006). "A functional analysis of PCNA-binding peptides derived from protein sequence, interaction screening and rational design." Oncogene **25**(20): 2850-2859.

Warren, A. J., A. E. Maccubbin and J. W. Hamilton (1998). "Detection of mitomycin C-DNA adducts in vivo by 32P-postlabeling: time course for formation and removal of adducts and biochemical modulation." Cancer Res **58**(3): 453-461.

Washington, M. T., R. E. Johnson, L. Prakash and S. Prakash (2002). "Human DINB1-encoded DNA polymerase kappa is a promiscuous extender of mispaired primer termini." Proc Natl Acad Sci U S A **99**(4): 1910-1914.

Williams, H. L., M. E. Gottesman and J. Gautier (2012). "Replication-independent repair of DNA interstrand crosslinks." Mol Cell **47**(1): 140-147.

Williams, H. L., M. E. Gottesman and J. Gautier (2013). "The differences between ICL repair during and outside of S phase." Trends Biochem Sci **38**(8): 386-393.

Wittschieben, J., M. K. Shivji, E. Lalani, M. A. Jacobs, F. Marini, P. J. Gearhart, I. Rosewell, G. Stamp and R. D. Wood (2000). "Disruption of the developmentally regulated Rev3l gene causes embryonic lethality." Curr Biol **10**(19): 1217-1220.

Wittschieben, J. P., S. C. Reshmi, S. M. Gollin and R. D. Wood (2006). "Loss of DNA polymerase zeta causes chromosomal instability in mammalian cells." Cancer Res **66**(1): 134-142.

Wolfle, W. T., M. T. Washington, L. Prakash and S. Prakash (2003). "Human DNA polymerase kappa uses template-primer misalignment as a novel means for extending mispaired termini and for generating single-base deletions." Genes Dev **17**(17): 2191-2199.

Woodward, A. M., T. Gohler, M. G. Luciani, M. Oehlmann, X. Ge, A. Gartner, D. A. Jackson and J. J. Blow (2006). "Excess Mcm2-7 license dormant origins of replication that can be used under conditions of replicative stress." J Cell Biol **173**(5): 673-683.

Wyatt, M. D. and D. L. Pittman (2006). "Methylating agents and DNA repair responses: Methylated bases and sources of strand breaks." Chem Res Toxicol **19**(12): 1580-1594.

Xie, K., J. Doles, M. T. Hemann and G. C. Walker (2010). "Error-prone translesion synthesis mediates acquired chemoresistance." Proc Natl Acad Sci U S A **107**(48): 20792-20797.

Xu, X., A. Lin, C. Zhou, S. R. Blackwell, Y. Zhang, Z. Wang, Q. Feng, R. Guan, M. D. Hanna, Z. Chen and W. Xiao (2016). "Involvement of budding yeast Rad5 in translesion DNA synthesis through physical interaction with Rev1." Nucleic Acids Res **44**(11): 5231-5245.

Yamada, M., K. Watanabe, M. Mistrik, E. Vesela, I. Protivankova, N. Mailand, M. Lee, H. Masai, J. Lukas and J. Bartek (2013). "ATR-Chk1-APC/CCdh1-dependent stabilization of Cdc7-ASK (Dbf4) kinase is required for DNA lesion bypass under replication stress." Genes Dev **27**(22): 2459-2472.

Yang, L., T. Shi, F. Liu, C. Ren, Z. Wang, Y. Li, X. Tu, G. Yang and X. Cheng (2015). "REV3L, a promising target in regulating the chemosensitity of cervical cancer cells." PLoS One **10**(3): e0120334.

Yang, Y., Y. Gao, A. Zlatanou, S. Tateishi, V. Yurchenko, I. B. Rogozin and C. Vaziri (2018). "Diverse roles of RAD18 and Y-family DNA polymerases in tumorigenesis." Cell Cycle **17**(7): 833-843.

Yarden, R. I., S. Metsuyanim, I. Pickholtz, S. Shabbeer, H. Tellio and M. Z. Papa (2012). "BRCA1-dependent Chk1 phosphorylation triggers partial chromatin disassociation of phosphorylated Chk1 and facilitates S-phase cell cycle arrest." Int J Biochem Cell Biol **44**(11): 1761-1769.

Yekezare, M., B. Gomez-Gonzalez and J. F. Diffley (2013). "Controlling DNA replication origins in response to DNA damage - inhibit globally, activate locally." J Cell Sci **126**(Pt 6): 1297-1306.

Yin, L., Y. Xie, S. Yin, X. Lv, J. Zhang, Z. Gu, H. Sun and S. Liu (2015). "The S-nitrosylation status of PCNA localized in cytosol impacts the apoptotic pathway in a Parkinson's disease paradigm." PLoS One **10**(2): e0117546.

Yoon, J. H., C. S. Lee, T. R. O'Connor, A. Yasui and G. P. Pfeifer (2000). "The DNA damage spectrum produced by simulated sunlight." J Mol Biol **299**(3): 681-693.

Yoon, J. H., M. J. McArthur, J. Park, D. Basu, M. Wakamiya, L. Prakash and S. Prakash (2019). "Error-Prone Replication through UV Lesions by DNA Polymerase theta Protects against Skin Cancers." Cell **176**(6): 1295-1309 e1215.

Yoon, J. H., L. Prakash and S. Prakash (2009). "Highly error-free role of DNA polymerase eta in the replicative bypass of UV-induced pyrimidine dimers in mouse and human cells." Proc Natl Acad Sci U S A **106**(43): 18219-18224.

Yoon, J. H., L. Prakash and S. Prakash (2010). "Error-free replicative bypass of (6-4) photoproducts by DNA polymerase zeta in mouse and human cells." Genes Dev **24**(2): 123-128.

Zan, H., A. Komori, Z. D. Li, A. Cerutti, A. Schaffer, M. F. Flajnik, M. Diaz and P. Casali (2001). "The translesion DNA polymerase zeta plays a major role in Ig and bcl-6 somatic hypermutation." Immunity **14**(5): 643-653.

Zegerman, P. and J. F. Diffley (2010). "Checkpoint-dependent inhibition of DNA replication initiation by Sld3 and Dbf4 phosphorylation." Nature **467**(7314): 474-478.

Zellweger, R., D. Dalcher, K. Mutreja, M. Berti, J. A. Schmid, R. Herrador, A. Vindigni and M. Lopes (2015). "Rad51-mediated replication fork reversal is a global response to genotoxic treatments in human cells." J Cell Biol **208**(5): 563-579.

Zeman, M. K. and K. A. Cimprich (2014). "Causes and consequences of replication stress." Nat Cell Biol **16**(1): 2-9.

Zhang, M., N. Huang, X. Yang, J. Luo, S. Yan, F. Xiao, W. Chen, X. Gao, K. Zhao, H. Zhou, Z. Li, L. Ming, B. Xie and N. Zhang (2018). "A novel protein encoded by the circular form of the SHPRH gene suppresses glioma tumorigenesis." Oncogene.

Zhang, S., J. Chea, X. Meng, Y. Zhou, E. Y. Lee and M. Y. Lee (2008). "PCNA is ubiquitinated by RNF8." Cell Cycle **7**(21): 3399-3404.

Zhang, S., H. Chen, X. Zhao, J. Cao, J. Tong, J. Lu, W. Wu, H. Shen, Q. Wei and D. Lu (2013). "REV3L 3'UTR 460 T>C polymorphism in microRNA target sites contributes to lung cancer susceptibility." Oncogene **32**(2): 242-250.

Zhao, Y., C. Biertumpfel, M. T. Gregory, Y. J. Hua, F. Hanaoka and W. Yang (2012). "Structural basis of human DNA polymerase eta-mediated chemoresistance to cisplatin." Proc Natl Acad Sci U S A **109**(19): 7269-7274.

Ziv, O., N. Geacintov, S. Nakajima, A. Yasui and Z. Livneh (2009). "DNA polymerase zeta cooperates with polymerases kappa and iota in translesion DNA synthesis across pyrimidine photodimers in cells from XPV patients." Proc Natl Acad Sci U S A **106**(28): 11552-11557.

Paper 1

Article

APIM-Mediated REV3L–PCNA Interaction Important for Error Free TLS Over UV-Induced DNA Lesions in Human Cells

Synnøve Brandt Ræder [1], Anala Nepal [1,2,†], Karine Øian Bjørås [1,†], Mareike Seelinger [1,†], Rønnaug Steen Kolve [1], Aina Nedal [1], Rebekka Müller [1] and Marit Otterlei [1,2,*]

[1] Department of Clinical and Molecular Medicine, Faculty of Medicine and Health Sciences, Norwegian University of Science and Technology (NTNU), N-7491 Trondheim, Norway; synnove.b.rader@ntnu.no (S.B.R.); anala.nepal@ntnu.no (A.N.); karine.bjoras@ntnu.no (K.Ø.B.); mareike.seelinger@ntnu.no (M.S.); ronnaugsk@gmail.com (R.S.K.); ainanedal11@gmail.com (A.N.); rebekka.muller.phd@gmail.com (R.M.)

[2] Clinic of Surgery, St. Olavs Hospital, Trondheim University Hospital, N-7006 Trondheim, Norway

* Correspondence: marit.otterlei@ntnu.no; Tel.: +47-92889422

† These authors contributed equally to this work.

check for updates

Abstract: Proliferating cell nuclear antigen (PCNA) is essential for the organization of DNA replication and the bypass of DNA lesions via translesion synthesis (TLS). TLS is mediated by specialized DNA polymerases, which all interact, directly or indirectly, with PCNA. How interactions between the TLS polymerases and PCNA affects TLS specificity and/or coordination is not fully understood. Here we show that the catalytic subunit of the essential mammalian TLS polymerase POLζ, REV3L, contains a functional AlkB homolog 2 PCNA interacting motif, APIM. APIM from REV3L fused to YFP, and full-length REV3L-YFP colocalizes with PCNA in replication foci. Colocalization of REV3L-YFP with PCNA is strongly reduced when an APIM-CFP construct is overexpressed. We also found that overexpression of full-length REV3L with mutated APIM leads to significantly altered mutation frequencies and mutation spectra, when compared to overexpression of full-length REV3L wild-type (WT) protein in multiple cell lines. Altogether, these data suggest that APIM is a functional PCNA-interacting motif in REV3L, and that the APIM-mediated PCNA interaction is important for the function and specificity of POLζ in TLS. Finally, a PCNA-targeting cell-penetrating peptide, containing APIM, reduced the mutation frequencies and changed the mutation spectra in several cell lines, suggesting that efficient TLS requires coordination mediated by interactions with PCNA.

1. Introduction

DNA damage is continuously induced by exogenous and endogenous sources. If not repaired prior to replication, these may result in replication fork collapse, strand breaks, cell death, or genomic instability. Cells have; therefore, evolved fine-tuned systems to handle replication fork stalling via two main pathways: translesion DNA synthesis (TLS) and template switching (TS). TLS is intrinsically error-prone and a major source of mutations, while TS is mostly error-free [1].

Proliferating cell nuclear antigen (PCNA) belongs to the conserved DNA clamp family, and the earliest known function of PCNA was docking of replicative polymerases to DNA. PCNA is a hub protein and essential for multiple DNA replication-associated processes, for example, chromatin remodeling/epigenetics, DNA repair, recombination/TS, and TLS [2,3]. When the replication fork

encounters a DNA lesion, mono-ubiquitination of PCNA is suggested to be important for mediating a polymerase switch, from the replicative polymerase to a TLS polymerase, which is able to synthesize over the lesion. In addition to the polymerase switch at replication forks, TLS polymerases are also believed to be important for the filling of post-replicative gaps left by replicative polymerases [1].

Several hundred proteins contain one or two of the PCNA-interacting motifs, called PCNA interacting peptide (PIP)-box and AlkB homolog 2 PCNA interacting motif (APIM), both of which are conserved in yeast [4,5]. These PCNA-binding motifs have an overlapping interaction site on PCNA [6–9]. The selection of which proteins interact with PCNA at any given time is likely coordinated by multi-layered regulatory mechanisms, including affinity-driven competition, post translational modifications (PTMs) of PCNA or PCNA-binding proteins, complex partners, as well as translational and proteolytic regulations [2].

The main polymerases in TLS are the Y-family polymerases, REV1, POLη, POLι POLκ and the B-family polymerase, POLζ. POLζ is an extender polymerase (i.e., it extends from the mismatch generated by the "inserter" TLS polymerases, POLη, POLι, or POLκ. However, POLζ has also been shown to insert bases opposite lesions [1]. The POLζ complex (here called POLζ consists of four subunits; REV3L, REV7, p50 (POLD2), and p66 (POLD3) [10]. The latter two are shared with the lagging strand replicative polymerase, POLδ. REV3L was recently also shown to be localized in mitochondria, where it associated with POLγ [11]. REV3L, the catalytic subunit, is essential for development and survival, for example, embryonic lethality is observed after REV3L knock out (KO) in mice [12,13], and higher sensitivity to UVC irradiation and chemotherapeutics, such as mitomycin-C (MMC), is seen in human cells with catalytically dead REV3L and REV3L KO cells [14]. The mammalian REV3L is 3130 amino acids (aa) long, which is twice the size of its yeast ortholog [12], and it contains the PCNA-interacting motif APIM in the predicted unstructured region (PCD) (aa 1240–1244), which is not present in yeast [5,15]. Whether APIM in mammalian REV3L is functional is not known.

REV1 acts as a scaffold for TLS via interactions with POLη, POLι, POLκ, POLζ subunit REV7, and PCNA. It is suggested that REV1 interacts with PCNA via its N-terminus BRCA1 C terminus (B RCT) domain and/or polymerase-associated (PAD) domain. POLη, POLι and POLκ contain the PIP-box, and interact directly with PCNA [1], but still they are dependent on REV1 for replicating over UV lesions [16]. POLζ, which contains a potential APIM in REV3L, can replicate over UV lesions independently of REV1. How exactly the most appropriate TLS polymerase is selected when needed likely depends both on the type of DNA lesion and on their ability to interact with their two main hub proteins, REV1 and PCNA.

In this study, we examined the in vivo properties of overexpressed full-length REV3L, and the functionality of APIM found in the predicted unstructured region of REV3L. Colocalization experiments, as well as analysis of mutation frequencies and mutations spectra after overexpression of full-length REV3L, supports that APIM in REV3L, and its direct interaction with PCNA, is important for REV3L's function in TLS. Furthermore, we found that an APIM-containing cell-penetrating peptide (APIM-peptide) targeting PCNA [6,17] reduced the mutation frequency more in the isogenic normal cell line than in POLζ-mutated cells. This data supports a role of APIM–PCNA interactions in TLS, and specifically in POLζ-mediated TLS.

2. Results and Discussion

2.1. REV3L Localization Increases in the Nuclei upon Genotoxic Stress and Inhibition of Nuclear Export

To determine REV3L localization, we overexpressed full-length REV3L tagged with YFP. REV3L localized both in the nucleus and cytosol, but the fraction of cells with nuclear localization increased after MMC treatment and UV irradiation (Figure 1a,b, and data not shown). This is in accordance with increased chromatin association after genotoxic stress previously reported [18]. Recently, REV3L was found to contain both functional nuclear and mitochondrial localization signals, and to associate with POLγ in mitochondria [11]. Some of the cytosolic REV3L could; therefore, be mitochondrial, but it

could also be due to overexpression. However, lack of specific antibodies against REV3L makes this hard to examine. Cytosolic localization could also indicate that the level of REV3L in nuclei is tightly regulated, for example by active nuclear export followed by protein degradation, to avoid mutagenic events. When the cells were treated with a specific inhibitor of active nuclear export, Leptomycin B [19], the fraction of cells with mainly nuclear REV3L-YFP localization increased (Figure 1b). This was not seen in cells expressing only the YFP-tag, where no cells had nuclear localization, even after Leptomycin B treatment (Supplementary Figure S1a,b). These results support that nuclear levels of REV3L are regulated via active nuclear export.
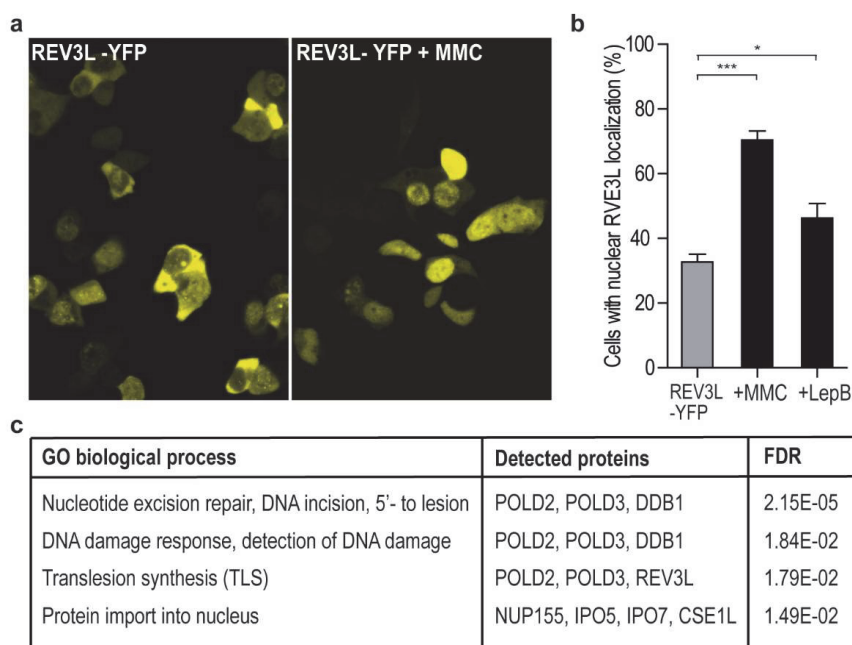

Figure 1. Increased nuclear REV3L localization after mitomycin-C (MMC) or Leptomycin B treatment. (**a**) Overview of subcellular localization of REV3L-YFP in HEK293T cells with and without MMC treatment (0.5 μM), measured after 12 h treatment. (**b**) Quantification of REV3L-YFP nuclear localization with and without MMC (0.5 μM) and Leptomycin B (LepB; 10 ng/mL, 1 h) treatment. Data from three independent biological experiments, each counting a minimum of 150 cells. (Student *t*-test, * $p = 0.017$, *** $p < 0.0001$). (**c**) Gene ontology (GO) analysis of proteins co-immunoprecipitated with REV3L-YFP using a PANTHER overrepresentation test. GO biological processes with a Benferroni-corrected *p*-value < 0.05 are shown. p-values given as false discovery rate (FDR).

In order to further characterize REV3L and its interaction partners, pull down experiments, using an anti-YFP antibody on extracts from weakly cross-linked cells overexpressing REV3L-YFP or YFP only, were performed. A weak PCNA band was detected on western blots after immunoprecipitation (IP) with anti-GFP from REV3L-YFP expressing cells, but also in some IPs from the control cells (YFP expressing cells). Thus, it was hard to determine if PCNA pull downs were significantly enriched in the REV3L-pull downs (data not shown). Next, we analyzed the same samples by mass spectrometry (MS). We did not detect PCNA, likely because PCNA is a "bad" flyer and not easily detected by MS [20]. However, we detected numerous proteins specifically pulled down by REV3L, including the subunits shared with POLδ, POLD2, and POLD3 (Figure 1c and Supplementary Table S1a). This suggests that the overexpressed tagged REV3L is functional and in complex with its normal partners. Gene ontology (GO) analysis revealed that the potential REV3L interaction partners were associated with the

following biological processes: nucleotide excision repair, DNA damage response, detection of DNA damage, protein import into nucleus and TLS (Figure 1c). We filtered proteins using the "CRAPome" database (www.crapome.org) prior to this analysis, however the biological processes detected did not change much from the list, including all proteins regarded as significantly enriched in REV3L-YFP pull downs (Supplementary Table S1b).

2.2. REV3L Colocalizes with PCNA and Contains a Functional APIM Sequence

The four subunit yeast POLζ complex is reported to have higher activity in presence of PCNA [10], thus how the different subunits interact with PCNA may be important, both for proper regulation of their activity and possibly also for fidelity/substrate specificity. The POLζ complex has two PCNA interacting motifs, POLD3 contains a PIP-box and REV3L contains the APIM sequence KFVLK (1240-1244). Previous data has shown that the second amino acid in APIM (consensus sequence: R/K-F/W/Y-L/I/V/A-L/I/V/A-K/R) is vital for affinity to PCNA [5,6,17,21]. After mutation of this amino acid, we found that both REV3L and REV3L F1241A colocalized in PCNA foci resembling replication foci (Figure 2a). This was not unexpected since REV3L pulled down both POLD2 and POLD3, both having the ability to interact directly or indirectly with PCNA [22–24]. Therefore, reducing the APIM-mediated REV3L–PCNA interaction by the F1241A mutation might not be sufficient to abolish colocalization with PCNA. However, KFVLK is a functional PCNA interacting motif, as KFVLK-YFP colocalizes with HcRed-PCNA in foci resembling replication foci (Figure 2b), similarly to the previously reported hABH2$_{1-7}$F4W APIM-variant (RWLVK) with increased affinity [5] (Supplementary Figure S1c), here shown as a CFP-fusion. Furthermore, when F in KFVLK is mutated (corresponds to F1241A in REV3L), colocalization with PCNA is strongly reduced (Figure 2c).
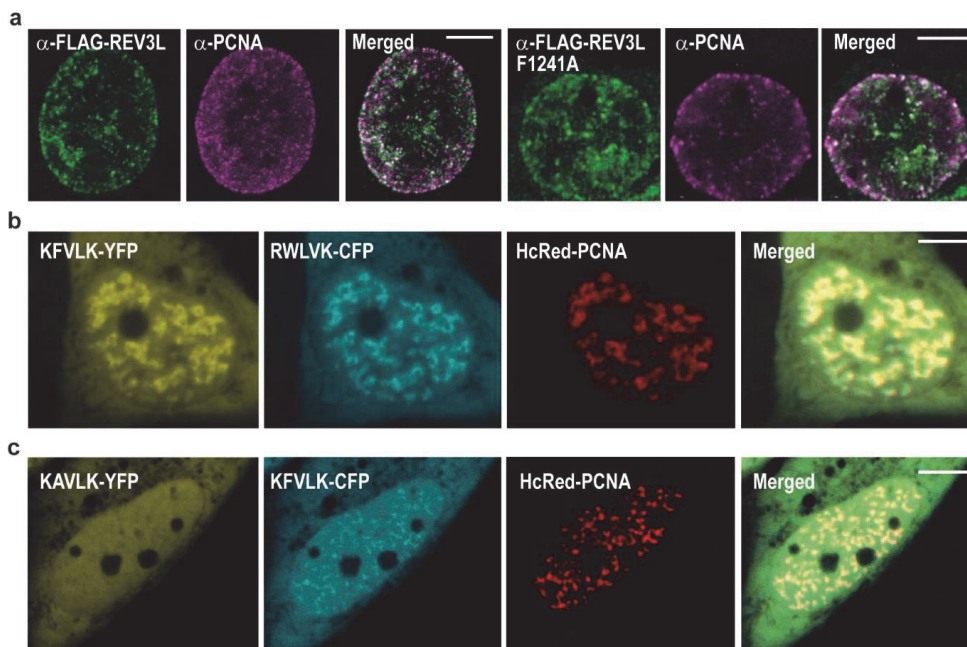

Figure 2. Overexpressed full-length REV3L and APIM peptide from REV3L (KFVLK-YFP) colocalizes with endogenous and overexpressed PCNA. White line on merged images represents 5 µm scale. Representative images display: (**a**) REV3L or REV3L F1241A (α-FLAG) and endogenous PCNA (α-PCNA) in transfected HEK293T cells (STED image); (**b**) KFVLK-YFP (REV3L APIM), RWLVK-CFP, and HcRed-PCNA in transfected HeLa cells (live cell images); and (**c**) KAVLK-YFP (REV3L F1241A-APIM), KFVLK-CFP (REV3L APIM), and HcRed-PCNA in transfected HeLa cells (live cell image).

In order to visually detect reduced colocalization/affinity, a large change is required. Fluorescence resonance energy transfer (FRET) measurements would have been the preferred technique, as it can quantifiably differentiate between direct interaction (<20 nm distance) and colocalization (~50–100 nm distance). For example, in a previous study, we found that the direct Xeroderma pigmentosum group-A complementing protein (XPA)–PCNA interaction determined by FRET was abolished when APIM in XPA was mutated; however, XPA with mutated APIM still colocalized with PCNA in replication foci [25]. We have made several attempts to measure FRET between REV3L-YFP (WT and F1241A) and CFP-PCNA. However, the large size of REV3L results in low expression levels and; therefore, low fluorescence intensity compared to PCNA. Therefore, FRET measurements were not technically possible. Second best to FRET, we have measured fold increase in intensity in foci over the background of REV3L-YFP (WT and F1241A), in the absence and presence of overexpressed APIM-CFP. When selecting images taken with the same confocal settings and comparing only cells with equal protein expression levels, we detected higher intensity in foci of REV3L than REV3L F1241A-YFP (Figure 3a). The foci intensities of both full-length proteins were reduced upon overexpression of the APIM motif in REV3L (KFVLK) and importantly, we detected a larger (>2×) reduction for REV3L F1241A than REV3L (26% versus 11%, Figure 3b), suggesting that REV3L F1241A has lower affinity for PCNA than REV3L.

When the high affinity APIM variant (RWLVK) was overexpressed, it nearly abolished the foci formation of both REV3L and REV3L F1241A (Figure 3c). APIM and PIP-box motifs have overlapping interaction sites on PCNA [6,9], and different PIP-box variants are shown to have up to 700× differences in their affinities for PCNA [23], with the PIP-box from p21 being the strongest. The high affinity APIM variant (RWLVK), which has a ~5× lower dissociation constant than the p21 PIP-box in microscale thermophoresis (MST) experiments [17], may be able to compete with both the PIP-box in POLD3 and the APIM in REV3L, for binding to PCNA, explaining the strong reduction of REV3L foci localization observed. We could not detect any differences in colocalization and/or intensities of REV3L in PCNA foci after treatments with DNA inducing damaging agents such as cisplatin, MMC, or UV irradiation (data not shown), although a stronger nuclear localization of REV3L was detected. In summary, these results suggest that REV3L is present in unperturbed replication foci and that the REV3L APIM–PCNA interaction is important for its affinity for PCNA.

2.3. Mutation of APIM in REV3L Affects the Mutation Frequency

Biochemical assays to test APIM functionality in REV3L is very difficult because REV3L is a very large protein (3130 aa) in complex with multiple other proteins, and interactions with PCNA is a process which is tightly regulated via, for example, PTMs. Therefore, in order to investigate APIM functionality in REV3L, REV3L-YFP (WT and F1241A) were overexpressed in one repair-proficient (HEK293) and one TLS-deficient cell line (POLη KO), together with an UV-irradiated reporter plasmid (SupF mutagenesis assay). The transfection efficiency was 30–50%, and no differences were detected between expression of REV3L and REV3L F1241A (Supplementary Figure S2a). The difference in mutation frequencies between independent experiments detected in the SupF assays was large, still we repeatedly detected a 2–3 times reduction in mutation frequency in cells overexpressing REV3L, compared to cells overexpressing REV3L F1241A, in both cell lines (Figure 4a). Differences in mutation frequencies after REV3L and REV3L F1241A overexpression were also found in two DNA repair-deficient cell lines; a nucleotide excision repair (NER) deficient fibroblast cell line (XPA$^{-/-}$) and a mismatch repair (MMR) deficient cell line (MLH1$^{-/-}$) (Supplementary Figure S2b). Overexpression of REV3L in HEK293 and POLη KO cells reduced the mutation frequency compared to both the control and the REV3L F1241A expressing cells, and this could suggest that APIM in REV3L, and; thus, a direct REV3L–PCNA interaction, contributes to the correct bypass of UV-lesions. Human POLζ has previously been reported to perform error-free replicative bypass of (6-4) photoproducts [26]. However, whether REV3L can bypass lesions correctly or not likely depends upon the damage type and load, and, the DNA repair capacity of the cells. Human POLζ is reported to be able to replicate over UV lesions independently of REV1 [16]. Whether the APIM-mediated PCNA interaction in POLζ is more

important for REV1 independent than REV1-dependent bypass of DNA lesions is not possible to predict from our data, and requires additional studies beyond the scope of this paper.
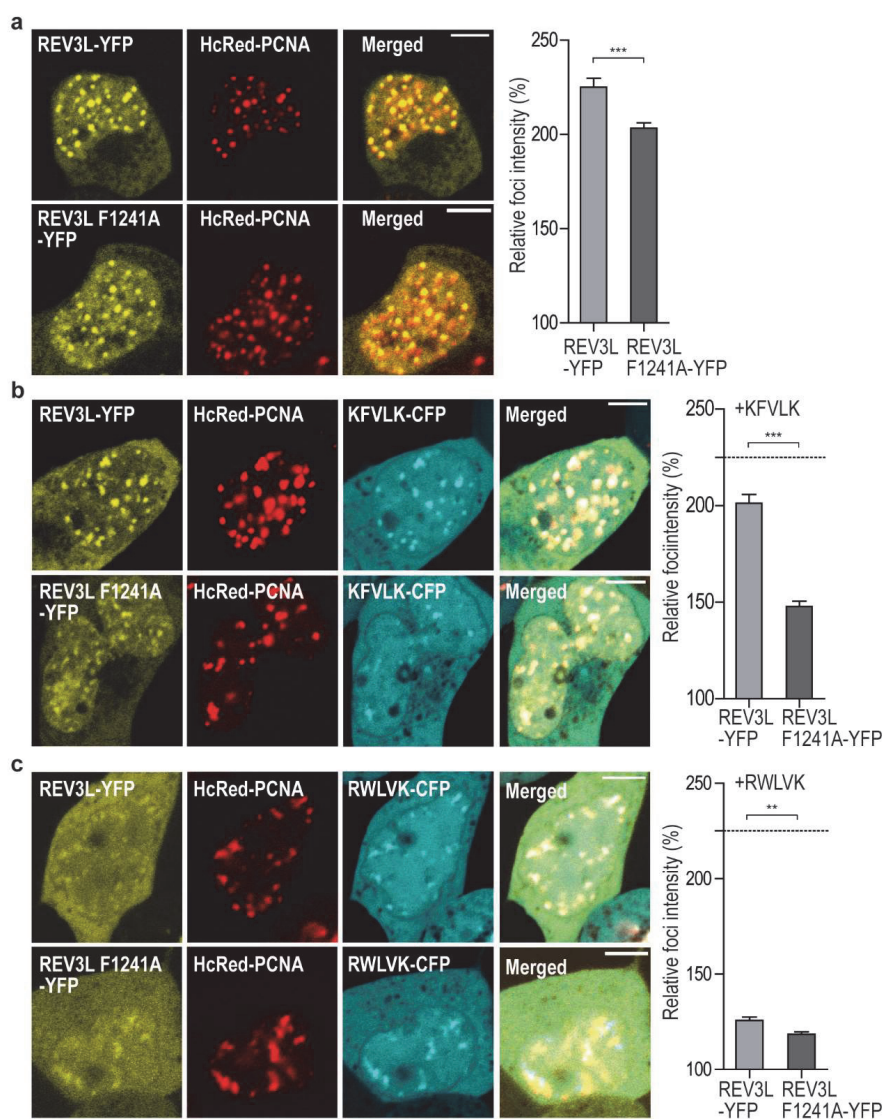

Figure 3. REV3L colocalization with PCNA in replication foci is reduced upon F1241A mutation and overexpression of APIM-peptides. Left panel: Representative live cell images of HEK293T cells overexpressing REV3L-YFP (upper row) or REV3L F1241A-YFP (lower row) and HcRed-PCNA. Scale bar = 5 μm. Right panel: Quantification of foci intensities of REV3L-YFP and REV3LF1241A-YFP in PCNA foci relative to background intensities (Image J). Data is from a minimum of 50 foci taken from 7 to 15 cells with comparable protein expression levels of both YFP and CFP tagged proteins. Student two-tailed unpaired *t*-test: (**a**) REV3L and REV3L F1241A-YFP and HcRed-PCNA (*** p = 0.0002); (**b**) REV3L and REV3L F1241A-YFP, HcRed-PCNA and KFVLK-CFP (*** p < 0.0001). Dotted line represents the value of REV3L-YFP foci intensity without peptide overexpression from (**a**). (**c**) REV3L and REV3L F1241A-YFF, HcRed-PCNA and RWLVK-CFP (** p = 0.0011). Dotted line represents the value of REV3L-YFP foci intensity without peptide overexpression from (**a**).
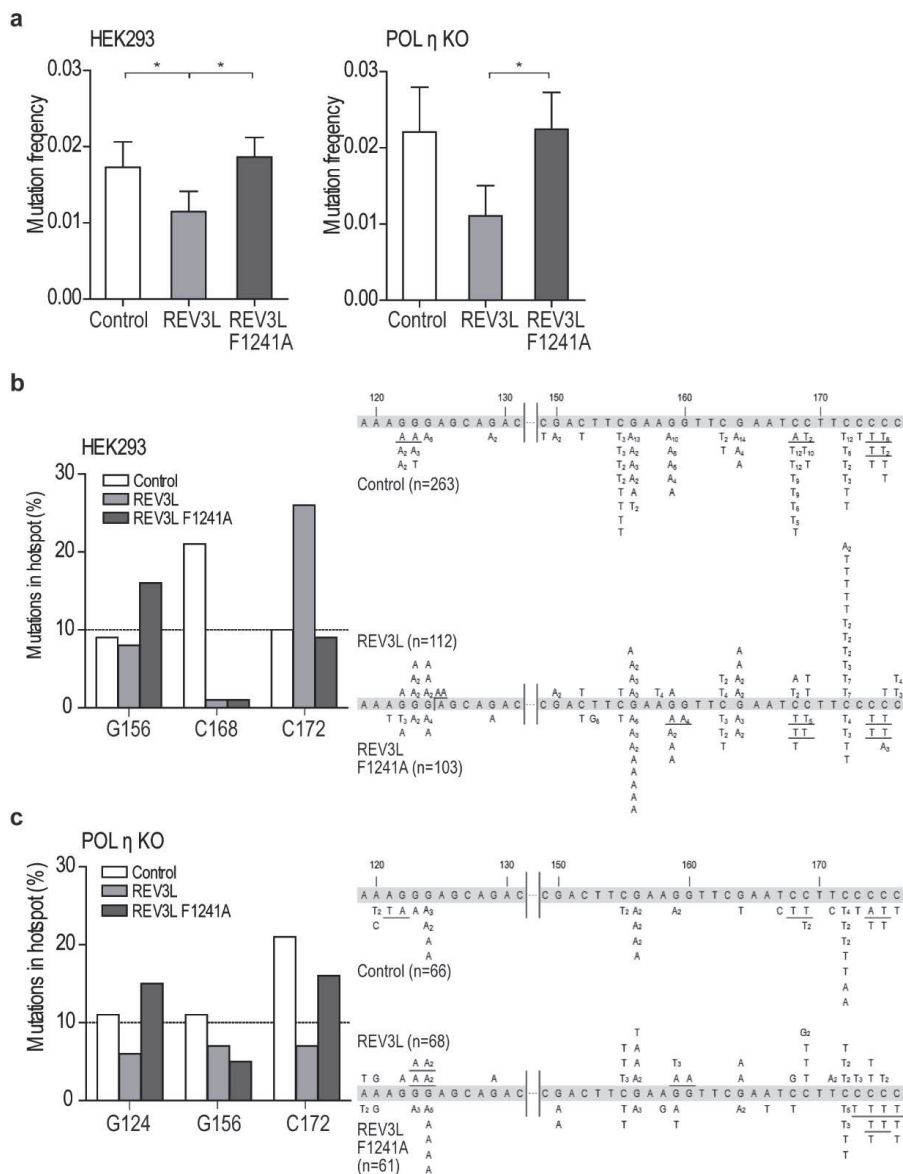
Figure 4. Mutation in APIM in REV3L (F1241A) affects the mutation frequency and pattern. (**a**) Mutation frequency determined by the supF assay from overexpression of REV3L-YFP or REV3L F1241A-YFP in HEK 293 and POLη KO (HAP-1) cells. Cells expressing only UVB-irradiated pSP189 (supF reporter plasmid) represents the control. Four independent experiments are shown for each cell line. Students two-tailed paired *t*-test, * $p < 0.05$. (**b**,**c**) Mutation spectra (*supF* gene) isolated from cells overexpressing REV3L-YFP, REV3L F1241A-YFP, or only pSP189 (control) in HEK293 cells (**b**) and POLη KO cells (**c**) from four independent experiments. Left panel: Mutations at sites in the *supF* gene occurring with a frequency > 10% in either control (white bars), REV3L (light grey bars), or REV3L F1241A-expressing cells (dark grey bars). Right panel: Mutation spectra. The number in subscript indicates how many times the specific mutation was detected in the same transformation. Tandem and quadruple mutations are underlined.

2.4. Mutation of APIM in REV3L Affects the Mutation Spectra in Four Cell Lines

The mutation spectra of the *supF* gene isolated from REV3L and REV3L F1241A overexpressing HEK293 cells showed a clear reduction of mutations at position 168 compared to the control cells (Figure 4b, left panel). This verifies that both proteins were expressed in sufficient levels to affect TLS. The spectra importantly also revealed differences between REV3L and REV3L F1241A overexpression (e.g., in the frequency of mutations at position 172 and 156). This suggests that the mutation of APIM in REV3L affected the specificity/function of POLζ.

The mutation spectra from the POLη-deficient cells also showed clear differences between cells overexpressing REV3L and REV3L F1241A at multiple positions, further supporting that APIM in REV3L is important for POLζ's specificity (Figure 4c). Additionally, and importantly in this context, the mutation spectra from cells overexpressing REV3L and REV3L F1241A were different also in the $XPA^{-/-}$ and $MLH1^{-/-}$ cell lines (Supplementary Figure S2c,d).

Because of the large size of POLζ, previous studies on the polymerase functionality have been done on yeast protein [15] or truncated human REV3L variants [10,14]. This is the first study of the functionality of full-length proteins including the APIM-containing PCD region in REV3L. The differences detected in both the mutation frequencies and the mutation spectra after overexpression of REV3L and REV3L F1241A, in all four cell lines tested, further suggest that APIM in REV3L is a functional PCNA interacting motif. The F1241A mutation is not expected to change the REV3L binding to REV7 nor REV3L's catalytic activity, because both the REV7 binding region and the catalytic domain are located distant to the PCD region [15]. We hypothesize that the changes in mutation frequency and mutation spectra observed by mutating APIM is due to reduced direct interaction between REV3L and PCNA. Impairing the direct interaction between REV3L and PCNA could either slightly change the proximity of REV3L to DNA, or the switch between the inserter and the extender TLS polymerase, and this could affect TLS and give rise to the differences in mutation frequency and mutation spectra observed between REV3L and REV3F1241A.

POLη interacts with PCNA via the two modules, PIP-box and ubiquitin-binding zinc-finger domain (UBZ), and mutations of one of these modules only partly reduce POLη's ability to complement Xeroderma pigmentosum variant (XP-V) cells after UV-irradiation [27]. Thus, multiple PCNA interacting modules working cooperatively to stabilize interaction of TLS POLs with PCNA in vivo is known also for other TLS polymerases. Recent data additionally suggests POLη travels with unperturbed replication forks [28]. If TLS polymerases are following a "piggyback" model as suggested (reviewed in [29]) (i.e., they ride on the PCNA ring until the replicative polymerases encounter a DNA lesion), then several interaction motifs of the functional polymerase complex might be required for regulation of their activities.

2.5. Targeting PCNA with APIM-Containing Peptides Reduce the Mutation Frequency

In order to further investigate the potential importance of APIM in REV3L, we wanted to make a cell line with an endogenous mutation in the APIM sequence of REV3L. We were not able to create a guide RNA including APIM in REV3L, and therefore decided to use a guide RNA targeting a sequence upstream of APIM. We initially selected mutated cells based on their hypersensitivity to MMC and UV-irradiation, and normal sensitivity to methyl methanesulfonate (MMS), and, surprisingly, the most sensitive clone obtained contained a homozygote single amino acid deletion, two amino acids upstream of APIM (REV3L ΔA1237) (Supplementary Figure S3a–d). No off-targets of significance could explain the observed phenotype in the REV3L ΔA1237 cell line (Supplementary Figure S3e). Because commercial antibodies against REV3L are not available, we tried to establish a targeted MS/MS method for determination of cellular REV3L levels. The level of endogenous REV3L in HEK293 was, as also found by others [11], low and below the detection limit, thus MS/MS detection was not technically possible (levels not detected in four out of five experiments, data not shown). In order to explore the consequence of the ΔA1237 deletion in REV3L, we overexpressed REV3L ΔA1237 as an YFP fusion (REV3L ΔA1237-YFP) and detected reduced nuclear localization of REV3L ΔA1237-YFP compared to

REV3L-YFP (Figure 5a,b). Despite this difference, overexpressed REV3L ΔA1237-YFP still colocalized with PCNA when co-expressed with HcRed-PCNA (Figure 5c). Reduced nuclear localization was not detected for the REV3L F1241A mutant (Supplementary Figure S1d), even though both REV3L ΔA1237 and REV3L F1241A have reduced foci intensities compared to REV3L WT (Figures 5c and 3a, respectively). Overexpression of APIM from REV3L (KFVLK) reduced REV3L ΔA1237-YFP foci less than REV3L F1241A-YPF (13% versus 26%, respectively), but slightly more than REV3L WT (11%) (Figures 5c and 3b), indicating that the reduced nuclear localization caused by the ΔA1237 deletion is not mainly due to its reduced PCNA affinity. The single amino acid deletion does not affect nuclear export of REV3L ΔA1237, as Leptomycin B treatment still increased nuclear fraction (data not shown). Thus, reduced nuclear localization and/or stability of REV3L ΔA1237 compared to REV3L WT is likely the main reason for the observed hypersensitivity towards UV-irradiation and MMC in this cell line.
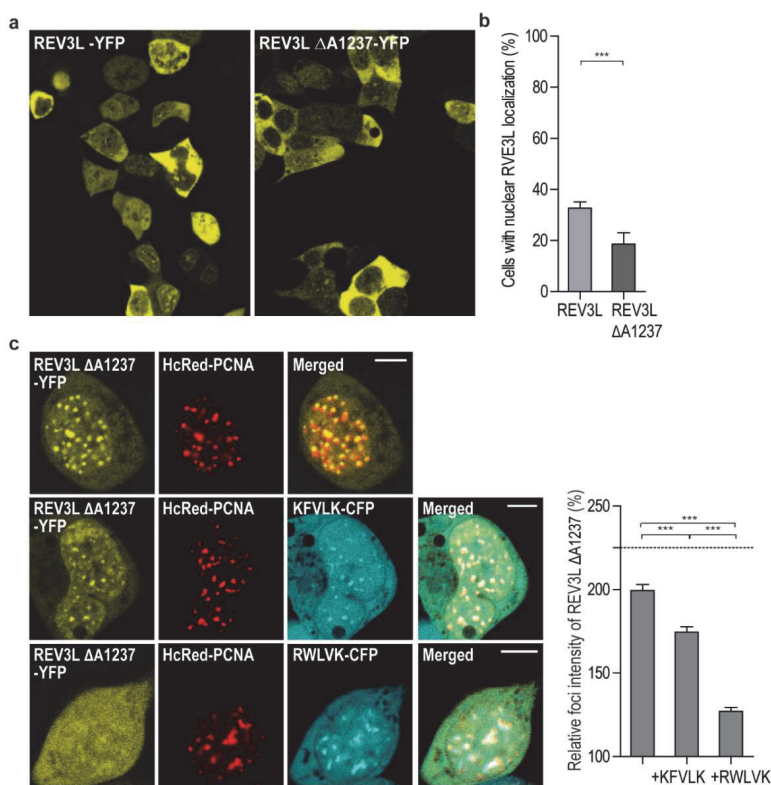

Figure 5. Deletion of A1237 in REV3L affects nuclear localization. (**a**) Overview of cells expressing REV3L-YFP and REV3L ΔA1237-YFP in HEK293T cells (live cell images). (**b**) Quantification of the cells with nuclear localization of REV3L-YFP (also shown in Figure 1b) compared to REV3L ΔA1237-YFP. Data from three independent biological experiments from a minimum of 150 cells. (Student *t*-test, *** $p < 0.0001$). (**c**) Left panel: Representative confocal images of HEK293T cells overexpressing REV3L ΔA1237-YFP and HcRed-PCNA (upper row); REV3L ΔA1237–YFP, HcRed-PCNA, and KFVLK-CFP (mid row); and REV3L ΔA1237-YFP, HcRed-PCNA, and RWLVK-CFP (bottom row). White line on merged images represents 5 μm scale. Right panel: Quantification of foci intensities of REV3L ΔA1237 -YFP in PCNA foci over background intensities (Image J). Data from a minimum of 50 foci taken from a minimum of 7 to 10 cells with comparable protein expression levels of both YFP and CFP tagged proteins. (Student two-tailed unpaired *t*-test, *** $p \leq 0.0002$). Dotted line represents the value of REV3L foci intensity without peptide overexpression from Figure 1a.

The mutation spectra of the *supF* gene isolated from REV3L ΔA1237 cells and its isogenic control HEK293 were different, supporting a reduced level of REV3L and an altered TLS pattern in the REV3L ΔA1237 cell line (Figure 6b). For example, mutations in position 168 that are frequent in HEK293 cells were absent in REV3L ΔA1237, and mutations in position 108 were found only in REV3L ΔA1237 (white bars, Figure 6a,b, left panel). Cumulatively, these results show that the REV3L ΔA1237 cell line has an altered TLS response, which, together with its hypersensitivity to MMC, might suggest that it is partly POLζ deficient.

We have previously designed a cell penetrating peptide containing the APIM sequence RWLVK (APIM-peptide), with high PCNA affinity, and a mutated version of this peptide (W4A) with ~50% reduced PCNA affinity [6,17]. Co-treatments with the APIM-peptide are shown to increase the efficacy of multiple chemotherapeutic drugs in multiple cancer cells and preclinical animal models [6,30–32]. In Figure 3c we showed that overexpression of RWLVK strongly reduced the colocalization between REV3L and PCNA. We have unpublished data indicating that a significant part of the increased growth inhibitory efficacy observed when combining APIM-peptide with cisplatin (another inter-strand crosslinking agent), is mediated via REV3L inhibition, because siRNA knock down of REV3L had less effect in cells overexpressing the APIM-peptide (data not shown). In order to explore the impact of inhibiting the APIM-mediated REV3L–PCNA interaction on TLS, HEK293 and the REV3L ΔA1237 cells were treated with the APIM-peptide during the SupF assay. In agreement with previous results [6,30], this treatment did not inhibit replication and we were able to isolate newly replicated SupF reporter plasmid. Interestingly, APIM-peptide treatment reduced the mutation frequency in HEK293 cells by ~70% compared to the control, while the reduction was only ~30% in the REV3L ΔA1237 cells (Figure 6c, $p < 0.05$). No reduction in the mutation frequency was detected in similar experiments using the mutant APIM-peptide (Supplementary Figure S4a). There is a tendency towards reduced mutation frequency in REV3L ΔA1237 compared to HEK293 cells when no peptide is added (not significant, $p = 0.08$), suggesting lower levels of REV3L, and reduced TLS, in this cell line. Furthermore, the APIM-peptide was >2× more efficient in reducing the mutation frequency in HEK293 than REV3L ΔA1237 cells. The latter suggests that part of the APIM-peptide's effect in HEK293 cells is the inhibition of POLζ-mediated TLS. The mutation frequency in the XPA$^{-/-}$ cells was, as expected, elevated compared to the repair proficient HEK293 (~2×); however, a ~50% reduction in mutation frequency was still detected in this cell line after treatments with the APIM-peptide (Figure 6c).

2.6. Targeting PCNA with APIM-Peptide Affects the Mutation Spectra

The mutation spectra in the *supF* gene, isolated from both HEK293 and the REV3L ΔA1237 cells, were changed by the APIM-peptide treatment. For example, the mutations at position 168 were strongly reduced compared to the control in HEK293 (Figure 6a, left panel), whereas, in the REV3L ΔA1237 cells, mutations at this position were only detected after treatment with the APIM-peptide (Figure 6b). Similar effects of the APIM-peptide were also detected in the two cell lines, for example, the relative amount of mutations at position 156 were increased after treatment with the APIM-peptide in both cell lines. The APIM-peptide treatment reduced the mutation frequency and changed the mutation spectra in both cell lines, but not similarly. Because the main difference in these two cell lines likely is the level of REV3L, we hypothesize that a major part of the APIM-peptide's effect on TLS is due to inhibition of the REV3L APIM–PCNA interaction. However, in addition to REV3L, the two Rad5 homologs, HLTF and SHPRH, believed to be important in regulation of TLS [33], and XPA, essential for NER [25], also contain APIM [5]. The function of these proteins could; therefore, also be affected by the APIM-peptide treatment. Of note, the reduction in mutation frequencies shows that the APIM-peptide reduces TLS more efficiently than error free DNA repair, and this could be beneficial in cancer therapies if the APIM-peptide were used in combination with chemotherapeutics.
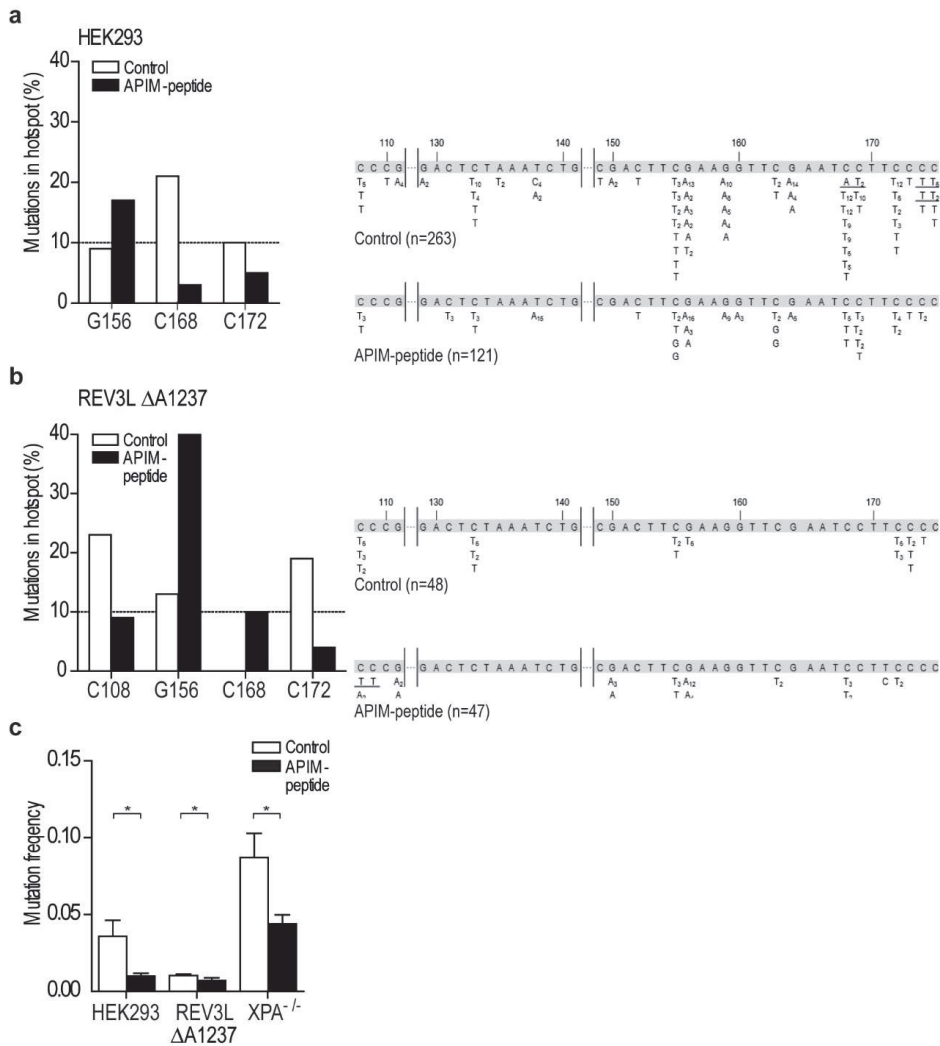
Figure 6. Treatment with APIM-peptide modulates the mutation spectra and reduces the mutation frequencies. (**a**,**b**) Mutation spectra (*supF* gene) from cells transfected with UVB irradiated pSP189 (supF reporter plasmid), with and without treatment with APIM-peptide (10 μM), isolated from (**a**) HEK293 and (**b**) REV3L ΔA1237 cells from four independent experiments. Left panel: Mutations at sites in the *supF* gene occurring with a frequency >10% in either control (white bars) or APIM-peptide treated cells (black bars). Right panel: Mutation spectra. The number in subscript indicates how many times the specific mutation was detected in the same transformation. Tandem mutations are underlined. (**c**) Mutation frequency in HEK293, REV3L ΔA1237, and XPA$^{-/-}$ cells after APIM-peptide treatment (black bars, 10 μM in HEK293 and REV3L ΔA1237, and 8 μM in XPA$^{-/-}$) relative to untreated cells (white bars). Data from each cell line includes data from a minimum of three independent experiments. A significant reduction in mutation frequency after addition of APIM-peptide compared to control (untreated) was detected in all three cell lines (student two-tailed paired *t*-test, * $p < 0.05$).

The aim of this study was to examine if APIM in REV3L is a functional PCNA interacting motif. Our data suggests that the APIM sequence in REV3L is a PCNA interacting motif and that mutation of APIM in full-length REV3L changes the functionality and/or specificity of TLS in vivo.

Additionally, we find that targeting PCNA with the APIM-peptide reduces mutagenesis, likely by impairing the efficacy of POLζ. Cumulatively, our data suggests that APIM in REV3L is a functional PCNA interacting motif and that direct interaction with PCNA is important for TLS coordination.

3. Material and Methods

3.1. Expression Constructs

KFVLK-YFP/CFP and KAVLK-YFP were constructed by annealing MDKFVLK and MDKAVLK encoding oligonucleotides (Sigma-Aldrich, Saint Louis, MO, USA) with EcoRI and XhoI overhang. These were cloned into yellow (YFP) and cyan (CFP) variants of green fluorescent protein (GFP) (Clonetech/TaKaRa Bio USA, Montain View, CA, USA), using the pEYFP-N1 or pECFP-N1 plasmids with mutated ATGsimilarly to RWLVK-CFP [5]. pREV3L-3xFLAG was a kind gift from Christine E. Canman, Department of Pharmacology, University of Michigan, USA [34]. A site-specific mutation F1241A was generated in pREV3L3xFLAG using Quick Change II (Agilent Technologies, Santa Clara, CA, USA). The Amp resistance in this plasmid was switched to Kanamycin (Km) using a Km-resistance gene flanked with AatII and FspI from the pUC57 vector. pREV3L-YFP was generated by GenScript (Piscataway, NJ, , USA) by replacement of the 3xFLAG tag with YFP using the pEYFP-N1. CFP-PCNA and HcRed-PCNA has previously been described [5,35]. pSP189 reporter plasmid and *Escherichia coli* strain MBM7070 were a gift from Professor Karlene Cimprich, Department of Chemical and Systems Biology, Stanford University, Stanford, CA, USA [33].

3.2. Cell Lines

HEK293, HEK293T, HCT116, and HeLa cells (ATCC: CRL 1573, CRL 11268, CCL-247, and CCL2, respectively) were cultured in Dulbecco´s Modified Eagle Medium (DMEM) (4.5 g/L; Sigma-Aldrich); and HAP1 cells (POLη KO, Horizon Genomics, Cambridge, UK) were cultured in Iscove's Modified Medium (IMDM) (Sigma Aldrich). Media was supplemented with 10% fetal bovine serum (FBS; Sigma-Aldrich), 2.5 μg/mL Fungizone® Amphotericin B (Gibco, Thermo Fischer Scientific, Waltham, MA, USA), 1 mM L-Glutamin (Sigma-Aldrich), and an antibiotic mixture containing 100 μg/mL penicillin and 100 μg/mL streptromycin (Gibco). The XP-A deficient cell line (XPA$^{-/-}$; Coriell Institute, GM04429) were cultured in Minimum Essential Medium-alpha (MEM-alpha, 4.5 g/L; Gibco) supplemented with 10% FBS, 2.5 μg/mL Fungizone® Amphotericin B, 1 mM L-Glutamin, and 100 μg/mL gentamicin (Gibco). The cells were cultured at 37 °C in a 5% CO_2-humidified atmosphere.

3.3. SupF Assay

The supF mutagenicity assay was performed essentially as previously reported [33]. Briefly, the reporter plasmid pSP189 was irradiated with 600 or 800 mJ/cm^2 UVB, depending on the cell line, with UV lamp, Vilber Lourmat Bio Spectra V5, 312 nm. Cells were transfected with UVB-irradiated pSP189 (including plasmids not exposed to UVR as controls) and co-transfected with constructs of interest or treated with APIM-peptide. Transfections were performed using X-treme GENE HP transfection reagent according to manufacturer protocol (Roche diagnostics, Basel, Switzerland). Cells were harvested after 48 h for both isolation of plasmid and western analysis and/or confocal analysis. Isolated plasmids were DpnI (NEB) restriction digested to exclude original bacterial plasmids in order to only look at replicated plasmids. Blue/white screening was performed by transformation of the isolated plasmids into *E. coli* MBM7070 cells, followed by plating on indicator X-gal/IPTG/Amp agar plates. Mutation frequency (white/blue colonies) was calculated for the different samples for several transformations. White mutant colonies were picked for re-streak and DNA sequencing of *supF* gene.

3.4. Imaging

HEK293T, transfected with pREV3L-3xFLAG, were fixed in paraformaldehyde (2%) and permeabilized in ice-cold methanol for 5 min at −20 °C. The cells were washed in phosphate buffered

saline (PBS) and blocked in bovine serum albumin (BSA)-PBS (2%), prior to incubation with primary antibodies against PCNA (ab18197) and FLAG-peptide (α-FLAG, mouse monoclonal, SIGMA F1804) overnight at 4 °C. Samples were washed in PBS and stained with tetramethylrhodamine (TRITC) goat α-rabbit and Alexa fluor 532 goat α-mouse (Life Technologies), and then diluted 1:200 in BSA-PBS (2%) for 1 hour at room temperature (RT). Samples were washed and maintained in PBS. Images were captured on a Leica SP8 stimulated emission depletion (STED) 3X confocal microscope using a $100\times/1.4$ oil immersion objective, using the 660 and 775 nm lasers.

For immunofluorescence staining and confocal imaging related to supF assay, cells were transfected in parallel with the SupF-assay transfection, with proportional amounts of cells and transfection mix. Cells were fixed with 2% paraformaldehyde, treated with methanol (-20 °C), and incubated overnight at 4 °C with primary antibody (α-FLAG), diluted 1:500 in FBS-PBS. The following day the cells were washed and treated with secondary antibody (goat α-mouse Alexa fluor 532), diluted 1:2000 in FBS-PBS for 45 min (37 °C). Images were captured using the Zeiss LSM 510 Meta confocal microscope (argon laser 514 nm and BP 530–600 nm for YFP; 543 nm argon laser and LP 560 for Alexa fluor 532). Live cell imaging was performed using a Zeiss LSM 510 Meta laser scanning microscope equipped with a Plan-Apochromate 63x/1.4 oil immersion objective. YFP, CFP, and HcRed were excited and detected at $\lambda = 514$ nm/530–600 nm, $\lambda = 458$ nm/470–500 nm, and $\lambda = 543$ nm/>615 nm, respectively, using consecutive scans. The thickness of the scanned optical slices was 1 μm.

3.5. Fluorescence Measurements and Fluorescence Resonance Energy Transfer (FRET)

FRET was done as previously described [6]. Fluorescence intensities was measured using the imaging processing software, Fiji (ImageJ) version 1.06.2016, and all images were taken with the exact same confocal settings. Average intensities within an area of interest (foci) was measured and divided with average intensity in the nucleus outside foci. We selected and compared only cells with equal fluorescence intensities (YFP and CFP) (i.e., equal levels of expressed proteins), and we selected cells within a narrow region of intensities. A minimum of 50 foci were measured per sample from 7 to 15 cells.

3.6. Preparation of Cell Lysates

Exponentially grown HEK293T cells were transfected with p-REV3L-YFP or pYFP using X-tremeGENE HP transfection reagent (Roche diagnostics). The cells were crosslinked in 0.25% formaldehyde for 20 min at room temperature, and harvested as previously described [36]. Briefly, the cell pellet was resuspended in $3\times$ packed cell volume in buffer I: 20 mM, pH 7.8, HEPES-KOH, 100 mM KCl, 1.5 mM $MgCl_2$, 0.2 mM EDTA, 20% glycerol, 0.5% NP-40, 1 mM DTT, $1\times$ complete protease inhibitor, and 1x phosphatase-inhibitor cocktails I and II (Sigma-Aldrich). 200 U OmniCleave Endonuclease (Epicenter Technologies, Thane, India) was added to each 100 μL of cell pellet before sonication (Branson Sonifier 250). Residual DNA/RNA in the lysates were digested for 1 h at 37 °C using an endonuclease cocktail of 400 U OmniCleave, 10 U DNase I (Roche diagnostics), 250 U benzonase (Merck, Darmstadt, Germany), 100–300 U micrococcal nuclease (Sigma-Aldrich), and 20 μg RNase (Sigma-Aldrich) per 30 mg protein in the lysate. Digestion was followed by clearance by centrifugation.

3.7. Immunoprecipitation

Immunoprecipitations were performed using Dynabeads protein A magnetic beads coupled to polyclonal GFP antibodies (ab290, Abcam, Cambridge, UK), which also recognize YFP and CFP, using the crosslinker, Bis(sulfosuccinimidyl)suberate (BS3), according to the manufacturer's instructions (Thermo Fisher Scientific). Coupled beads were incubated with cleared lysates, under gentle rotation at 4 °C overnight, and further washed, three times, with 10 mM Tris-HCl, pH 7.5, 100 mM KCl before elution. Immunoprecipitated proteins were eluted in lithium dodecyl sulfate (LDS) loading buffer

(Invitrogen, Thermo Fisher Scientific), containing 100 mM DTT, by heating the beads for 10 minutes at 70 °C, and separated briefly on a NuPAGE 3–8% Tris-Acetate protein gel (Invitrogen).

3.8. Mass Spectrometry (MS) Analysis

The gel lanes were cut into pieces (~100 mg) and submitted to in-gel tryptic digestion, as described by [37]. Tryptic digests were dried out, resuspended in 0.1% formic acid, and analyzed on an Orbitrap Elite mass spectrometer (Thermo Scientific) coupled to an Easy-nLC 1000 UHPLC system (Thermo Scientific). Peptides were injected into an Acclaim PepMap100 C-18 column (75 μm i.d. × 2 cm, C18, 3 μm, 100 Å, Thermo Scientific) and further separated in an Acclaim PepMap RSLC Nanoviper analytical column (75 μm i.d. × 50 cm, C18, 2 μm, 100 Å, Thermo Scientific). A 120-minute method with a 250 nL/minute flow rate was employed; it started with an 80-minute gradient from 2% to 40% of buffer B (99.9% acetonitrile, 0.1% formic acid; buffer A was 0.1% formic acid in water), then it was increased to 55% of buffer B in 15 min, and then to 100% of buffer B in 15 min, it was then kept at 100% of buffer B for 10 min. The peptides eluting from the column were analyzed in positive-ion mode using data dependent acquisition, using collision-induced dissociation (CID) fragmentation with normalized collision energy 35. Each profile MS scan (m/z 400–1600) was acquired at a resolution of 120,000 FWHM in the orbitrap, followed by 10 centroid MS/MS scans in the ion trap at rapid scan rate, with an isolation width of 2.0 m/z and an activation time of 10 ms. A 60-second dynamic exclusion was employed. MS spectra were analyzed using Proteome Discoverer (Thermo Scientific) version 1.4.0.288 software, running Mascot and the Sequest HT database search algorithms. Spectra were searched against a human proteome database from UniProt with the following parameters: maximum missed cleavage = 2, precursor mass tolerance = 10 ppm, fragment mass tolerance = 0.6 Da, and dynamic modification = carbamidomethyl (C: +57.021 Da). Peptides were identified with a high degree of confidence (defined as false discovery rate (FDR) ≤0.01) using Percolator. From three biological replicas, possible REV3L interaction partners were identified as proteins detected with a Sequest score >5 in at least two or more experiments in the REV3L-YFP IP, compared to the YFP control sample.

3.9. Guide RNA Cloning

LentiCRISPRv2 vector (Addgene plasmid #52961), containing two expression cassettes, hSpCas9 and the chimeric guide RNA, was used as a vector for the CRISPR/Cas9 system. The guide RNA was chosen to target REV3L upstream of its APIM sequence. The following oligonucleotides were used: 5′caccgAAAATCTCAGTCTGGTGCTG-3′ on plus-strand and 5′aaacCAGCACCAGACTGAGATTTTc-3′ on minus-strand. The vector was digested using BsmBI (NEB) and the annealed oligonucleotides (guide RNA) were cloned into the guide RNA scaffold by using Quick Ligase (NEB). Constructs were heat shock transformed into Stbl3 chemically-competent *E. coli*, and plated on LB Ampicillin plates (100 μg/mL). Plasmids from three bacterial colonies were isolated, digested by restriction enzyme HindIII (NEB), and applied on a 0.8% agarose gel for screening. Further, the constructs were sequenced to verify if the guide RNA was cloned correctly into the vector.

3.10. Transfection of CRISPR/Cas9 Vector and Single Clone Expansion.

HEK293 cells, seeded in a 12-well plate (150,000 cells/well), were transfected (Xtreme Gene HP, Roche) with 1 μg lentiCRISPR v2 guide plasmid per well. Selection medium containing 2 μg/mL puromycin was added 72 h after transfection and renewed every 3 to 4 days. Potential single-cell colonies could be observed after 14 days. Cell colonies were washed with PBS, trypsinized, resuspended, and transferred into a 24-well plate. Cells were further expanded and DNA was harvested for screening. Briefly, 100,000 cells were resuspended in 50 μL of alkaline solution (25 mM NaOH/0.2 mM EDTA, pH 12) and heated for 10 min at 95 °C. After cooling, 50 μL of neutralizing solution (40mM tris-HCl, pH 5) was added and the lysate was isolated after centrifugation. The target sequence in the REV3L was PCR amplified using forward primer 5′ ATTCTTCTCCACCTCGCTGC-3′ and reverse primer

3′CCGCTATGCACACAATCTGC-5′, and the PCR product was sequenced using forward primer 5′ GCGCAAGAGCACAGATTAAG-3′ and reverse primer 3′ TGGGTAGGGAAGCAGAAAGG-5′.

3.11. Viability

HEK293 (4000 cells/well) and REV3L ∆A1237 (5000 cells/well) were seeded in 96-well plates. After 4 h, cells were treated with mitomycin-C (MMC, Medac) (0.05, 0.1, 0.2, and 0.4 µM), exposed to UVB-irradiation (20, 40, and 60 mJ/cm^2) or treated with methyl methanesulfonate (MMS) (0.025, 0.05, 0.1, and 0.2 µM). Cell viability was measured at different timepoints by the MTT (3-(4.5-Dimethylthiazol-2-yl)-2.5 diphenyl-tetrazolium bromide) assay as previously described [5].

Supplementary Materials: The following are available online at http://www.mdpi.com/1422-0067/20/1/100/s1.

Conflicts of Interest: APIM Therapeutics is a spin-off company of the Norwegian University of Science and Technology, where Professor Marit Otterlei is an inventor, founder, minority shareholder, and CSO. APIM Therapeutics is developing APIM-peptides for use in cancer therapy.

References

1. Zhao, L.; Washington, M.T. Translesion Synthesis: Insights into the Selection and Switching of DNA Polymerases. *Genes* **2017**, *8*, 24. [CrossRef] [PubMed]

2. Choe, K.N.; Moldovan, G.L. Forging Ahead through Darkness: PCNA, Still the Principal Conductor at the Replication Fork. *Mol. Cell* **2017**, *65*, 380–392. [CrossRef] [PubMed]

3. Mailand, N.; Gibbs-Seymour, I.; Bekker-Jensen, S. Regulation of PCNA-protein interactions for genome stability. *Nat. Rev. Mol. Cell Biol.* **2013**, *14*, 269–282. [CrossRef] [PubMed]

4. Olaisen, C.; Kvitvang, H.F.N.; Lee, S.; Almaas, E.; Bruheim, P.; Drablos, F.; Otterlei, M. The role of PCNA as a scaffold protein in cellular signaling is functionally conserved between yeast and humans. *FEBS Open Biol.* **2018**, *8*, 1135–1145. [CrossRef] [PubMed]

5. Gilljam, K.M.; Feyzi, E.; Aas, P.A.; Sousa, M.M.; Muller, R.; Vagbo, C.B.; Catterall, T.C.; Liabakk, N.B.; Slupphaug, G.; Drablos, F.; et al. Identification of a novel, widespread, and functionally important PCNA-binding motif. *J. Cell Biol.* **2009**, *186*, 645–654. [CrossRef] [PubMed]

6. Müller, R.; Misund, K.; Holien, T.; Bachke, S.; Gilljam, K.M.; Våtsveen, T.K.; Rø, T.B.; Bellacchio, E.; Sundan, A.; Otterlei, M. Targeting Proliferating Cell Nuclear Antigen and Its Protein Interactions Induces Apoptosis in Multiple Myeloma Cells. *PLoS ONE* **2013**, *8*, e70430. [CrossRef]

7. Bacquin, A.; Pouvelle, C.; Siaud, N.; Perderiset, M.; Salomé-Desnoulez, S.; Tellier-Lebegue, C.; Lopez, B.; Charbonnier, J.-B.; Kannouche, P.L. The helicase FBH1 is tightly regulated by PCNA via CRL4 (Cdt2)-mediated proteolysis in human cells. *Nucleic Acids Res.* **2013**, *41*, 6501–6513. [CrossRef]

8. Fu, D.; Samson, L.D.; Hubscher, U.; van Loon, B. The interaction between ALKBH2 DNA repair enzyme and PCNA is direct, mediated by the hydrophobic pocket of PCNA and perturbed in naturally-occurring ALKBH2 variants. *DNA Repair* **2015**, *35*, 13–18. [CrossRef]

9. Sebesta, M.; Cooper, C.D.O.; Ariza, A.; Carnie, C.J.; Ahel, D. Structural insights into the function of ZRANB3 in replication stress response. *Nat. Commun.* **2017**, *8*, 15847. [CrossRef]

10. Makarova, A.V.; Stodola, J.L.; Burgers, P.M. A four-subunit DNA polymerase zeta complex containing Pol delta accessory subunits is essential for PCNA-mediated mutagenesis. *Nucleic Acids Res.* **2012**, *40*, 11618–11626. [CrossRef]

11. Singh, B.; Li, X.R.; Owens, K.M.; Vanniarajan, A.; Liang, P.; Singh, K.K. Human REV3 DNA Polymerase Zeta Localizes to Mitochondria and Protects the Mitochondrial Genome. *PLoS ONE* **2015**, *10*, 18. [CrossRef] [PubMed]

12. Van Sloun, P.P.H.; Romeijn, R.J.; Eeken, J.C.J. Molecular cloning, expression and chromosomal localisation of the mouse Rev31 gene, encoding the catalytic subunit of polymerase zeta. *Mutat. Res. DNA Repair* **1999**, *433*, 109–116. [CrossRef]

13. Van Sloun, P.P.H.; Varlet, I.; Sonneveld, E.; Boei, J.; Romeijn, R.J.; Eeken, J.C.J.; De Wind, N. Involvement of mouse Rev3 in tolerance of endogenous and exogenous DNA damage. *Mol. Cell. Biol.* **2002**, *22*, 2159–2169. [CrossRef] [PubMed]

14. Suzuki, T.; Gruz, P.; Honma, M.; Adachi, N.; Nohmi, T. The role of DNA polymerase zeta in translesion synthesis across bulky DNA adducts and cross-links in human cells. *Mutat. Res.* **2016**, *791–792*, 35–41. [CrossRef] [PubMed]

15. Lee, Y.S.; Gregory, M.T.; Yang, W. Human Pol zeta purified with accessory subunits is active in translesion DNA synthesis and complements Pol. in cisplatin bypass. *Proc. Natl. Acad. Sci. USA* **2014**, *111*, 2954–2959. [CrossRef] [PubMed]

16. Yoon, J.H.; Park, J.; Conde, J.; Wakamiya, M.; Prakash, L.; Prakash, S. Rev1 promotes replication through UV lesions in conjunction with DNA polymerases eta, iota, and kappa but not DNA polymerase zeta. *Genes Dev.* **2015**, *29*, 2588–2602. [PubMed]

17. Olaisen, C.; Muller, R.; Nedal, A.; Otterlei, M. PCNA-interacting peptides reduce Akt phosphorylation and TLR-mediated cytokine secretion suggesting a role of PCNA in cellular signaling. *Cell. Signal.* **2015**, *27*, 1478–1487. [CrossRef] [PubMed]

18. Brondello, J.M.; Pillaire, M.J.; Rodriguez, C.; Gourraud, P.A.; Selves, J.; Cazaux, C.; Piette, J. Novel evidences for a tumor suppressor role of Rev3, the catalytic subunit of Pol zeta. *Oncogene* **2008**, *27*, 6093–6101. [CrossRef]

19. Kudo, N.; Matsumori, N.; Taoka, H.; Fujiwara, D.; Schreiner, E.P.; Wolff, B.; Yoshida, M.; Horinouchi, S. Leptomycin B inactivates CRM1/exportin 1 by covalent modification at a cysteine residue in the central conserved region. *Proc. Natl. Acad. Sci. USA* **1999**, *96*, 9112–9117. [CrossRef]

20. Bj Ras, K.O.; Sousa, M.M.L.; Sharma, A.; Fonseca, D.M.; CK, S.G.; Bj Ras, M.; Otterlei, M. Monitoring of the spatial and temporal dynamics of BER/SSBR pathway proteins, including MYH, UNG2, MPG, NTH1 and NEIL1-3, during DNA replication. *Nucleic Acids Res.* **2017**, *45*, 8291–8301. [CrossRef]

21. Hara, K.; Uchida, M.; Tagata, R.; Yokoyama, H.; Ishikawa, Y.; Hishiki, A.; Hashimoto, H. Structure of proliferating cell nuclear antigen (PCNA) bound to an APIM peptide reveals the universality of PCNA interaction. *Acta Crystallogr. F Struct. Biol. Commun.* **2018**, *74 Pt 4*, 214–221. [CrossRef]

22. Ducoux, M.; Urbach, S.; Baldacci, G.; Hubscher, U.; Koundrioukoff, S.; Christensen, J.; Hughes, P. Mediation of proliferating cell nuclear antigen (PCNA)-dependent DNA replication through a conserved p21(Cip1)-like PCNA-binding motif present in the third subunit of human DNA polymerase delta. *J. Biol. Chem.* **2001**, *276*, 49258–49266. [CrossRef] [PubMed]

23. Bruning, J.B.; Shamoo, Y. Structural and thermodynamic analysis of human PCNA with peptides derived from DNA polymerase-delta p66 subunit and flap endonuclease-1. *Structure* **2004**, *12*, 2209–2219. [CrossRef] [PubMed]

24. Pustovalova, Y.; Magalhaes, M.T.Q.; D'Souza, S.; Rizzo, A.A.; Korza, G.; Walker, G.C.; Korzhnev, D.M. Interaction between the Rev1 C-Terminal Domain and the PolD3 Subunit of Pol xi Suggests a Mechanism of Polymerase Exchange upon Rev1/Pol xi-Dependent Translesion Synthesis. *Biochemistry* **2016**, *55*, 2043–2053. [CrossRef] [PubMed]

25. Gilljam, K.M.; Muller, R.; Liabakk, N.B.; Otterlei, M. Nucleotide Excision Repair Is Associated with the Replisome and Its Efficiency Depends on a Direct Interaction between XPA and PCNA. *PLoS ONE* **2012**, *7*, e49199. [CrossRef] [PubMed]

26. Yoon, J.H.; Prakash, L.; Prakash, S. Error-free replicative bypass of (6-4) photoproducts by DNA polymerase zeta in mouse and human cells. *Genes Dev.* **2010**, *24*, 123–128. [CrossRef]

27. Bienko, M.; Green, C.M.; Sabbioneda, S.; Crosetto, N.; Matic, I.; Hibbert, R.G.; Begovic, T.; Niimi, A.; Mann, M.; Lehmann, A.R.; et al. Regulation of translesion synthesis DNA polymerase eta by monoubiquitination. *Mol. Cell* **2010**, *37*, 396–407. [CrossRef]

28. Despras, E.; Sittewelle, M.; Pouvelle, C.; Delrieu, N.; Cordonnier, A.M.; Kannouche, P.L. Rad18-dependent SUMOylation of human specialized DNA polymerase eta is required to prevent under-replicated DNA. *Nat. Commun.* **2016**, *7*, 15. [CrossRef]

29. Slade, D. Maneuvers on PCNA Rings during DNA Replication and Repair. *Genes* **2018**, *9*, 28. [CrossRef]

30. Søgaard, C.K.; Moestue, S.A.; Rye, M.B.; Kim, J.; Nepal, A.; Liabakk, Ni.; Bachke, S.; Bathen, T.F.; Otterlei, M.; Hill, D.K. APIM-peptide targeting PCNA improves the efficacy of docetaxel treatment in the TRAMP mouse model of prostate cancer. *Oncotarget* **2018**, *9*, 11752–11766. [CrossRef]

31. Gederaas, O.A.; Sogaard, C.D.; Viset, T.; Bachke, S.; Bruheim, P.; Arum, C.J.; Otterlei, M. Increased Anticancer Efficacy of Intravesical Mitomycin C Therapy when Combined with a PCNA Targeting Peptide. *Transl. Oncol.* **2014**, *7*, 812–823. [CrossRef] [PubMed]

32. Søgaard, C.K.; Blindheim, A.; Røst, L.M.; Petrovic, V.; Nepal, A.; Bachke, S.; Liabakk, N.B.; Gederaas, O.A.; Viset, T.; Arum, C.J.; et al. "Two hits—One stone"; increased efficacy of cisplatin-based therapies by targeting PCNA's role in both DNA repair and cellular signaling. *Oncotarget* **2018**, *9*, 32448. [CrossRef] [PubMed]

33. Lin, J.R.; Zeman, M.K.; Chen, J.Y.; Yee, M.C.; Cimprich, K.A. SHPRH and HLTF act in a damage-specific manner to coordinate different forms of postreplication repair and prevent mutagenesis. *Mol. Cell* **2011**, *42*, 237–249. [CrossRef] [PubMed]

34. Sharma, S.; Hicks, J.K.; Chute, C.L.; Brennan, J.R.; Ahn, J.Y.; Glover, T.W.; Canman, C.E. REV1 and polymerase zeta facilitate homologous recombination repair. *Nucleic Acids Res.* **2012**, *40*, 682–691. [CrossRef] [PubMed]

35. Aas, P.A.; Otterlei, M.; Falnes, P.O.; Vagbo, C.B.; Skorpen, F.; Akbari, M.; Sundheim, O.; Bjoras, M.; Slupphaug, G.; Seeberg, E.; et al. Human and bacterial oxidative demethylases repair alkylation damage in both RNA and DNA. *Nature* **2003**, *421*, 859–863. [CrossRef] [PubMed]

36. Akbari, M.; Solvang-Garten, K.; Hanssen-Bauer, A.; Lieske, N.V.; Pettersen, H.S.; Pettersen, G.K.; Wilson, D.M., 3rd; Krokan, H.E.; Otterlei, M. Direct interaction between XRCC1 and UNG2 facilitates rapid repair of uracil in DNA by XRCC1 complexes. *DNA Repair* **2010**, *9*, 785–795. [CrossRef]

37. Shevchenko, A.; Wilm, M.; Vorm, O.; Mann, M. Mass spectrometric sequencing of proteins silver-stained polyacrylamide gels. *Anal. Chem.* **1996**, *68*, 850–858. [CrossRef]

Supplementary material

APIM mediated REV3L-PCNA interaction important for error free TLS over UV induced DNA lesions in human cells

Synnøve Brandt Ræder[1], Anala Nepal[1,2,#], Karine Øian Bjørås[1,#], Mareike Seelinger[1,#], Rønnaug Steen Kolve[1], Aina Nedal[1], Rebekka Müller[1] and Marit Otterlei[1,2*].

[1]Department of Clinical and Molecular Medicine, Faculty of Medicine and Health Sciences, Norwegian University of Science and Technology (NTNU), Trondheim, Norway

[2]Clinic of Surgery, St. Olavs Hospital, Trondheim University Hospital, Trondheim, Norway

[#]Equal contributions

Supplementary Figure S1
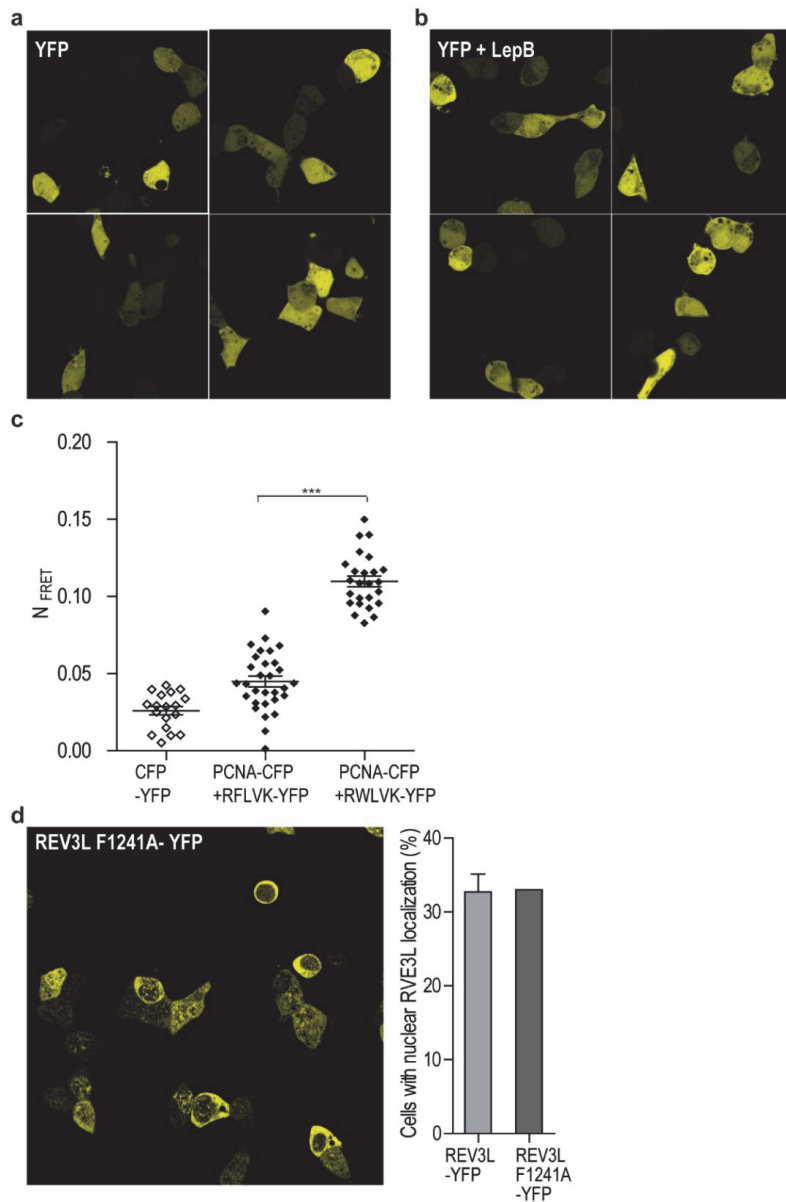
Supplementary Figure S1, related to Figure 1. Subcellular localization of YFP and REV3L F1241-YFP and FRET between PCNA and APIM variants. **(a)** Overview of subcellular localization of YFP expressed in HEK293T cells. **(b)** Overview of subcellular localization of YFP expressed in HEK293T cells with Leptomycin B treatment (10 ng/ml, after 1 hour treatment). **(c)** Normalized FRET measurement between overexpressed PCNA-CFP and RFLVK-YFP or RWLVK-YFP in Hela cells. CFP-YFP (vectors only) was used as background control. Data is from one out of 2 similar experiments. The p-value (***= p> 0.0001) is calculated from a two-tailed unpaired t-test. **(d)** *Left panel:* Overview of subcellular localization of REV3L F1241A- YFP in HEK293T cells. *Right panel:* Quantification of REV3L F1241A-YFP nuclear localization (dark grey bar) from one experiment with in total 267

cells, compared with the quantified REV3L-YFP nuclear localization (light grey bar) also shown previously in Fig. 1b and 5b.

Supplementary Table S1, related to Figure 1. All proteins pulled down with REV3L-YFP used for gene ontology (GO) analysis. **(a)** Proteins immonoprecipitatated from REV3L-YFP expressing cells. Only proteins detected in maximum one out of three IPs from similarly crosslinked YFP-expressing cell are included. Only proteins detected with average sequest score larger than 5 is regarded as a significant detection. Proteins found in the CRAPome database at a frequency of more than 50% of experiments with magnetic Dynabeads are shown in *italic*. These are excluded from the list prior to the GO analysis shown in Fig. 1c. **(b)** GO-analysis of complete list shown in (a) using a PANTHER overrepresentation test. GO biological processes with a Benferroni corrected P-value <0.05 are shown. P-values given as false discovery rate (FDR).

a

Uniprot ID	Symbol	Description	Average sequest score		#Replica detected		CRAPome frequency occurance (%)
			EYFP	REV3L	EYFP	REV3L	
P52292	*KPNA2*	*Importin subunit alpha-1*	*4*	*36*	*0*	*3*	*63*
Q03252	*LMNB2*	*Lamin-B2*	*3*	*13*	*0*	*3*	*58*
P49005	POLD2	DNA polymerase delta subunit 2		17	0	3	5
Q15054	POLD3	DNA polymerase delta subunit 3		11	0	3	2,6
O60884	DNAJA2	DnaJ homolog subfamily A member 2	3	11	0	3	50
P34932	HSPA4	Heat shock 70 kDa protein 4	3	8	0	3	39
O60673	DPOLZ	DNA polymerase zeta catalytic subunit	6	671	1	3	0
P45880	*VDAC2*	*Voltage-dependent anion-selective channel protein 2*	*7*	*14*	*1*	*3*	*58*
Q9Y265	*RUVB1*	*RuvB-like 1*	*7*	*29*	*1*	*3*	*66*
O00410	IPO5	Importin-5	7	31	1	3	31,6
Q9Y230	*RUVB2*	*RuvB-like 2*	*7*	*28*	*1*	*3*	*58*
P02545	*LMNA*	*Prelamin-A/C*	*7*	*22*	*1*	*3*	*71*
P55060	CSE1L	Exportin-2	14	30	1	3	45
Q9Y2L1	DIS3	Exosome complex exonuclease RRP44	11	15	1	3	13
O75694	NUP155	Nuclear pore complex protein Nup155	4	13	1	3	42
Q00341	HDLBP	Vigilin	4	8	1	3	18
Q14204	*DYNC1H1*	*Cytoplasmic dynein 1 heavy chain 1*	*12*	*22*	*1*	*3*	*53*
P62906	*RPL10A*	*60S ribosomal protein L10a*	*3*	*5*	*0*	*2*	*58*
P46060	RANGAP1	Ran GTPase-activating protein 1	3	6	0	2	45
P31689	DNAJA1	DnaJ homolog subfamily A member 1	9	14	0	2	50
Q13765	NACA	Nascent polypeptide-associated complex subunit alpha	7	6	0	2	45
O95373	IPO7	Importin-7	14	37	0	2	26
P33992	*MCM5*	*DNA replication licensing factor MCM5*	*3*	*6*	*0*	*2*	*55*
P49588	AARS	Alanine--tRNA ligase, cytoplasmic	4	9	0	2	29
Q16531	DDB1	DNA damage-binding protein 1		7	0	2	50
Q8IX12	CCAR1	Cell division cycle and apoptosis regulator protein 1	2	6	0	2	26
Q86VP6	CAND1	Cullin-associated NEDD8-dissociated protein 1	3	6	0	2	45
Q9Y5V3	MAGED1	Melanoma-associated antigen D1		6	0	2	47
Q6Y7W6	GIGYF2	PERQ amino acid-rich with GYF domain-containing prot 2	3	8	0	2	13
Q92598	HSPH1	Heat shock protein 105 kDa	3	5	0	2	26
Q92616	GCN1L1	Translational activator GCN1	2	12	0	2	34

b

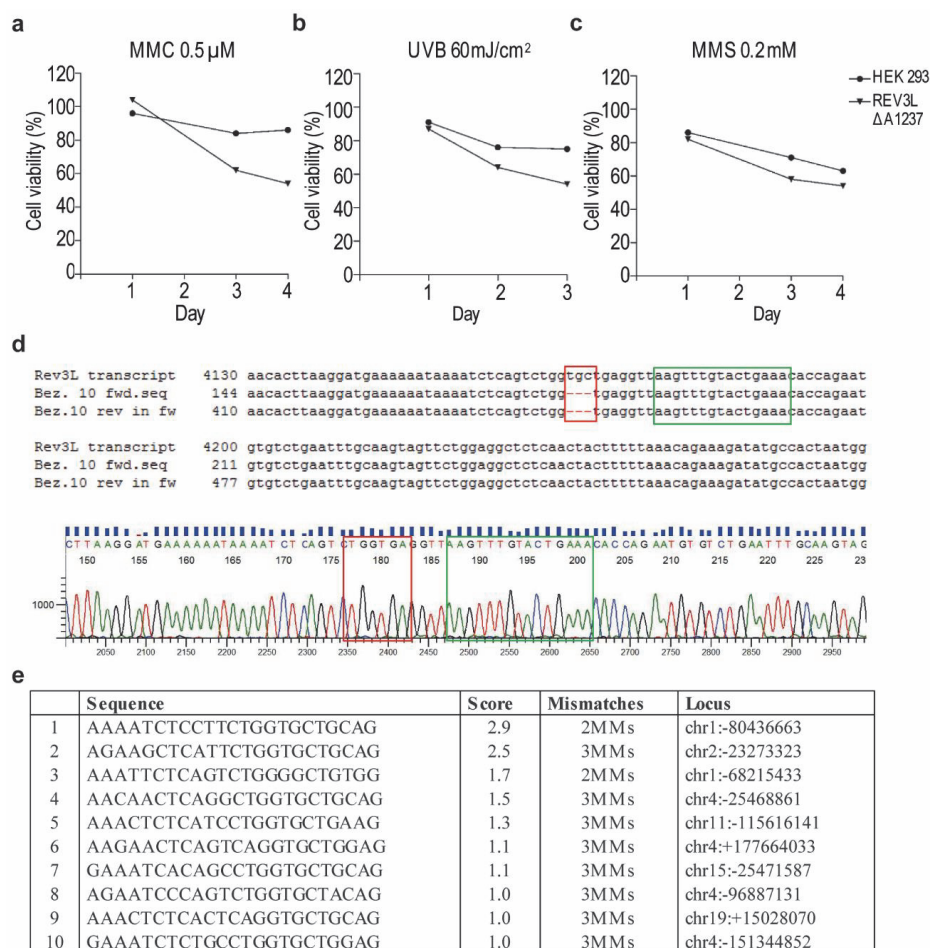| GO biological process	Detected proteins	FDR
Protein import into nucleus	KPNA2, LMNA, NUP155, IPO7, IPO5, CSE1L	3,13E-05
Response to unfolded protein	LMNA, HSPA4, DNAJA1, HSPH1	4,56E-02
DNA-dependent DNA replication	MCM5, POLD2, POLD3, REV3L	3,00E-02
Nucleotide excision repair, DNA incision, 5'- to lesion	POLD2, POLD3, DDB1	2,99E-02
Translesion synthesis	POLD2, POLD3, REV3L	2,85E-02
DNA damage response, detection of DNA damage	POLD2, POLD3, DDB1	2,78E-02
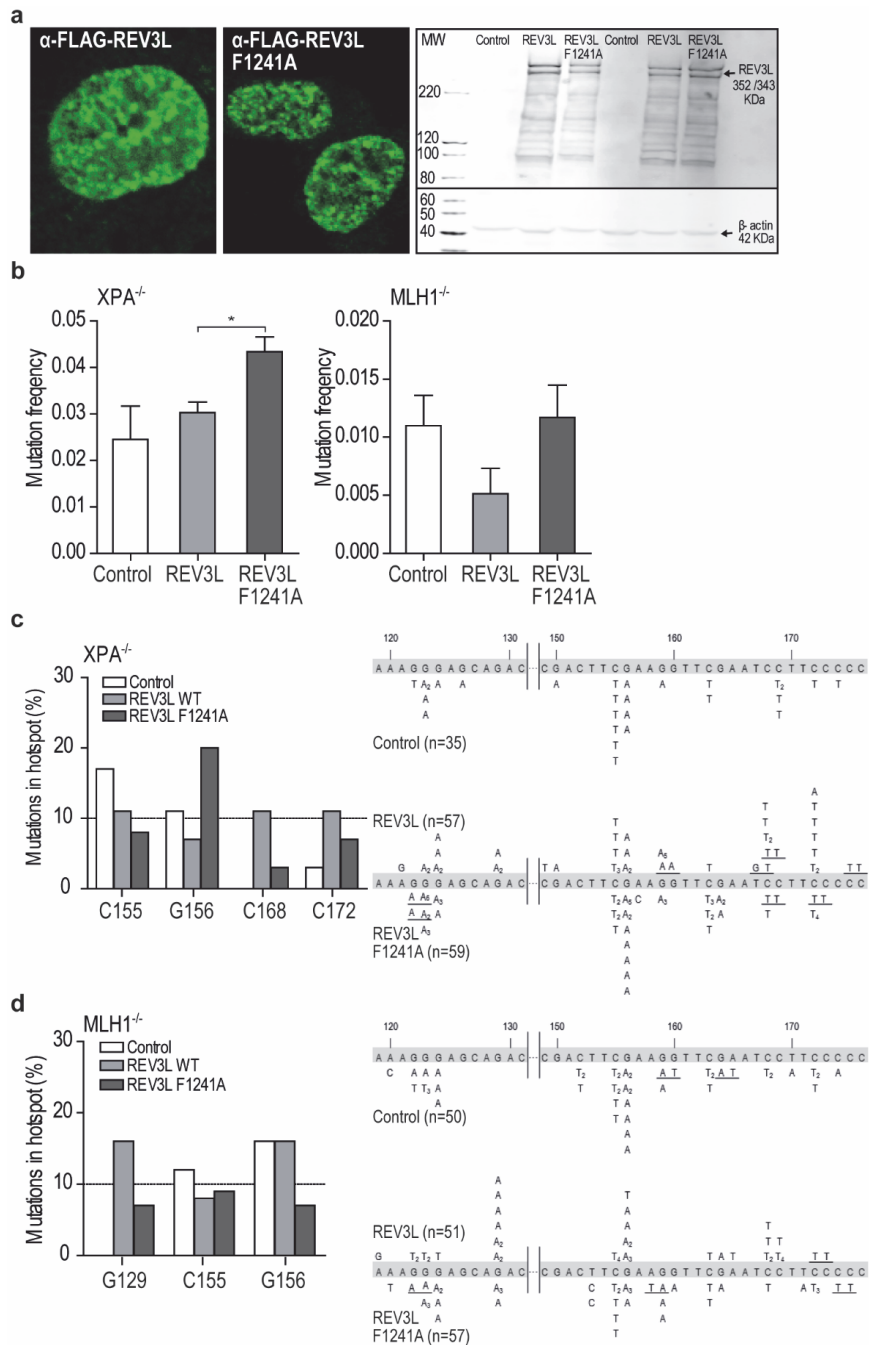
Supplementary Figure S2, related to Figure 3. Mutation frequencies and mutation spectra in XPA and MLH1 deficient cell lines after overexpression of REV3L or REV3L F1241A. **(a)** *Left panel:* Determination of expression levels of FLAG-tagged REV3L and REV3L F1241A by immunofluorescence in HCT116 cells. *Right panel:* Western blot showing expression of FLAG-tagged REV3L and REV3L F1241A in two representative independent experiments (transfections) in HEK293T cells. At least six transfections in HEK293T, HCT116 or XPA^{-/-} cell lines

showed similar results. Western blot analysis was performed as previously described (Olaisen et al., 2015, *Cellular signalling.* 27, (7), 1478-87). Bands below REV3L indicate some degradation of the overexpressed constructs, as these are not detected in the control. **(b)** Mutation frequency determined by SupF assay in XPA $^{-/-}$ (NER deficient) and MLH1 $^{-/-}$ (HCT116, MMR deficient) cells. REV3L WT-FLAG, REV3L F1241A-FLAG or YFP were co-transfected with the UV irradiated reporter plasmid pSP189 (600 and 800 mJ/cm^2 respectively). Cells expressing YFP represents the control. Minimum three independent experiments are shown for each cell line. Students two-tailed paired t-test were performed, *=p<0.05. **(c-d)** Mutation spectra (*supF* gene) isolated from cells overexpressing REV3L-FLAG, REV3L F1241A-FLAG or YFP (control) in (c) XPA $^{-/-}$ cells and (d) MLH1 $^{-/-}$ cells from three independent experiments. *Left panel*: Mutations at sites from the *supF* gene occurring with a frequency >10% in either control-(white bars), REV3L- (light grey bars) or REV3L F1241A-expressing (dark grey bars) cells. *Right panel:* Mutation spectra. The number in subscript indicates how many times the specific mutation was detected in the same transformation. Tandem mutations are underlined.
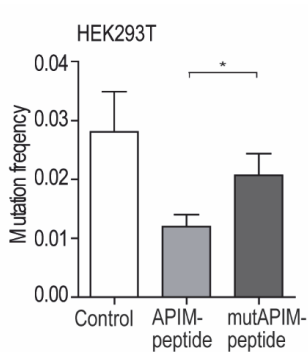
Supplementary Figure S3

	Sequence	Score	Mismatches	Locus
1	AAAATCTCCTTCTGGTGCTGCAG	2.9	2MMs	chr1:-80436663
2	AGAAGCTCATTCTGGTGCTGCAG	2.5	3MMs	chr2:-23273323
3	AAATTCTCAGTCTGGGGCTGTGG	1.7	2MMs	chr1:-68215433
4	AACAACTCAGGCTGGTGCTGCAG	1.5	3MMs	chr4:-25468861
5	AAACTCTCATCCTGGTGCTGAAG	1.3	3MMs	chr11:-115616141
6	AAGAACTCAGTCAGGTGCTGGAG	1.1	3MMs	chr4:+177664033
7	GAAATCACAGCCTGGTGCTGCAG	1.1	3MMs	chr15:-25471587
8	AGAATCCCAGTCTGGTGCTACAG	1.0	3MMs	chr4:-96887131
9	AAACTCTCACTCAGGTGCTGCAG	1.0	3MMs	chr19:+15028070
10	GAAATCTCTGCCTGGTGCTGGAG	1.0	3MMs	chr4:-151344852

Supplementary Figure S3, related to Figure 4 and 5. Characterization of the REV3L ΔA1237 cell line. **(a-c)** Viability of HEK293 and REV3L ΔA1237 after different treatments (treated on day 0)**.** Cells treated with (a)

mitomycin C (MMC), 0.5 µM (b) UVB-irradiation (UVB), 60 mJ/cm² and (c) methyl methanesulfonate (MMS), 0.2 mM. One representative experiments out of three independent experiments is presented. **(d)** Confirmation of the deletion of A1237 in REV3L by genome sequencing. *Upper panel:* Genomic REV3L transcript variant 1 isoform gene aligned with REV3L sequenced from REV3L deletion mutant cell line REV3L ΔA1237 (forward and reverse sequence) aligned using software Clone Manager 9. Deleted codon marked with red box, APIM marked with green box. *Lower panel:* Sequence chromatogram from REV3L ΔA1237 investigated in software Sequence Scanner v1.0. Codon triplet upstream and downstream the deleted codon marked with a red box, APIM marked with green box. **(e)** OFF-targets of guide RNA used for mutating genomic REV3L in HEK293 cells with CRISPR/Cas9. Guide RNAsequence including PAM sequence (AAAATCTCAGTCTGGTGCTGAGG) analysed by CRISPR design tool http://crispr.mit.edu/. ON-target chr6:+111695842 (quality score 59), 279-OFF targets found in human genome (18 in genes).

Supplementary Figure S4

Supplementary Figure S4, related to Figure 6. Mutation frequency after treatment with APIM-peptide variants. APIM-peptide, but not the mutAPIM-peptide, reduced the mutation frequency in HEK293T. Mutation frequency determined by the SupF assay after treatment with APIM-peptide or mutAPIM-peptide (10 µM). Data from four independent experiments. Two-tailed paired t-test (*=p<0.05).

Paper 2

Roles of HLTF and SHPRH in DNA damage tolerance depend on direct interactions with PCNA

Mareike Seelinger and Marit Otterlei[*]

Department of Clinical and Molecular Medicine, Faculty of Medicine and Health Sciences, Norwegian University of Science and Technology NTNU, Trondheim, Norway

[*]To whom correspondence should be addressed:

Tel: +4792889422

E-Mail: marit.otterlei@ntnu.no

Marit Otterlei

Department of Clinical and Molecular Medicine, Norwegian University of Technology (NTNU), PO Box 8905, N-7491, Trondheim, Norway

Key words: TLS, mutagenicity, DDT, APIM, RAD5

Running title: Functional APIM in HLTF and SHPRH

Abbreviations: APIM, AlkB homolog 2 PCNA-interating motif; CPD, cyclo-pyrimidine dimer; DDT, DNA damage tolerance; HLTF, helicase-like transcription factor; MMS, methyl methanesulfonate; NER, nucleotide excision repair; SHPRH, SNF2 histone-linker PHD and RING finger domain-containing helicase; TLS, translesion synthesis; TS, template switch; XPV, Xeroderma Pigmentosum Variant; 6-4PPs, (6-4)photoproducts

Abstract

To prevent replication fork collapse and genome instability under replicative stress, DNA damage tolerance (DDT) mechanisms have evolved. The RAD5 homologs, HLTF (helicase-like transcription factor) and SHPRH (SNF2, histone-linker, PHD and RING finger domain-containing helicase), both ubiquitin ligases, are involved in several DTT mechanisms; DNA translesion synthesis (TLS), fork reversal/remodeling and template switch (TS). Here we show for the first time that these two human RAD5 homologs contain a functional APIM PCNA-interaction motif. Our results show that both, stimulation of error-free bypass in presence of HLTF overexpression and nuclear localization of SHPRH, are dependent on the interaction of HLTF and SHPRH with PCNA. Additionally, we detected multiple changes in the mutation spectra when APIM in overexpressed HLTF or SHPRH were mutated, compared to overexpressed wildtype proteins. In plasmids from cells overexpressing the APIM mutant version of HLTF we observed a decrease in C to T transitions, the most common mutation caused by UV-irradiation, and an increase of mutations on the transcribed strand. These results strongly suggest that direct binding of HLTF and SHPRH to PCNA is vital for their function in DDT.

1   Introduction

Cells are constantly exposed to endogenous and exogenous agents that cause DNA lesions. DNA translesion synthesis (TLS), fork reversal and template switch (TS) are DNA damage tolerance (DDT) mechanisms handling DNA lesions or other obstacles during replication. This is achieved by one or more specialized low fidelity polymerases in TLS (TLS polymerases), by converting the replication fork into a stabilized chickenfoot structure intermediate, or by using the nascent strand in the sister chromatid as a template in TS. These mechanisms allow cells to continue replication and to prevent replication fork collapse [1].

One day of sun exposure is estimated to originate up to 10^5 UV-induced photolesions per cell [2]. UVB irradiation is absorbed by the DNA and induces mainly two types of UV-photodimers: cyclobutane pyrimidine dimers (CPDs) and pyrimidine pyrimidone (6-4)photoproducts (6-4PPs). CPDs account for the largest fraction of all photoproducts [3, 4]. They are the major mutagenic UV-lesions in mammalian cells, because they exhibit a slower repair-rate and are therefore often bypassed by TLS polymerases [5-7]. 6-4PPs on the other hand are bulky lesions which are rapidly detected and repaired by nucleotide excision repair (NER) [8]. The Xeroderma Pigmentosum variant (XPV) syndrome is associated POLη deficiency, but intact nucleotide excision repair (NER) [9]. XPV patients are hypersensitive towards sunlight and have an ~1000 times higher skin cancer incidence rate [10-12], illustrating the importance of properly regulated TLS, even in presence of functional NER (reviewed in [13]).

The DDT mechanisms are at least partly coordinated by mono- and polyubiquitination of K164 on PCNA (reviewed in [14]). The RAD5 homologues, HLTF and SHPRH, are both ubiquitin ligases containing a RING domain which is involved in polyubiquitination of PCNA [15]. They are therefore believed to be important for inducing TS. In addition, HLTF mediates fork reversal via its HIRAN domain interacting with the 3`ends of a frayed fork [16]. For SHPRH, which lacks a HIRAN domain, fork reversal has not been reported yet. Human cells have at least two additional important fork reversal proteins, SMARCAL1 and ZRANB3. The latter contains a functional PCNA-interacting sequence, AlkB homolog 2 PCNA interating motif (APIM) [17]. In addition, SMARCAL1, ZRANB3 and HLTF can restore a three-way-replication fork from a four-way-reversed replication fork [16, 18]. Furthermore, both RAD5 homologs are reported to be involved in TLS; HLTF by recruiting POLη after UV-induced DNA damage and SHPRH by recruiting POLκ after methyl methanesulfonate (MMS) induced DNA damage [19]. HLTF

and SHPRH are suggested as tumor suppressor genes, because loss of function or dysregulation has been linked to cancer development [20-22], and HLTF is often epigenetically silenced by promotor hypermethylation in colon cancers (~40 %) [23]. Interestingly, both RAD5 homologs contain potential PCNA interaction motifs, APIMs, within the helicase domain at their C-terminus; KFIVK (amino acid (aa) 959-963) in HLTF and RFLIK (aa 1631-1635) in SHPRH.

Serving as a scaffold protein, PCNA switches between protein interaction partners using either of the two motifs; the PIP-box or APIM. While the majority of APIM-containing proteins are involved in various cellular stress responses, including DNA repair, TS and TLS, the PIP-box is found in multiple proteins essential for replication [24-26]. The two motifs share the same interaction site on PCNA, which is a potential binding site for over 600 proteins [27-30]. Interactions with PCNA are therefore coordinated at multiple levels, including affinity driven competitive inhibition, context/cellular state and posttranslational modifications on PCNA or the interacting proteins [17, 31]. Data suggests that cellular stress, e.g. replication stress, is important for increased APIM - PCNA affinity [17, 24, 26, 27, 32-34]. Indeed, functional APIM is verified in three proteins directly involved in DDT, ZRANB3 [17], TFII-I [24, 35], and the catalytic subunit of POLζ, REV3L [36], and in two proteins involved in the regulation of TS, FBH1 [28] and RAD51B [24]. We show here that APIM in both HLTF and SHPRH directly interacts with PCNA, and that the binding of HLTF and SHPRH to PCNA is important for their function in DDT after UV-induced DNA damage.

2   Results and Discussion

2.1   APIM in HLTF is a functional PCNA-interacting motif

APIM in HLTF (KFIVK) fused to CFP and co-expressed with HcRed-tagged PCNA colocalized with PCNA in foci resembling replication foci (Figure 1A, mid two images). We have previously shown that mutation of the second position in APIM from an aromatic amino acid to alanine reduced the affinity to PCNA by ~50 % [37]. Accordingly, the HLTF APIM F2A mutant (K**A**IVK) fused to YFP did not colocalize with PCNA in foci when co-expressed with K**F**IVK-CFP and HcRed-PCNA (Figure 1A), a first indication for the importance of APIM in HLTF. However, both wildtype and APIM mutant versions (F960A) of full-length YFP-HLTF colocalized with overexpressed HcRed-PCNA (Figure 1D, H). The persistent colocalization of YFP-HLTF F960A with PCNA in replication foci indicates that the mutation in APIM only reduces, and not abolishes the interaction with PCNA and that other proteins partners participating in the same complex may interact with PCNA. The cellular localization of YFP-HLTF F960A was, however, slightly different from the wildtype protein, i.e. we detected a higher level of fluorescence in the cytosol. Thus, the mutation in APIM of HLTF might have reduced the stability, reduced the nuclear retention or increased the nuclear export of the protein (Figure 1B, quantified in C). Therefore, we next tested if the nuclear level of HLTF is actively regulated. Nuclear HLTF levels were measured after overexpression and treatment of the cells with Leptomycin B (an active nuclear export blocking drug). We found increased nuclear levels of both YFP-HLTF and YFP-HLTF F960A (Figure 1C). This indicates that the level of HLTF in the nucleus is actively regulated, but that the export of HLTF is independent of APIM and thus independent of a direct HLTF - PCNA interaction (Figure 1C).

To further investigate the importance of APIM in HLTF for colocalization with PCNA in replication foci, HLTF and HLTF F960A were overexpressed together with APIM-peptides and PCNA. The intensity of YFP-HLTF in PCNA foci was significantly reduced by co-expression of KFIVK-CFP (APIM in HLTF), and an even stronger reduction could be achieved by overexpression of RWLVK-CFP, an APIM-version with increased PCNA-affinity [36] (Figure 1E, F, quantified in G). The intensity of YFP-HLTF F960A in PCNA foci was initially stronger than YFP-HLTF, however, after overexpression of APIM-peptides (KFIVK-CFP or RWLVK-CFP), foci intensity was reduced to the same or lower level as measured for YFP-HLTF (Figure 1I, J, quantified in K). These results show that localization of both wildtype HLTF and HLTF

5

F960A in PCNA foci are reduced by overexpression of peptides containing the APIM sequence of HLTF, supporting that APIM in HLTF is a functional PCNA-interacting motif.
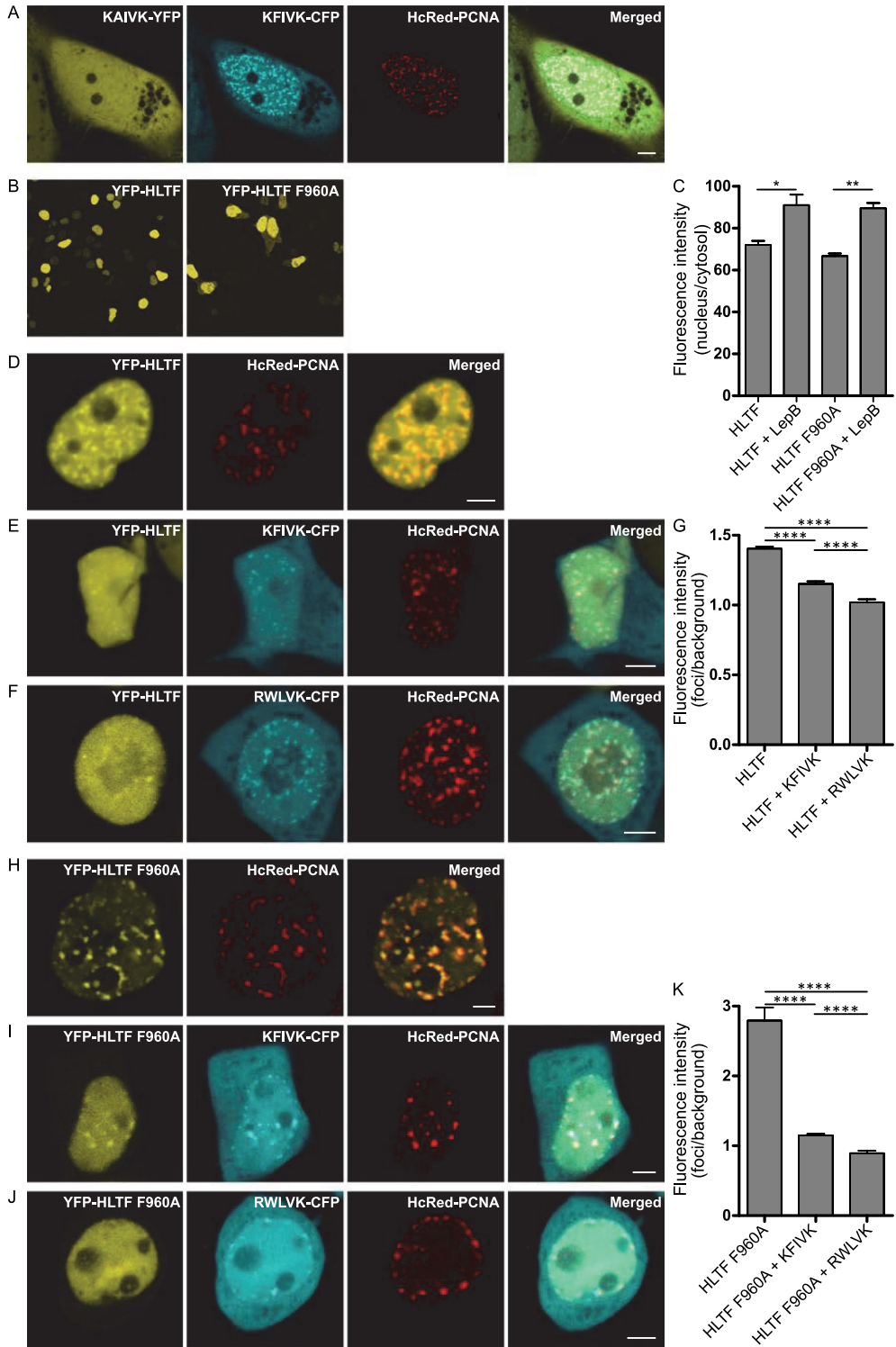
Figure 1: APIM in HLTF is a functional PCNA-interacting motif. (A) Overexpressed KAIVK-YFP (mutAPIM in HLTF), KFIVK-CFP (APIM in HLTF) and HcRed-PCNA. (**B**) Overview of subcellular localization of YFP-HLTF and YFP-HLTF F960A, and (**C**) quantification of their nuclear localization in cells treated with Leptomycin B (LepB; 30 ng/ml, 45 min) (n=>90 cells per sample). (**D**) Overexpressed YFP-HLTF and HcRed-PCNA, (**E**) YFP-HLTF, KFIVK-CFP (APIM of HLTF) and HcRed-PCNA, and (**F**) YFP-HLTF, RWLVK-CFP and HcRed-PCNA. (**G**) Quantification of YFP-HLTF foci intensities with and without co-transfection of KFIVK-CFP (n=76) or RWLVK-CFP (n=59). (**H**) Overexpressed YFP-HLTF F960A and HcRed-PCNA, (**I**) YFP-HLTF F960A, KFIVK-CFP (APIM of HLTF) and HcRed-PCNA, and (**J**) YFP-HLTF F960A, RWLVK-CFP and HcRed-PCNA. (**K**) Quantification of YFP-HLTF F960A foci intensities with and without co-transfection of KFIVK-CFP (n=103) or RWLVK-CFP (n=98). Foci intensity quantifications were done using Image J software. All images done in live cells. Scale bar = 5 μm. Two-sided Student`s t-test, * p< 0.05, ** p< 0.01, **** p< 0.0001.

2.2 Nuclear localization of SHPRH depends on the interaction of SHPRH with PCNA

Like HLTF, APIM in SHPRH (RFLIK) was fused to CFP and co-expressed with HcRed-tagged PCNA. RFLIK-CFP colocalized with PCNA, while the F2A APIM mutant version (RALIK-CFP) did not (Figure 2A). The same APIM mutation in full-length SHPRH (F1632A), led to a strong reduction in nuclear localization compared to wildtype SHPRH (Figure 2B, quantified in C, first and forth bar). These results could suggest that the interaction with PCNA is necessary for the nuclear localization of SHPRH or that the mutant SHPRH protein is less stable. To explore if the nuclear localization of SHPRH is dependent on a direct interaction with PCNA, we examined if the fraction of nuclear SHPRH can be reduced by treatment with an APIM-containing cell penetrating peptide (APIM-peptide), which has earlier been shown to block the binding of APIM-containing proteins to PCNA [27]. Indeed, the fluorescence intensity of GFP-SHPRH in the nucleus was reduced upon APIM-peptide treatment (Figure 2C), and this effect was not achieved by treatment with a mutant version of the APIM-peptide with reduced affinity for PCNA (MutAPIM-peptide, W2A)[37]. Together these results indicate that nuclear localization of SHPRH is dependent on its direct binding to PCNA via APIM.

Like HLTF, both GFP-SHPRH and GFP-SHPRH F1632A colocalized with overexpressed HcRed-PCNA in replication foci (Figure 2D, E). Thus, the residual affinity of SHPRH F1632A to PCNA and/or its interaction with other PCNA-interacting proteins is sufficient to cause localization of SHPRH F1632A in replication foci.

2.3   APIM in SHPRH and HLTF is required for maximal pull down of PCNA after DNA damage

Our results suggest that APIM in both HLTF and SHPTH are functional PCNA-interacting motifs. To further verify this, we examined if endogenous PCNA can be pulled down by the GFP-SHPRH and YFP-HLTF fusion proteins. As APIM - PCNA interactions are relatively weak, and PCNA interactions with HLTF and SHPRH are expected to be dynamic and to increase upon DNA damage, we treated the cells with MMS and gently cross-linked the cells with formaldehyde before making extracts (see material and methods and [24]). We could not detect any specific PCNA pull down in absence of MMS treatment (data not shown), but both YFP-HLTF and GFP-SHPRH pulled down more endogenous PCNA than the YFP control (Figure 2F, normalized against total GFP pulled down). Importantly, mutated APIM versions of the proteins abolished (HLTF F960A) or reduced PCNA pulldown by at least 50 % (SHPRH F1632A) compared to wildtype protein versions. We detected less full-length protein and more degraded protein in APIM mutants compared to the wildtype proteins (Supplementary Figure S1), further supporting that PCNA interactions are important for the stability of both HLTF and SHPRH.
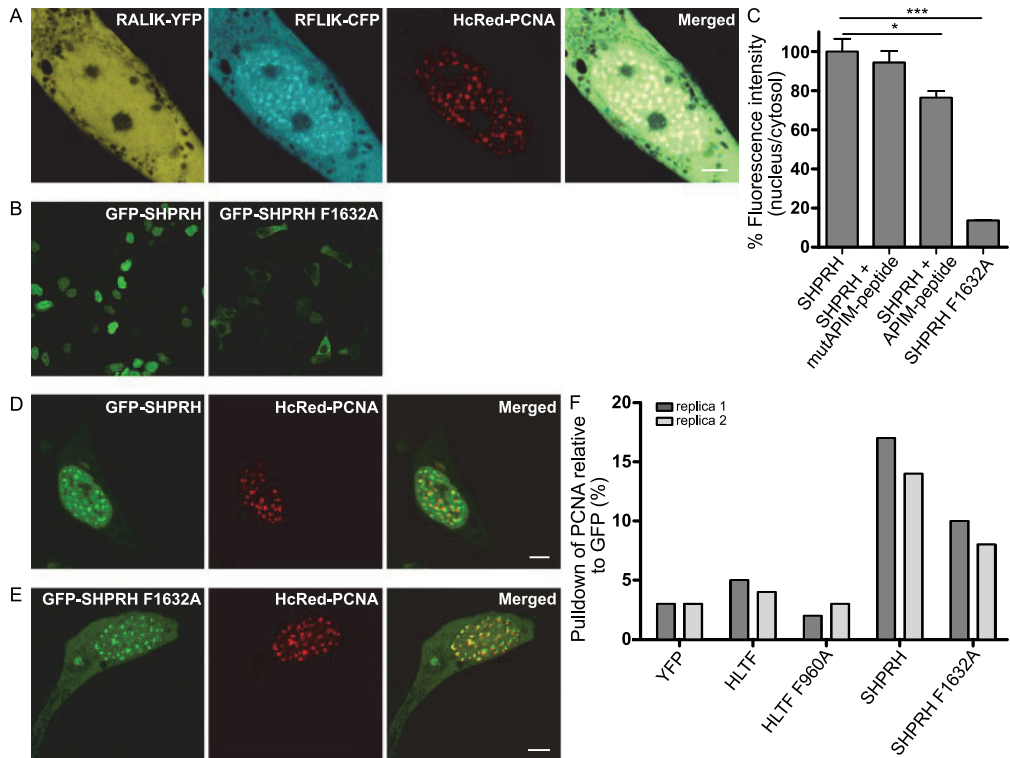
Figure 2: SHPRH localization in the nucleus is dependent on APIM. (**A**) Overexpressed RALIK-YFP (mutAPIM in SHPRH), RFLIK-CFP (APIM in SHPRH) and HcRed-PCNA. (**B**) Overview of subcellular localization of GFP-SHPRH and GFP-SHPRH F1632A and (**C**) quantification of nuclear localization of GFP-SHPRH (n(number of foci)= 484) and GFP-SHPRH F1632A (n=123), and GFP-SHPRH after treatment with an APIM peptide (n=247) or mutAPIM-peptide (n=319), average of 3 replicas, normalized to untreated control, two-sided Student`s t-test, * p< 0.05, *** p< 0.001. (**D**) Overexpressed GFP-SHPRH and HcRed-PCNA and (**E**) GFP-SHPRH F1632A and HcRed-PCNA. All images are live cells. Scale bar = 5 µm (**F**) Quantification of PCNA levels pulled down by anti-GFP from YFP-HLTF, YFP-HLTF F960A, GFP-SHPRH and GFP-SHPRH F1632A transfected cells after weak cross-linking and MMS treatment. Levels of PCNA is given as % of total GFP-protein pulled down. Two independent biological replicas are shown.

2.4 Direct interaction with PCNA is important for the regulation of DDT by HLTF and SHPRH

To further examine the functionality and the impact of APIM in HLTF and SHPRH in DDT, we performed SupF mutagenesis assays. We therefore measured the mutation frequency and analysed the mutation spectra in UV damaged reporter plasmids in cells overexpressing wildtype or APIM mutant versions of HLTF or SHPRH. Overexpression of HLTF did not significantly change the mutation frequency compared to control, although a tendency towards

a reduction was observed. However, overexpression of HLTF F960A significantly increased the mutation frequency by 45 % compared to both control and HLTF wildtype overexpressing cells (Figure 3A). This suggests that a direct interaction with PCNA is important for HLTF´s ability to support error-free repair. One of the most studied TLS polymerase, POLη, is important in bypassing UV-lesions and essential for error-free bypass of TT-CPDs [38]. HLTF has previously been reported to stimulate bypass by POLη [19]. Thus, our results could indicate a lack of POLη stimulation in HLTF F960A overexpressing cells and that POLη stimulation by HLTF is dependent on a direct interaction with PCNA. Recently, a loss-of-function mutation in HLTF has been reported to increase the amount of DNA damage due to a decrease in PCNA polyubiquitination [39]. Thus, the increase in the mutation frequency in presence of HLTF F960A overexpression could also be caused by a reduction of PCNA polyubiquitination and TS, indicating that APIM in HLTF is important for PCNA polyubiquitination mediated by HLTF. Recently, Masuda and colleagues reported that a HLTF - PCNA interaction at stalled primer ends reduced the polyubiquitination activity of HLTF *in vitro*, and that the polyubiquitination activity of HLTF could be partly restored by a mutation in the putative APIM in HLTF (F960A) [40]. However, they did not know if APIM was a functional PCNA-interacting motif. We show here that APIM in HLTF is a functional PCNA-interacting motif, thus our results support that the restoration of HLTF`s polyubiquitination activity seen by Masuda and colleagues, was due to a reduced PCNA interaction. Therefore, the increased mutation frequency in HLTF F960A overexpressing cells detected in our study is probably not caused by reduced, but rather by in increased polyubiquitination and excessive fork reversal. The latter is associated with genomic instability [41].
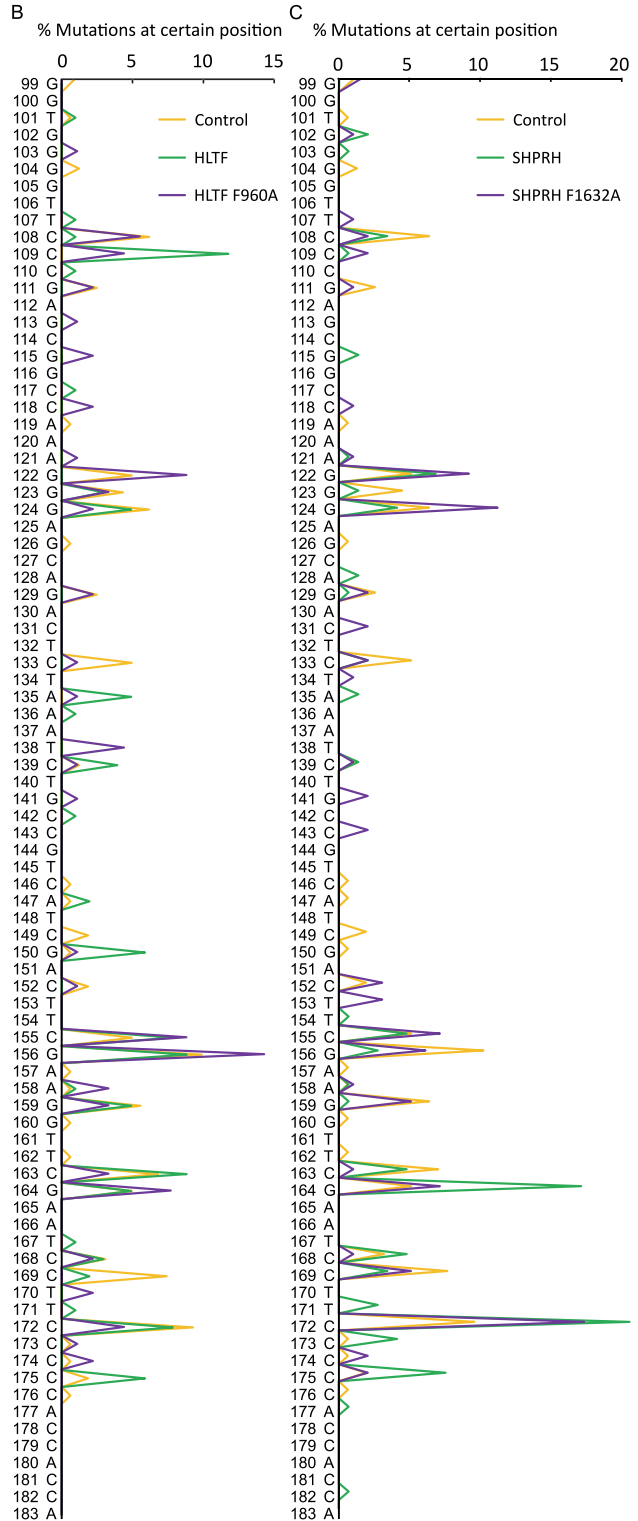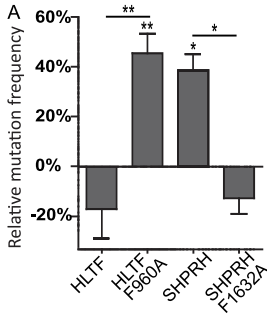
SHPRH overexpression increased the mutation frequency compared to both SHPRH F1632A overexpressing and control cells (Figure 3A), suggesting a dysregulation of DDT after SHPRH overexpression.

In line with our data it is reported that HLTF is more important for the regulation towards error-free DDT over UV-induced DNA damage than SHPRH, i.e. the mutation frequency was increased after HLTF knockdown but not after SHPRH knockdown [19]. The mutation spectra of SupF reveal multiple differences between plasmids replicated in cells overexpressing wildtype and APIM mutant versions of the RAD5 homologs. This further illustrates the impact of a direct interaction with PCNA for both HLTF and SHPRH (Figure 3B, C).

2.5 Direct binding of HLTF to PCNA is important for error-free DDT and/or DNA repair

When analyzing the mutations in *SupF* isolated from the different cells, we found mainly C to T transitions (corresponding G to A mutations on the transcribed strand) in plasmids from control cells (Figure 3D, G). DNA mutations resulting from UV-exposure are usually ~80 % C to T transitions [42], and accordingly C to T mutations are frequently found in skin cancers [43]. Thus, our results follow the expected mutation pattern from UV-irradiation *in vitro* and *in vivo*. Overexpression of HLTF led to an increase of transitions from 83 % (in control) to 90 %, and this increase was mainly caused by an increase of tandem CC to TT mutations (Figure 3D). UV-induced 6-4PPs are quickly repaired by NER while CPDs are repaired at a slower rate. Therefore, the main amount of mutations received in our experiments likely arised from bypass of CPDs (TT, TC and CC). C to T transitions are the most frequent mutations found in both XPV cells (lacking POLη, [44]) and normal cells. However, knockdown of POLη in mammalian cells does not change the amount of C to T mutations after UV-irradiation [38, 45]. This suggests that also other TLS polymerases than POLη can bypass CPDs leading to C to T transitions. Thus, wheather the increase of CC to TT mutations is a result of HLTF mediated stimulation of POLη or stimulation of other TLS polymerases cannot be concluded based on our data.

Overexpression of HLTF F960A resulted in fewer transition mutations compared to HLTF overexpression, especially on the coding strand (26 % versus 42 % C to T mutations, and 7 % versus 12 % CC to TT mutations), and an overall increase of mutations on the transcribed/non-coding/template strand (Figure 3D). At the same time, HLTF F960A overexpression led to an increase in the mutation frequency (Figure 3A). Since transcription-coupled NER is error-free and probably repairs a part of the lesions on the transcribed strand, HLTF F960A overexpression is suggested to either dysregulate NER and/or other error-free repair/bypass processes, for example fork reversal or TS. Thus, our results suggest that a direct interaction between PCNA and APIM in HLTF is important for error-free TLS and/or repair regulated by HLTF.

A

Relative mutation frequency; HLTF, HLTF F960A, SHPRH, SHPRH F1632A (** , ** , * , *)

B % Mutations at certain position (0 5 10 15)

Control — HLTF — HLTF F960A

Positions 99–183

C % Mutations at certain position (0 5 10 15 20)

Control — SHPRH — SHPRH F1632A

Positions 99–183

D Types of mutations in reporter plasmid (%)

Mutation		Control	HLTF	HLTF F960A	SHPRH	SHPRH F1632A
C	T	43	42	26	51	46
G	A	34	29	48	30	37
CC	TT	4	12	7	4	0
C	A	4	0	4	0	0
G	T	4	1	0	1	6
GG	AA	2	2	2	2	1
T	A	1	3	4	0	0
T	C	1	0	0	2	4
A	G	0	5	2	1	1
Transitions		83	90	84	91	89
Transversions		9	6	12	5	8
at C or T		56	60	45	60	54

E 164 (positions 162 163 **164** 165 166) — Number of mutations; Control, HLTF, HLTF F960A, SHPRH, SHPRH F1632A

172 (positions 170 171 **172** 173 174)

F 109 (positions 107 108 **109** 110 111) — Number of mutations

122 (positions 120 121 **122** 123 124)

G
- C to T 43%
- G to A 34%
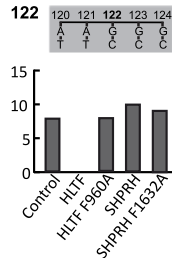- G to T (3%)
- CC to TT (4%)
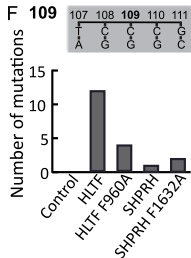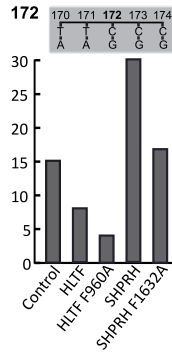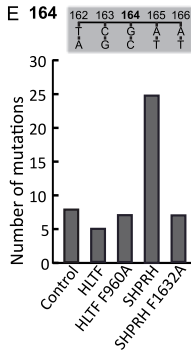- C to A (4%)
- GG to AA (2%)
- Rest 10%
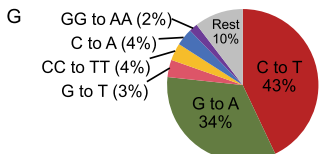
Figure 3: Mutation of APIM in HLTF and SHPRH results in differences in mutation frequencies and mutation spectra

(**A**) Mutation frequencies after overexpression of HLTF, HLTF F960A, SHPRH, or SHPRH F1632A together with SupF reporter plasmid pSP189 relative to control (reporter plasmid only) in HEK293 cells with number of colonies counted for HLTF (n=14700), HLTF F960A (n=13321), SHPRH (n=11183), SHPRH F1632 (n=14709), control (n=17560), two-sided student`s t-test, ** p<0.01. (**B, C**) Mutation spectra received from sequencing mutant colonies from (A). HLTF (n=102), HLTF F960A (n=91), SHPRH (n=152), SHPRH F1632 (n=102), control (n=163). (**D**) Quantification of different mutations using sequencing results from (B, C). Mutations with prevalence ≥ 2 % are shown. Mutations at T or C bases (putative codings strand mutations) in *supF* (**E**) Mutations at position 164 and 172 in *supF* isolated from cells expressing HLTF, HLTF F960A, SHPRH, or SHPRH F1632A compared to control. (**F**) Mutations at position 109 and 122 in *supF* isolated from cells expressing HLTF, HLTF F960A, SHPRH, or SHPRH F1632A compared to control. (**G**) Distribution of mutations using sequencing results from (B, C) received from reporter plasmid isolated from control cells.

2.6 SHPRH overexpression stimulates error-prone TLS

Overexpression of SHPRH led to an increase in the mutation frequency by 38 % (Figure 3A) and an increase of transitions, mainly due to a higher amount of C to T transitions (51 % compared to 43 % in control) (Figure 3D). Mutations at position 164 and 172 further illustrate this higher amount of mutations at Cs in SHPRH overexpressing cells (Figure 3E). POLκ has been shown to be activated by SHPRH overexpression [19], thus the observed C to T transitions could be by mediated POLκ. In presence of SHPRH F1632A overexpression, we observed a mutation spectrum that was more similar to the control than to SHPRH wildtype overexpression. This might be caused by lower nuclear level of SHPRH F1632A, because we found that function and nuclear localization of SHPRH is dependent on a direct APIM-mediated PCNA interaction (Figure 3B).

Since HLTF and SHPRH are reported to be partly competetive [19, 38], the changes in mutation patterns observed after overexpression of both wildtype and APIM mutants of SHPRH and HLTF result from a disturbance of the HLTF/SHPRH ratio.

2.7 Reduced levels of putative transcribed strand mutations after overexpression of HLTF and SHRPH

Due to the nature of UV-lesions (mainly occuring at C and T bases) and to the fact that we sequenced the coding strand only, we categorized mutations into mutations which with high probability occurred on the coding strand versus transcribed strand. We found a lower fraction of mutations on the coding strand (44 % v.s. 56 % on transcribed strand) in *SupF* isolated from

control cells (Figure 3D). This could be explained by transcription coupled NER repairing lesions on the transcribed strand and/or by a higher TLS rate on the coding strand. When HLTF or SHPRH were overexpressed the mutations on the coding strand decreased to 40 %. This could be explained by increased TLS on the coding strand (e.g. POLη or κ) or decreased error-free repair/bypass on the transcribed strand (e.g. TS, NER or error-free TLS). Overexpression of HLTF F960A resulted in an increased amount of G to A (48 %) transitions compared to overexpression of wildtype HLTF (29 %)(Figure 3D). In addition, mutations on the transcribed strand increased from 40 % for HLTF to 55 % for HLTF F960A. The number of mutations at position 109 (mutations on coding strand CC) and 122 (mutations on transcribed strand CC) in the *SupF gene* (Figure 3F), further illustrate the large difference between HLTF and HLTF F960A overexpression on coding and transcribed strand mutations. The same trends, although less pronouced, were detected for SHPRH wildtype versus SHPRH F1632A, in spite of the low nuclear abundance of the mutated protein. SHPRH overexpression resulted in a shift from G to A (30 %) mutations to C to T (51 %) mutations in comparison to SHPRH F1632A overexpression (37 % and 46 %, respectively) (Figure 3D), and differences in the mutation spectra, especially in the amout of mutations at positions 124 and 164 and in the type of mutation e.g. at position 122 (Figure 3B, E). In total, these results further support that APIMs in HLTF and SHPRH are functional PCNA-interacting motifs which seem to be especially important for reducing mutations on the transcribed strand.

In conclusion, the results presented here show that both mammalian RAD5 homologs, HLTF and SHPRH, contian a functional APIM sequence and that their direct interaction with PCNA is important for the regulation of the DDT pathways. Our data also shows that increased levels of wildtype HLTF and SHPRH disturb the balance of error-free and error-prone DDT pathways, suggesting that their levels are normally strictly regulated.

3   Material and methods

3.1. Expression constructs.

pEGFP-C2-HLTF and pEGFP-C2-SHPRH, the pSP189 reporter plasmid and *E. coli* strain MBM7070 described in [19], were kind gifts from Professor Karlene Cimprich, Department of Chemical and Systems Biology, Stanford University, USA. HLTF was sub-cloned into pEYFP-C1 vector (YFP-HLTF) and site-specific mutations at position F960A in HLTF, and F1632A in SHPRH were generated as described [24]. The wildtype APIM sequences from HLTF (aa 959-963, KFIVK) and SHPRH (aa 1631-1635, RFLIK) as well as the corresponding APIM mutant (F2A) was cloned as fusions with CFP or YFP, respectively, by using pECFP-N1 and pEYFP-N1 vectors with mutated ATG, similarly to RWLVK-CFP [24]. CFP-PCNA and HcRed-PCNA have previously been described [46].

3.2. Cell lines.

HEK293, HEK293T, and Hela cells (ATCC: CRL-1573, CRL 11268, and CCL-2, respectively) were cultured in D-MEM (4.5 g/L; Sigma-Aldrich). Media was supplemented with 10 % fetal bovine serum (FBS; Sigma-Aldrich), 2.5 µg/ml Fungizone ® Amphotericin B (Gibco, Life Sciences), 1 mM L-Glutamine (Sigma-Aldrich) and antibiotic mixture containing 100 µg/ml penicillin and 100 µg/ml streptromycin (Gibco, Invitrogen^{TM}). The cells were cultured at 37 °C in a 5 % CO_2-humidified atmosphere.

3.3. SupF assay.

The SupF mutagenicity assay was performed essentially as previously reported [19]. Briefly, the reporter plasmid pSP189 was irradiated with 600 mJ/cm^2 UVB (312 nm), with UV lamp Vilber Lourmat, Bio Spectra V5. Cells were transfected with constructs of interest and UVB-irradiated pSP189 (including plasmids not exposed to UVR as controls) using X-treme GENE HP transfection reagent according to manufacturer protocol (Roche diagnostics); at least 3 biological replicas were conducted (3 transfections). Cells were harvested after 48 h for both isolation of plasmid and western analysis. Isolated plasmids were DpnI (NEB) restriction digested to exclude original bacterial plasmids in order to continue with only replicated plasmids. Isolated plasmids were transformed into *E. coli* MBM7070 cells and plated on indicator X-gal/IPTG/Amp agar plates. Blue/White screening was performed and mutation frequency (white/ blue colonies) was calculated for the different samples for several transfections (at least 3 replicas). White and light blue colonies were picked for re-streaking

and DNA sequencing of SupF gene. Colonies that did not show a mutation in the sequencing results were afterwards excluded and the mutation frequency was recalculated.

3.4. Imaging.

Live cell imaging of HEK293 transfected with pGFP-SHPRH, pGFP-SHPRH F1632A, pYFP-HLTF, pYFP-HLTF F960A, pHcRed-PCNA, and YFP/CFP constructs of the APIM/mutated APIM in HLTF or SHPRH were performed 24 h after transfection using a Zeiss LSM 510 Meta laser scanning microscope equipped with a Plan-Apochromate 63x /1.4 oil immersion objective. GFP and CFP were excited/detected at λ=458 nm/BP470-500 nm YFP was excited/detected at λ=514 nm/BP530-600 nm, and HcRed was excited/detected at λ=543 nm/LP615 nm, using consecutive scans. The thickness of the scanned optical slices was 1 μm.

Live cell imaging of HEK293T transfected with pYFP-HLTF or pYFP-HLTF F960A together with pKFIVK-CFP or pRWLVK-CFP and pHcRed-PCNA was performed as described above, but YFP was detected at BP535-590 nm in these experiments. Fluorescence intensities were measured in cells with comparable expression levels of YFP and CFP using the imaging processing software Fiji (ImageJ) version 1.06.2016. Average intensity within an area of interest (foci) was measured and divided by average intensity in the nucleus outside foci.

For SupF assay transfection control, HEK293 cells were transfected with proportional amounts of transfection mix as used in the SupF assay. Live cell imaging was performed 48 h after transfection using Zeiss LSM 510 Meta laser scanning microscope as described above, in order to evaluate the transfection efficacy.

3.6. Measurement of fluorescence intensities after APIM-peptide or Leptomycin B treatment. HEK293 cells were transfected with pGFP-SHPRH, pGFP-SHPRH F1632A, pYFP-HLTF or pYFP-HLTF F960A, using X-treme GENE HP transfection reagent according to manufacturer protocol (Roche diagnostics). After 24 h and 30 h the cells were treated with 8 μM APIM-peptide (Innovagen, Sweden), 8 μM APIM-peptide (Innovagen) or 30 ng/mL Leptomycin B. Not treated is the negative control. 45 min after the treatment, images were taken and the fluorescence intensity (mean) in the region of interest covering at least 200 pixels using Zeiss LSM 510 software were measured.

3.7. Preparation of cross-linked cell extracts

HEK293T cells were transfected with the construct of interest and treated with 50 μM methyl methanesulfonate (MMS) the next day. 48 h after MMS treatment intact cells were gently cross-linked with 0.2 % formaldehyde as previously described [24]. Cells were lysed using 3 x PCV

M-PER Mammalian Protein Extraction Reagent (Thermo Scientific), PIC2 (10 µl/ml buffer) and PIC 3 (10 µl/ml buffer) (Sigma Aldrich) and complete protease inhibitor (20 µl/ml buffer)(Roche) for 1 hour at 4 ˚C and sonicated in a sonication water bath 5 rounds of 30 sec on 30 sec off (Picoruptor SA, Diagenode). 1 µl Omnicleave was added to 100 µl PCV. The lysate was cleared by centrifugation for 10 min at 16000 g, 4 °C.

3.8. Immunoprecipitation.

An in-house affinity-purified rabbit polyclonal antibody raised against GFP protein, which also recognizes YFP and CFP proteins (called α-GFP), was covalently linked to protein A paramagnetic beads (Invitrogen) according to instructions provided by New England Biolabs, Inc. 750 µg cell extract was incubated with 30 µl antibody-coupled beads and 0.3 ml IP buffer (20 mM Hepes, pH 7.9, 1.5 mM MgCl$_2$, 100 mM KCl, 0.2 mM EDTA, 10 % glycerol, 1 mM DTT, 10mM Na-butyrate, 0.1mM NaVO3 and 1x complete protease inhibitor) under constant rotation at 4 °C overnight. The beads were washed three times with 500 µl 10 mM Tris-HCl pH 7.4 with a 5 min incubation on ice in between each wash. The beads were resuspended in 30µl NuPAGE (Invitrogen) loading buffer including DTT (final concentration 0.1 M) and heated 30 min at 95 °C to reverse crosslinks before the samples were run on 4–12 % Bis-Tris-HCl (NuPAGE) gels. 100 µg cell extract was used for input. The primary antibodies α-GFP (ab290, Abcam) and α-PCNA (sc-56, Santa Cruz Biotechnology) as well as the secondary antibodies IRDye 800CW (Goat Anti-Rabbit) and IRDye 700RD (Goat Anti-Mouse) (LI-COR Bioscience) were diluted in 5 % dry milk in PBS and the proteins were visualized and quantified using the Odyssey Imager.

18

AUTHOR CONTRIBUTIONS:

M.O. and M.S. planned the study, M.S. performed the experiments, M.O. supervised and M.O. and M.S. wrote the manuscript.

4   References

1.   Marians, K.J., *Lesion Bypass and the Reactivation of Stalled Replication Forks.* Annu Rev Biochem, 2018. **87**: p. 217-238.

2.   Hoeijmakers, J.H., *DNA damage, aging, and cancer.* N Engl J Med, 2009. **361**(15): p. 1475-85.

3.   Yoon, J.H., et al., *The DNA damage spectrum produced by simulated sunlight.* J Mol Biol, 2000. **299**(3): p. 681-93.

4.   Pfeifer, G.P., *Formation and processing of UV photoproducts: effects of DNA sequence and chromatin environment.* Photochem Photobiol, 1997. **65**(2): p. 270-83.

5.   Kemp, M.G. and A. Sancar, *DNA excision repair: where do all the dimers go?* Cell Cycle, 2012. **11**(16): p. 2997-3002.

6.   Hu, J., et al., *Genome-wide analysis of human global and transcription-coupled excision repair of UV damage at single-nucleotide resolution.* Genes Dev, 2015. **29**(9): p. 948-60.

7.   Riou, L., et al., *The relative expression of mutated XPB genes results in xeroderma pigmentosum/Cockayne's syndrome or trichothiodystrophy cellular phenotypes.* Hum Mol Genet, 1999. **8**(6): p. 1125-33.

8.   Garinis, G.A., et al., *Transcriptome analysis reveals cyclobutane pyrimidine dimers as a major source of UV-induced DNA breaks.* EMBO J, 2005. **24**(22): p. 3952-62.

9.   Cordonnier, A.M., A.R. Lehmann, and R.P. Fuchs, *Impaired translesion synthesis in xeroderma pigmentosum variant extracts.* Mol Cell Biol, 1999. **19**(3): p. 2206-11.

10.   Inui, H., et al., *Xeroderma pigmentosum-variant patients from America, Europe, and Asia.* J Invest Dermatol, 2008. **128**(8): p. 2055-68.

11.   Kraemer, K.H., et al., *The role of sunlight and DNA repair in melanoma and nonmelanoma skin cancer. The xeroderma pigmentosum paradigm.* Arch Dermatol, 1994. **130**(8): p. 1018-21.

12.   Kraemer, K.H., M.M. Lee, and J. Scotto, *Xeroderma pigmentosum. Cutaneous, ocular, and neurologic abnormalities in 830 published cases.* Arch Dermatol, 1987. **123**(2): p. 241-50.

13.   Menck, C.F. and V. Munford, *DNA repair diseases: What do they tell us about cancer and aging?* Genet Mol Biol, 2014. **37**(1 Suppl): p. 220-33.

14.   Leung, W., et al., *Mechanisms of DNA Damage Tolerance: Post-Translational Regulation of PCNA.* Genes (Basel), 2018. **10**(1).

15.   Masuda, Y., et al., *En bloc transfer of polyubiquitin chains to PCNA in vitro is mediated by two different human E2-E3 pairs.* Nucleic Acids Res, 2012. **40**(20): p. 10394-407.

16.   Chavez, D.A., B.H. Greer, and B.F. Eichman, *The HIRAN domain of helicase-like transcription factor positions the DNA translocase motor to drive efficient DNA fork regression.* J Biol Chem, 2018. **293**(22): p. 8484-8494.

17.   Ciccia, A., et al., *Polyubiquitinated PCNA recruits the ZRANB3 translocase to maintain genomic integrity after replication stress.* Mol Cell, 2012. **47**(3): p. 396-409.

18.   Betous, R., et al., *Substrate-selective repair and restart of replication forks by DNA translocases.* Cell Rep, 2013. **3**(6): p. 1958-69.

19.   Lin, J.R., et al., *SHPRH and HLTF act in a damage-specific manner to coordinate different forms of postreplication repair and prevent mutagenesis.* Mol Cell, 2011. **42**(2): p. 237-49.

20.   Kim, J.J., et al., *Promoter methylation of helicase-like transcription factor is associated with the early stages of gastric cancer with family history.* Ann Oncol, 2006. **17**(4): p. 657-62.

21.   Capouillez, A., et al., *Expression of the helicase-like transcription factor and its variants during carcinogenesis of the uterine cervix: implications for tumour progression.* Histopathology, 2011. **58**(6): p. 984-8.

22.   Zhang, M., et al., *A novel protein encoded by the circular form of the SHPRH gene suppresses glioma tumorigenesis.* Oncogene, 2018.

23.   Moinova, H.R., et al., *HLTF gene silencing in human colon cancer.* Proc Natl Acad Sci U S A, 2002. **99**(7): p. 4562-7.

24.   Gilljam, K.M., et al., *Identification of a novel, widespread, and functionally important PCNA-binding motif.* J Cell Biol, 2009. **186**(5): p. 645-54.

25.   Warbrick, E., *PCNA binding through a conserved motif.* Bioessays, 1998. **20**(3): p. 195-9.

26.   Olaisen, C., et al., *The role of PCNA as a scaffold protein in cellular signaling is functionally conserved between yeast and humans.* FEBS Open Bio, 2018. **8**(7): p. 1135-1145.

27.   Muller, R., et al., *Targeting proliferating cell nuclear antigen and its protein interactions induces apoptosis in multiple myeloma cells.* PLoS One, 2013. **8**(7): p. e70430.

28.   Bacquin, A., et al., *The helicase FBH1 is tightly regulated by PCNA via CRL4(Cdt2)-mediated proteolysis in human cells.* Nucleic Acids Res, 2013. **41**(13): p. 6501-13.

29.   Fu, D., et al., *The interaction between ALKBH2 DNA repair enzyme and PCNA is direct, mediated by the hydrophobic pocket of PCNA and perturbed in naturally-occurring ALKBH2 variants.* DNA Repair (Amst), 2015. **35**: p. 13-8.

30.   Sebesta, M., et al., *Structural insights into the function of ZRANB3 in replication stress response.* Nat Commun, 2017. **8**: p. 15847.

31. Choe, K.N. and G.L. Moldovan, *Forging Ahead through Darkness: PCNA, Still the Principal Conductor at the Replication Fork.* Mol Cell, 2017. **65**(3): p. 380-392.

32. Gederaas, O.A., et al., *Increased Anticancer Efficacy of Intravesical Mitomycin C Therapy when Combined with a PCNA Targeting Peptide.* Transl Oncol, 2014. **7**(6): p. 812-23.

33. Sogaard, C.K., et al., *"Two hits - one stone"; increased efficacy of cisplatin-based therapies by targeting PCNA's role in both DNA repair and cellular signaling.* Oncotarget, 2018. **9**(65): p. 32448-32465.

34. Sogaard, C.K., et al., *APIM-peptide targeting PCNA improves the efficacy of docetaxel treatment in the TRAMP mouse model of prostate cancer.* Oncotarget, 2018. **9**(14): p. 11752-11766.

35. Fattah, F.J., et al., *The transcription factor TFII-I promotes DNA translesion synthesis and genomic stability.* PLoS Genet, 2014. **10**(6): p. e1004419.

36. Raeder, S.B., et al., *APIM-Mediated REV3L(-)PCNA Interaction Important for Error Free TLS Over UV-Induced DNA Lesions in Human Cells.* Int J Mol Sci, 2018. **20**(1).

37. Olaisen, C., et al., *PCNA-interacting peptides reduce Akt phosphorylation and TLR-mediated cytokine secretion suggesting a role of PCNA in cellular signaling.* Cell Signal, 2015. **27**(7): p. 1478-87.

38. Yoon, J.H., L. Prakash, and S. Prakash, *Highly error-free role of DNA polymerase eta in the replicative bypass of UV-induced pyrimidine dimers in mouse and human cells.* Proc Natl Acad Sci U S A, 2009. **106**(43): p. 18219-24.

39. Takaoka, K., et al., *A germline HLTF mutation in familial MDS induces DNA damage accumulation through impaired PCNA polyubiquitination.* Leukemia, 2019. **33**(7): p. 1773-1782.

40. Masuda, Y., et al., *Regulation of HLTF-mediated PCNA polyubiquitination by RFC and PCNA monoubiquitination levels determines choice of damage tolerance pathway.* Nucleic Acids Res, 2018. **46**(21): p. 11340-11356.

41. Bhat, K.P. and D. Cortez, *RPA and RAD51: fork reversal, fork protection, and genome stability.* Nat Struct Mol Biol, 2018. **25**(6): p. 446-453.

42. Pfeifer, G.P., Y.H. You, and A. Besaratinia, *Mutations induced by ultraviolet light.* Mutat Res, 2005. **571**(1-2): p. 19-31.

43. Pfeifer, G.P. and A. Besaratinia, *UV wavelength-dependent DNA damage and human non-melanoma and melanoma skin cancer.* Photochem Photobiol Sci, 2012. **11**(1): p. 90-7.

44. Giglia-Mari, G. and A. Sarasin, *TP53 mutations in human skin cancers.* Hum Mutat, 2003. **21**(3): p. 217-28.

45. Choi, J.H. and G.P. Pfeifer, *The role of DNA polymerase eta in UV mutational spectra.* DNA Repair (Amst), 2005. **4**(2): p. 211-20.

46.   Aas, P.A., et al., *Human and bacterial oxidative demethylases repair alkylation damage in both RNA and DNA.* Nature, 2003. **421**(6925): p. 859-63.
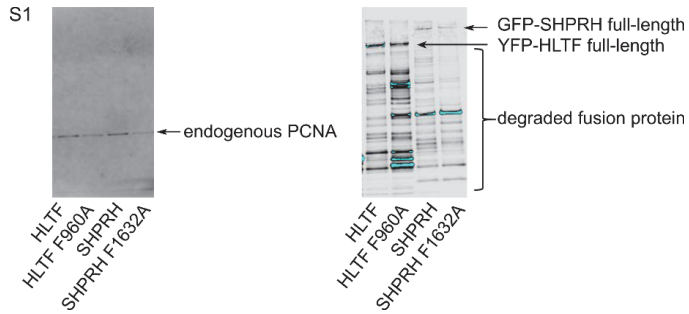
Supplementary material

S1

Figure S1. Mutation in APIM in HLTF or SHPRH reduced PCNA pulldown after DNA damage. Western blot analysis of proteins pulled down with α-GFP coupled beads from weakly crosslinked HEK293T cells after overexpression of YFP-HLTF, YFP-HLTF F960A, GFP-SHPRH, GFP-SHPRH F1632A and treatment with 50 μM MMS. Pull down of endogenous PCNA (upper panel, anti-PCNA), pull down of the overexpressed proteins (lower panel, anti-GFP).

Paper 3

The Human RAD5 homologs, HLTF and SHPRH, have distinct functions in DNA damage tolerance dependent on the DNA lesion type

Mareike Seelinger, Caroline Krogh Søgaard and Marit Otterlei[*]

Department of Clinical and Molecular Medicine, Faculty of Medicine and Health Sciences, Norwegian University of Science and Technology (NTNU), Trondheim, Norway

[*]To whom correspondence should be addressed:

Tel: +4792889422

E-mail: marit.otterlei@ntnu.no

Marit Otterlei

Department of Clinical and Molecular Medicine, Norwegian University of Technology (NTNU), PO Box 8905, N-7491, Trondheim, Norway

Key words: DDT, chemotherapeutics, CHK2, TLS, TS

Abbreviations: AT, Ataxia Telangiectasia; CPD, cyclo-pyrimidine dimer; DDR, DNA damage response; DDT, DNA damage tolerance; FA, Fanconi Anemia; HLTF, helicase-like transcription factor; ICL, interstrand crosslinks; MMC, mitomycin C; MMS, methyl methanesulfonate; NER, nucleotide excision repair; NHEJ, Non-Homologous End Joining; SHPRH, SNF2 histone-linker PHD and RING finger domain-containing helicase; TLS, translesion synthesis; TS, template switch; XP, Xeroderma Pigmentosum; dko, double knockout; 6-4PP, (6-4)photoproduct

Abstract

HLTF and SHPRH, the two human homologs of yeast Rad5, are believed to have a vital role in DNA damage tolerance (DDT). Here we show that HLTF, SHPRH and HLTF/SHPRH knockout cell lines have different sensitivities towards UV-irradiation, methyl methanosulfonate (MMS), Cisplatin and mitomycin C (MMC); drugs that induce different types of DNA lesions. In general, the HLTF/SHPRH double knockout cell line is less sensitive than the single knockouts in response to all drugs, and interestingly, especially to MMS and Cisplatin. Using the SupF assay, we detected an increase in the mutation frequency in HLTF knockout cells both after UV- and MMS-induced DNA damage, while we detected a decrease in the mutation frequency over UV-lesions in the HLTF/SHPRH double knockout cells. However, after MMS treatment no change in the mutation frequency was detected in the absence of HLTF and SHPRH, even though these cells were more resistant to MMS and grew faster than the other cell lines after DNA damaging treatments. This phenotype could possibly be explained by the reduced activation of CHK2 in cells lacking SHPRH, because this in turn could contribute to the reduced MCM2 phosphorylation observed after MMS treatment in these cells. Our data reveal both distinct and common roles of the human RAD5 homologs dependent on the nature of DNA lesions and identified SHPRH as a regulator of CHK2.

1   Introduction

Faithful replication of the genome is essential for life. DNA lesions that are not be repaired prior to replication can stall replication, which may lead to mutations, replication fork collapse and genome instability. Consequences of DNA repair deficiencies are for instance carcinogenesis or neurological problems, as illustrated by the diseases Xeroderma Pigmentosum (XP), Ataxia Telangiectasia (AT) or Fanconi Anemia (FA). These diseases exhibit defects in nucleotide excision repair (NER), in the central DNA damage sensing kinase ATM or in one of the 17 FA genes important for homologous recombination and the Fanconi Anemia Pathway, respectively [1-3].

Cells can tolerate lesions by activating so-called DNA damage tolerance (DDT) pathways; Translesion synthesis (TLS) which is often error-prone, fork reversal or template switch (TS) pathways which are error-free. These pathways ensure replication fork progression or restart upon replication stalling and promote the completion of DNA replication [4-6].

The human RAD5 homologs, HLTF (helicase-like transcription factor) and SHPRH (SNF2, histone-linker, PHD and RING finger domain-containing helicase), are multi-functional enzymes involved in TLS by activating POLη and POLκ, respectively [7], and in TS via polyubiquitination of PCNA [8]. HLTF and SHPRH are reported to suppress UV- or MMS-induced mutagenesis, respectively [7]. In addition, HLTF is an ATP-dependent translocase able to catalyze fork regression by its HIRAN domain [9]. Both proteins have been suggested as tumor suppressor genes, because dysregulation of HLTF and SHPRH is found in several types of cancers [10-13]. Structurally, HLTF is more similar to yeast Rad5 than SHPRH. SHPRH lacks a HIRAN domain and instead contains a histone H1 and H5 linker sequence, and a PHD domain [14]. Both RAD5 homologs bind to PCNA via their APIM sequence and this direct interaction is required to reduce the ratio of G to A (putative transcribed strand) versus C to T mutations after UV-irradiation. Furthermore, the PCNA - HLTF interaction is required for minimizing the overall mutation level (Seelinger and Otterlei, 2019, Paper 2 in this thesis). Still, little is known about the exact functions and interplay of HLTF and SHPRH in DDT.

In this study we show that both human RAD5 homologs have distinct functions in DDT, but that they are also dependent on each other. HLTF is important for minimizing the amount of

mutations after both UV- and MMS-treatment and SHPRH has a role in the regulation of the DNA damage response (DDR) via CHK2.

2 Results and Discussion

2.1 The two RAD5 homologs have different roles in DNA repair or tolerance depending on the DNA lesion

We wanted to explore the roles of HLTF and SHPRH in DDT using drugs inducing different types of DNA lesions. After the absence of HLTF and SHPRH expression in the knockout (ko) cell lines was confirmed by western analysis (Figure 1C). The different knockout (ko) cell lines were then exposed to various DNA damaging agents. MMC induces mainly mono-adducts and interstrand crosslinks (ICLs) with minor distortions in the DNA structure. The fraction of ICLs (~14 %) produced by MMC is the main contributor to the physiological challenges after MMC treatment [15, 16]. A reduction in cell survival was observed in all ko cell lines compared to the parental cell line, suggesting that both, HLTF and SHPRH are important for handling MMC-induced ICLs. However, the HLTF/SHPRH double ko (dko) cell line was less sensitive than the single ko cell lines (Figure 1A).

Cisplatin induces mainly DNA intrastrand crosslinks (> 95%), and only small amount of ICLs (2-5%) [17]. The intrastrand crosslinks formed by cisplatin were shown to be the main cause of cisplatin-mediated cytotoxicity [15]. In this case, the HLTF/SHPRH dko showed a significantly reduced sensitivity towards cisplatin compared to both parent and single ko cells, while HLTF ko cells were more sensitive to cisplatin than the parental cell line. Thus, HLTF seems to be important for handling intrastrand crosslinks formed by cisplatin, however, not in absence of SHPRH. This indicates that HLTF and SHPRH have diverse roles and are cooperating in repair/bypass of intrastrand crosslinks and ICLs. This could indicate roles in NER and/or TLS.

MMS induces mainly alkylated base lesions. The sensitivity to MMS was clearly reduced in both SHPRH and HLTF/SHPRH dko cells, while HLTF ko cells were slightly more sensitive than parent cells. SHPRH has been reported to stimulate POLκ after MMS-induced DNA lesions [7]. However, our results suggest that the stimulation of POLκ is not vital for survival, because cells lacking SHPRH were resistant to MMS (Figure 1A).

When examining the sensitivity to UV-irradiation, which induces cyclo-pyrimidine dimers (CPDs) and (6-4)photoproducts (6-4PPs), HLTF ko cells were again more sensitive, and SHPRH ko and HLTF/SHPRH dko cells were less sensitive than the parental cell line (Figure 1A). This supports a role for HLTF in repair/bypass of CPD UV-lesions, because 6-4PPs are rapidly repaired by NER. This is in accordance with the report showing that HLTF stimulates TLS over UV-lesions by recruiting POLη [7]. Stimulation of POLη could be important for survival not only after UV-irradiation, but also after MMS, Cisplatin and MMC treatment.

HLTF/SHPRH dko cells were less sensitive than the parent cells to almost all the DNA lesions induced in our experiments (except DNA lesions induced by MMC). Therefore, our results suggest that cells lacking both RAD5 homologs exhibit increased DNA repair and/or tolerance in response to intrastrand crosslinks, mono-adducts, CPDs, 6-4PP and alkylated bases. These lesions can be repaired by NER, BER, direct repair or bypassed by TLS. However, these dko cells did not increase DNA repair and/or tolerance in response to ICLs, possibly because the repair of ICLs requires the additional activation of HR and FA pathways.

Proliferation rates in absence of treatment revealed slightly slower growth rate of HLTF ko and the dko cells (Figure 1B); however, this should only marginally contribute to the differences in the growth rates detected after treatment. In summary, cell viability measurements of the HLTF and SHPRH single ko and dko cell lines treated with different DNA damaging agents suggest that the two RAD5 homologs have both distinct functions and inter-dependent functions in mediating repair/tolerance of different DNA lesions.
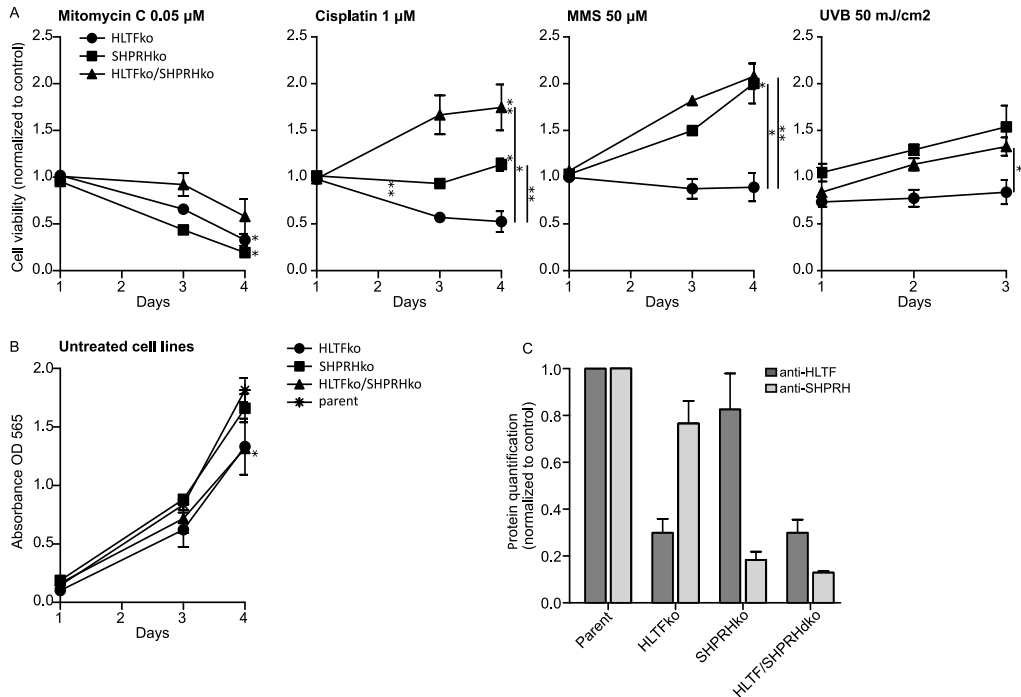
Figure 1. Knockouts of HLTF and SHPRH reduce the sensitivity towards several DNA damaging agents. (A) Cell growth of HLTF or SHPRH single knockout or HLTF/SHPRH double knockout Hap1 cell lines, compared to a Hap1 parent cell line measured by MTT assay after exposure to MMC, Cisplatin, MMS or UV-irradiation. Growth rates are normalized to the untreated control of each cell line. The average of 3 independent replica in proportion to the parent cell line is depicted +/- SD **(B)** Untreated control cell lines from (A) depicted. Two-sided student`s t-test, * p<0.05, ** p<0.01. **(C)** Hap1 knockout verification. Protein quantification by Western blot analysis.

2.2 Absence of HLTF and SHPRH reduces error-prone TLS over UV-induced DNA lesions

To evaluate the impact of TLS for the reduced sensitivity towards UV-irradiation and MMS exposure in cells lacking SHPRH (Figure 1A), we used a mutagenesis assay where a reporter plasmid was exposed to UV-irradiation and MMS (SupF assay).

The UV-damaged plasmids isolated from SHPRH ko cells did not show any change in the mutation frequency compared to plasmids form control cells, but somewhat unexpectedly, the simultaneous absence of HLTF and SHPRH resulted in a 24 % reduction in the mutation frequency. In contrast, the absence of only HLTF increased the mutation frequency by 18 % (Figure 2A).

Two possibilities have been suggested for how HLTF may reduce error-prone DDT: i) HLTF stimulates POLη and error-free bypass of TT-CPDs [7] and ii) HLTF induces PCNA polyubiquitination, triggering fork reversal and/or TS [8, 18]. Our data from the HLTF ko cells could support both decreased stimulation of POLη and/or PCNA polyubiquitination. However, the absence of HLTF, which possibly results in decreased lesion bypass by POLη, seems to be "rescued" by ko of SHPRH.

The mutation spectrum of *SupF* in the UV-damaged reporter plasmid isolated from HLTF/SHPRH dko cells revealed less C to T transitions (34 % compared to 50 % in parent cell line, 42 % in HLTF ko and 51 % in SHPRH ko), and more transversion mutations than plasmids isolated from the other cell lines (Figure 2B). Mutations at position 155, 172 and 156 are examples for this (Figure 2C). Thus, TLS across CPDs seems to be reduced in HLTF/SHPRH dko cells and instead these lesions are repaired/bypassed differently. The assumption of less TLS in HLTF/SHPRH dko cells is supported by the reduced mutation frequency in these cells. In addition, mutations at C and T bases, i.e. on the coding strand are also reduced in the absence of HLTF and SHPRH (dko cells) (44 % compared to 57 % in parental) (Figure 2B). This could theoretically be due to an increased repair on the transcribed strand and would then be an indication for a regulatory role of HLTF and SHPRH in transcription coupled repair.

However, the overall reduced mutation frequency in the dko cells suggests that these cells bypass/repair UV-lesions not by the "first choice" mechanisms, i.e. not by POLη or other TLS polymerases, and that these "second choice" mechanisms do not increase the mutation frequency in reporter plasmids. Polyubiquitination of PCNA can be performed by HLTF, SHPRH, or another unknown ubiquitin ligase [19]. Therefore, PCNA polyubiquitination might only be reduced in the absence of the RAD5 homologs, and the repair in the HLTF/SHPRH dko cells could therefore still mainly be facilitated by fork reversal or TS. In conclusion, the decreased sensitivity of dko cells towards UV-irradiation (Figure 1) is not caused by increased TLS, but could be mediated by fork reversal/TS in combination with other cellular changes such as increased repriming, increased firing of origins, increased post-replicative repair etc. The effect of HLTF ko and SHPRH ko on genome stability on chromosomal DNA can, however, not be determined by a plasmid-based assay.

2.3 HLTF and SHPRH are interdependent proteins in response to UV-lesions

The mutation spectrum in plasmids from HLTF ko cells contained less transition mutations compared to that of parent cells (81 versus 86 %, Figure 2B), an effect that is even more pronounced in plasmids from dko cells (74 %). The mutation spectrum showed different consequences of HLTF ko across identical template sequences, e.g. at position 156 the HLTF ko resulted in an increase of mutations relative to the other cell lines, whereas at position 164 the HLTF ko resulted in fewer mutations (Figure 2C and D). The opposite applies for the SHPRH ko cells at the same positions. This indicates that involvement of HLTF or SHPRH in TLS across UV-lesions depends on multiple mechanisms, which could be for example the distance from origins or location of the lesion (coding strand/transcribed strand, leading/lagging strand) and not only on the type of lesion and/or the sequence context.

In total, our mutation spectra analysis reveals a phenotype for the HLTF/SHPRH dko cells that differs from single HLTF and SHPRH ko cells and show that the two RAD5 homologs are interconnected.
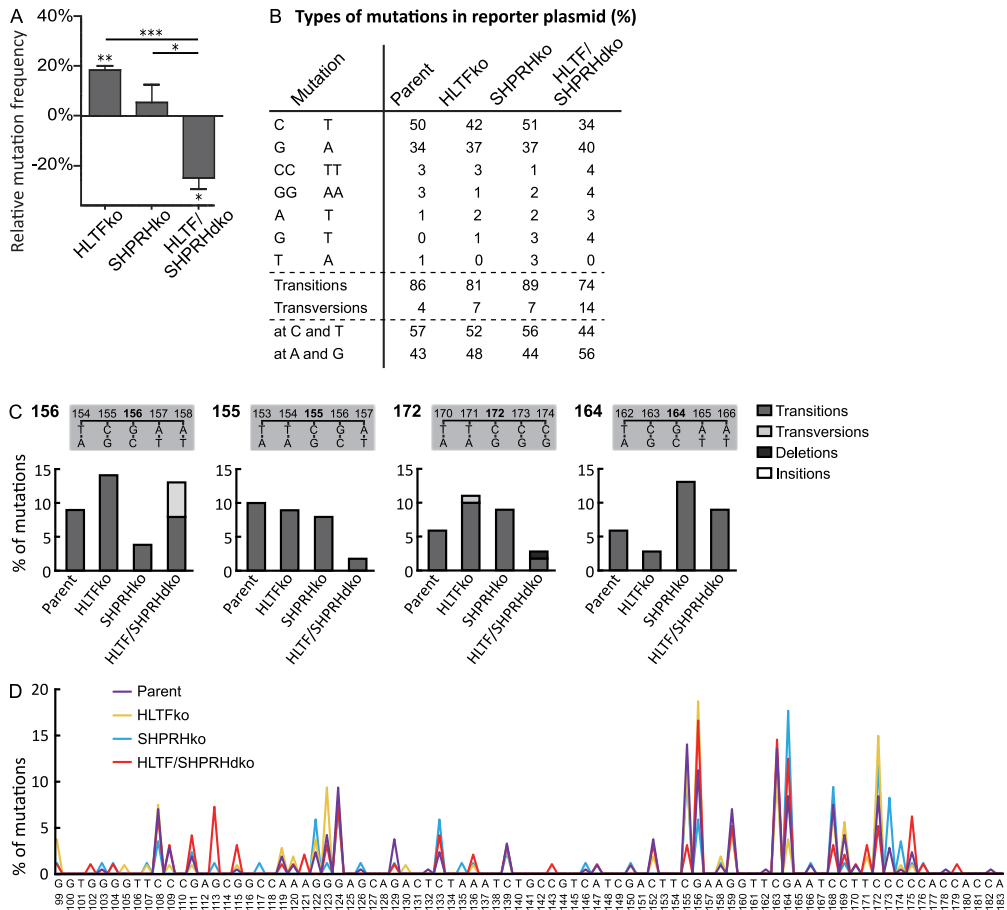
Figure 2. HLTF reduces error-prone DDT after UV-irradiation. (**A**) Mutation frequencies of UV irradiated SupF reporter plasmids (pSP189) relative to the Hap1 parent cell line with number of colonies counted for HLTF ko (n=11265), SHPRH ko (n=25059), HLTF/SHPRH dko (n=13325), Parent (n=25725), two-sided student`s t-test, * p<0.05, ** p<0.01, *** p<0.001. (**B**) Quantification of types of mutations from sequencing mutant colonies from (A). Mutations with prevalence ≥2 % are depicted. HLTF ko (n=141), SHPRH ko (n=112), HLTF/SHPRH dko (n=127), Parent (n=282). (**C**) Mutations at positions 155, 156, 164, 172 in *SupF* gene from (A) in % with a prevalence of ≥10 % in isolated plasmids from at least one cell line. (**D**) Mutation spectra of the *SupF* gene received from sequencing mutant colonies from (A). HLTF ko (n=141), SHPRH ko (n=112), HLTF/SHPRH dko (n=127), Parent (n=282).

2.4   HLTF is important for correct bypass and/or repair of MMS-induced DNA damage

While plasmids isolated from SHPRH ko and HLTF/SHPRH dko cells contained an almost equal amount of mutations as plasmids isolated from parent cells, the absence of HLTF resulted in an 45 % increased mutation frequency over MMS-induced lesions (Figure 3A). Thus, HLTF is important for error-free bypass of MMS-induced DNA lesions. POLη is able to bypass damages introduced by MMS, both 3meC and 3-deaza-3-methyl-2′-deoxyadenosine (a 3meA analog), partly correct [20, 21]. Thus, the increased mutation frequency observed could partly be due to a lack of POLη stimulation in HLTF ko cells. In addition, because PCNA polyubiquitination and strand invasion by D-loop formation is mediated by HLTF, absence of HLTF will likely stimulate a more error-prone TLS pathway.

Plasmids isolated from HLTF ko cells contained more C/G to A/T transversions (40 % compared to 18 % in parent, 26 % in SHPRH ko and 29 % in HLTF/SHPRH dko cells) and a general increase in mutations at C (50 % compared to maximum 18 % in parent cells) (Figure 3B and C). MMS causes methylations, predominantly at Gs (~83 % 7meG, 1 % 3meG, 16 % at As, including 3meA, 1meA, 7meA, and in dsDNA less than 1 % 3meC)(reviewed in [22]). Thus, the observed increase in C/G to A/T transversions likely mainly results from lesion bypass at Gs. Error-prone bypass of 3meC could also contribute to the increased C to A transversions, because a similar pattern, i.e. increased C to A transversions and increased mutation frequency, was detected in mouse cells lacking ABH2, which is a dioxygenase repairing 3meC (direct repair) [23]. Thus, even if 3meC is an infrequent DNA lesion after MMS in dsDNA, we cannot exclude that absence of HLTF causes a more mutagenic bypass of 3meC or that HLTF is involved in direct repair of 3meC. Interestingly, both ABH2 and HLTF contain APIM [24]. Plasmids from HLTF ko cells also contained more A to G transitions (12 % compared to 6 % in parent, 3 % in SHPRH ko and 3 % in HLTF/SHPRH dko cells) (Figure 3B). Since MMS does not cause damage at Ts, these mutations likely arise from 3meA, 1meA or 7meA (16% of the lesions introduced by MMS). Known mechanisms repairing these lesions are BER and direct repair by ABH2.

2.5 SHPRH has no central role in TLS over MMS-induced DNA lesions, but is important for avoiding strand breaks

The mutation frequencies of MMS-treated plasmids replicated in SHPRH ko and SHPRH/HLTF dko cells were similar to the parent cell line (Figure 3A); thus, SHPRH does not seem to have a central role in TLS over MMS-induced DNA lesions. The main change in the mutation spectrum in absence of only SHPRH (SHPRH ko) was a doubling in A to T mutations (from 5 % to 10 %, Figure 3B), thus, SHPRH could be involved in repair/error free bypass of MMS-induced lesions in As. Unlike the mutation spectrum of HLTF ko cells, the mutation spectrum from SHPRH ko cells was more similar to that of the parental cells. Still, the mutation spectra of all cell lines revealed cell line specific patterns (Figure 3 E, examples of patterns in positions 101, 102, 144, 178 and 183 are shown in Figure 3D). The most striking differences between the dko cell line and the parental cell line are the strong reduction in mutations at A (5 % in HLTF/SHPRH dko compared to at least 15 % in the other cell lines) (Figure 3C) and the absence of A to T transversions in plasmids from the dko cell line (Figure 3B), suggesting no/low bypass of lesions in A. We also detected a reduction in the total amount of transitions in HLTF/SHPRH dko cells (16%) compared to the other cell lines (32-34%) (Figure 3C).

SHPRH deficiency caused an increase in deletions; the amount of 1bp deletions was increased in plasmids from SHPRH ko cells, and the amount of larger, > 20bp, deletions was increased in plasmids from HLTF/SHPRH dko cells (Figure 3B). This is in contrary to the reported SHPRH mediated stimulation of TLS by POLκ [7], which itself often results in single-base deletions (Wolfle, Washington et al, 2003). The increased amount of deletions could indicate an increase in repair of strand breaks by Non-Homologous End Joining (NHEJ) in these cells. Interestingly, we repeatedly isolated less replicated reporter plasmid from the HLTF/SHPRH dko cells than from the other cells. This may indicate more frequently collapsed replication forks in this cell line. Thus, even though we do not see an increase in mutation frequency, these results suggest that SHPRH ko and HLTF/SHPRH dko cells have a reduced ability to handle MMS-induced lesions.
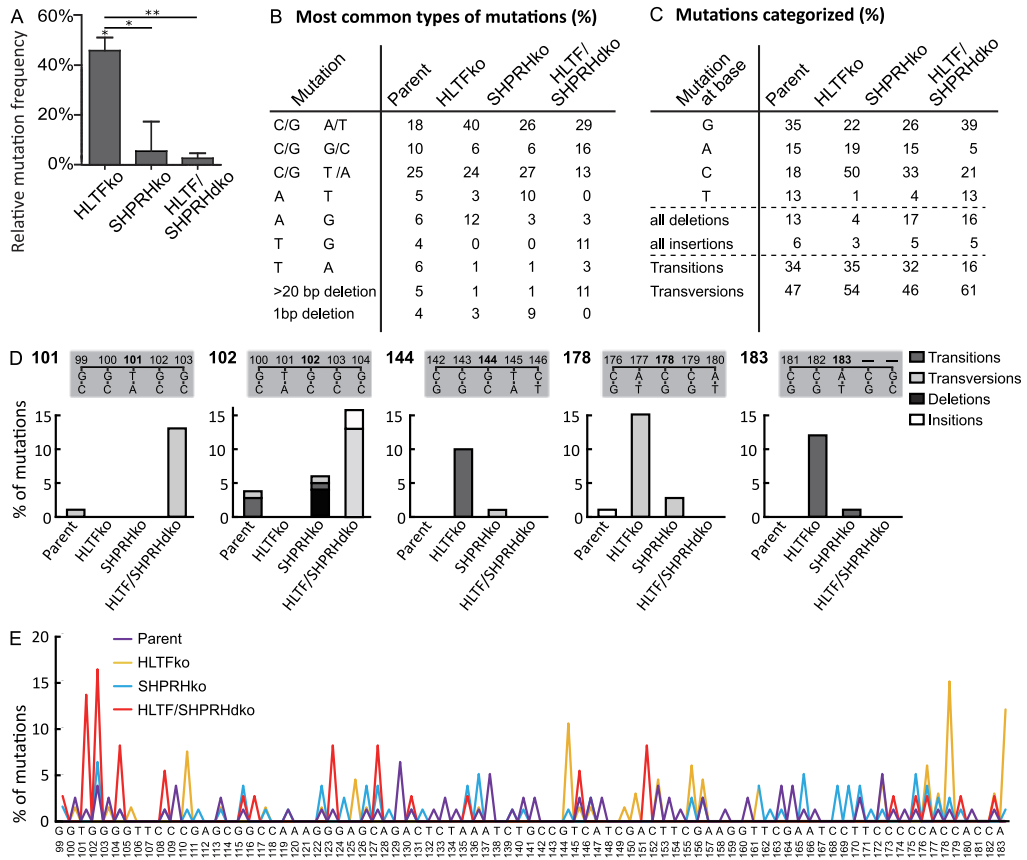
Figure 3. HLTF reduces error-prone DDT after MMS damage. (**A**) Mutation frequencies of MMS-damaged SupF reporter plasmids (pSP189) relative to the Hap1 parent cell line with number of colonies counted for HLTF ko (n=20104), SHPRH ko (n=22294), HLTF/SHPRH dko (n=19130), Parent (n=20538), two-sided student`s t-test, * p<0.05, ** p<0.01 (**B**) Quantification of types of mutations from sequencing mutant colonies from (A) with a prevalence ≥5 %. (**C**) Categorized mutations received from sequencing mutant colonies from (A). HLTF ko (n=68), SHPRH ko (n=78), HLTF/SHPRH dko (n=38), Parent (n=79). (**C**) Mutations at positions 101, 102, 144, 178 and 183 in *SupF* gene from (A) in % with a prevalence of ≥10 % in isolated plasmids from at least one cell line. (**D**) Mutation spectra received from sequencing mutant colonies from (A). HLTF ko (n=68), SHPRH ko (n=78), HLTF/SHPRH dko (n=38), Parent (n=79).

2.6　MMS results in a more diverse mutation pattern than UV-irradiation

Overall, the *SupF* mutation spectra contained a more diverse pattern of mutations after MMS- than after UV-treatment of the reporter plasmid isolated from the wild type/parental cells (Figure 4). MMS treatment also resulted in more deletions than UV-irradiation (13 % compared to 0 %). These results suggest a more diverse contribution of repair/bypass pathways upon MMS treatment than upon UV-irradiation.
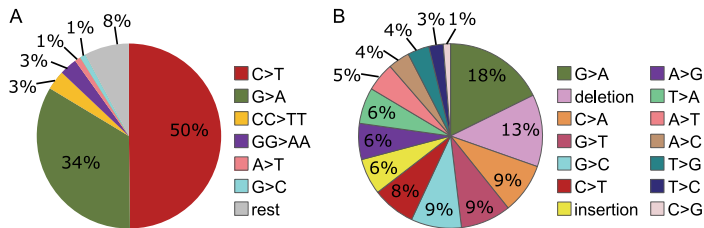
Figure 4: Distribution of mutation types caused by UV-irradiation or MMS (A) UV-irradiation (control/parent only) **(B)** MMS (control/parent only) in the SupF reporter plasmid replicated in a Hap1 parent cell line. Rest accounts for mutations with a prevalence < 1 %.

2.7   Knockout of the RAD5 homologs affects cell cycle distribution after MMS treatment

HLTF ko cells were slightly more sensitive and showed an increased mutation rate, indicating increased error-prone TLS, after MMS treatment, whereas SHPRH ko and HLTF/SHPRH dko cells were less sensitive and no increase in the mutation frequency was detected in replicated plasmids (Figure 1 and 3). The results from the viability assays and the SupF assays therefore suggest that the reduced sensitivity in absence of SHPRH is caused by other cellular DDT mechanisms than TLS. Because this also could include changes in cell cycle checkpoints and/or regulation of replication origin firing, we next examined how the absence of RAD5 homologs affects cell cycle distribution. After 12 hours, all ko cell lines treated with MMS were accumulated in S-phase compared to the parent cell line (Figure 5A), indicating a higher level of replicative stress. After 24 hours, the HLTF ko cells were accumulated in S-phase, while cells lacking SHPRH did not differ much from the parental cell line, even though these cells (SHPRH ko and dko) were less sensitive to MMS. This is an indication for HLTF affecting cell cycle progression.

2.8   CHK2 and MCM2 phosphorylations are reduced in cells lacking SHPRH

Next, we examined activation of CHK2, a kinase important for regulating cell cycle entry into mitosis as well as phosphorylation of multiple downstream factors such as p53 and MCM2 [25, 26]. Interestingly, we detected reduced levels of phosphorylated CHK2 in all ko cells, with the lowest levels in the cells lacking SHPRH (Figure 5B). At the same time, the levels of

unphosphorylated CHK2 were less reduced in these cell lines. This may suggest that SHPRH is directly or indirectly involved in CHK2 activation. All ko cells were also more arrested in S-phase 12 hours after MMS treatment (Figure 5A). In addition, P53 phosphorylation increased in all cell lines after MMS treatment. Despite low CHK2 phosphorylation, the increases in P53 phosphorylation in the HLTF/SHPRH single and dko cells, suggest that P53 phosphorylation in these cells is not only mediated by CHK2.

Further, we detected a tendency towards reduced phosphorylation of both MCM2 (S139) and MCM2 (S108) in cell lines lacking SHPRH upon MMS treatment, i.e. the cells with lowest CHK2 activation (Figure 5B). Phosphorylation of MCM2, a component of the pre-replication complex, is needed in order to recruit proteins to the CMG helicase complex and activate replication.

Reduced CHK2 phosphorylation upon DNA damage is expected to result in reduced activation of the G1/S and G2/M checkpoints. We found that the cell lines with reduced activation status of CHK2 accumulated in S-phase after 12 hours (Figure 5A and B). In addition, the basal levels of γH2AX was reduced in cells lacking SHPRH (Figure 5B). This was somehow unexpected, because reduced activation of the G2/M checkpoint allows cells to enter mitosis in the presence of unreplicated DNA [27]. Interestingly, this is in line with the observation that the cell lines lacking SHPRH (SHPRH ko and dko) used in our experiments were more resistant to MMS and continued to proliferate rapidly up to 4 days after the treatment.

Normally, in response to replication stress (late) origin firing is inhibited in presence of CHK1 and intra-S checkpoint activation [28]. We were not able to detect CHK1 phosphorylation in our western analysis (data not shown). However, CHK2, as well as other factors, might also be involved in regulation of origin firing. For example, in a recent study in yeast, inhibition of origin firing was observed in response to MMS before CHK1 was phosphorylated [29]. Interestingly, a similar phenotype, i.e. maintained replication upon MMS treatment, is reported in yeast cells with reduced Rad53-levels, the functional CHK2 homolog in yeast [30]. Furthermore, Rad53 was found to block origin firing through phosphorylation of Dbf4 [31], and in addition, Rad53 mutants contained an accumulation of reversed forks, abnormal replication intermediates and larger ssDNA regions at the replication fork than wild type yeast cells [32]. These reports support a role of CHK2 in the regulation of origin firing. If so, reduced CHK2 levels in SHPRH ko and dko cells may be responsible for the continuous proliferation

observed in SHPRH ko cells after MMS treatment. Thus, the unperturbed growth of the cell lines lacking SHPRH could be mediated by activation of dormant origins, without an inhibition of late origin firing.

As mentioned above, reduced CHK2 phosphorylation likely results in a premature entry into mitosis with increased levels of postreplicative gaps, leading to increased genomic instability. However, this cannot be detected by the SupF assay used in this study, but reduced recovery of DNA from the SupF assay in dko cells might be an indication of a high level of stalled/collapsed replication forks. However, validation of this hypothesis requires further investigation.
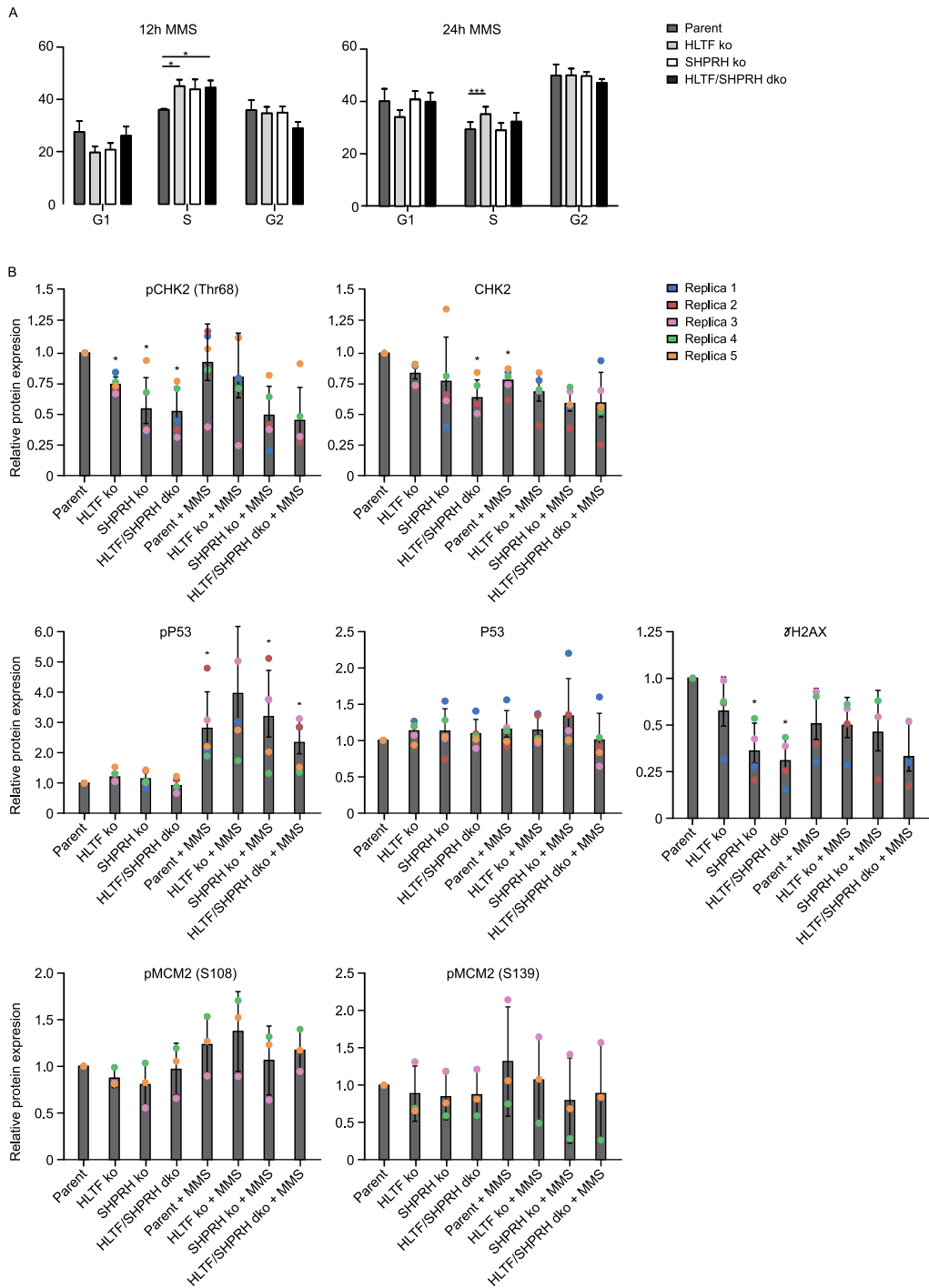
Figure 5. Effect on cycle distribution and protein expression after MMS in the ko cell lines. (A) Cell cycle analysis of knockout cell lines and parent Hap1 cell line 12h and 24h after MMS treatment; 4 replicas and 5 replicas, respectively. Student`s t-test * p<0.05, *** p< 0.001. (B) Levels of pCHK2 T68, CHK2, p53-P. p53, pMCM2-S139, pMCM2 S108 and γH2AX before and after MMS (50μM) treatment (12 h) in different cell lines relative to the levels in untreated parental cells. Level of proteins detected by Western blot analysis are determined using fluorescence and loading is normalized to β-actin. Average ± SD as well individual values of 3-5 replica (R1-R5) are shown. Student`s t-test * p<0.05 compared to untreated parent cell line.

In conclusion, in this study we show that HLTF and SHPRH have distinct properties/functions in presence of replication stress induced by different types of DNA lesions. HLTF is important for inhibiting error-prone DDT directly by stimulating error-free DDT, while SHPRH is modulating DDT also via regulation of checkpoint activation.

3   Material and methods

Cell lines. Hap1 parent cell line (Horizon) and CRISPR/Cas9-edited Hap1 HLTF[(-)], SHPRH[(-)], and HLTF[(-)]/SHPRH[(-)] cell lines (HZGHC004435c010, HZGHC006910c007, HZGHC006988c001, respectively, Horizon) were cultured in Iscove's Modified Dulbecco's Medium (IMDM) (ThermoFisher Scientific). Media was supplemented with 10 % fetal bovine serum (FBS; Sigma-Aldrich), 2.5 µg/ml Fungizone ® Amphotericin B (Gibco, Life Sciences), 1 mM L-Glutamine (Sigma-Aldrich) and antibiotic mixture containing 100 µg/ml penicillin and 100 µg/ml streptromycin (Gibco, Invitrogen[TM]). The cells were cultured at 37 °C in a 5 % CO_2– humidified atmosphere.

SupF assay. The SupF mutagenicity assay was performed essentially as previously reported [7]. Briefly, the reporter plasmid pSP189 was irradiated with 600 mJ/cm^2 UVB (312 nm), with UV lamp Vilber Lourmat, Bio Spectra V5 or incubated in MMS at a final concentration of 200mM (30min, 30˚C). Cells were transfected with the UV- or MMS- (Sigma Aldrich) damaged reporter plasmid or an undamaged reporter plasmid as control using X-tremeGENE HP transfection reagent according to manufacturer protocol (Roche diagnostics). At least 3 replicas were conducted (3 Hap1 cell transfections). After 48 hours the cells were harvested, and isolated plasmids were DpnI (NEB) restriction digested to exclude original bacterial plasmids in order to continue with only replicated plasmids. Isolated plasmids were transformed into *E. coli* MBM7070 cells and plated on indicator X-gal/IPTG/Amp agar plates. Blue/White screening was performed and mutation frequency (white/ blue colonies) was calculated for the different samples from multiple transformations using plasmid from the same biological replica. At least 13000 colonies were counted from each replica. White and light blue colonies were picked for re-streaking and DNA sequencing of *SupF gene*. Colonies that did not show a mutation in the sequencing results were afterwards excluded and the mutation frequency was recalculated.

Cell cycle and western blot analysis. Cells were seeded in 10 cm dishes (220000 cells/ml) and treated with 50 µM MMS (Sigma Aldrich) the next day. Cells were harvested for cell cycle and western blot analysis by trypsinization 12 and 24 hours after treatment. Cells for cell cycle analysis cells were fixed in ice-cold methanol, washed with PBS, RNAseA-treated (100 µg/ml in PBS, 37˚C, 30min) and DNA stained with propidium iodide (50 µg/ml in PBS). DNA

staining was quantified using a FACS Canto flow cytometer (BD-Life Science) and FlowJo software. Cells for western blot analysis were lysed in 3 x packed cell volume (PCV) M-PER Mammalian Protein Extraction Reagent (Thermo Scientific), PIC2 (10 μl/ml buffer) and PIC 3 (10 μl/ml buffer) (Sigma Aldrich) and complete protease inhibitor (20 μl/ml buffer)(Roche) and incubated for 1 hour at 4 ˚C. 1 μl Omnicleave was added to 100 μl packed cell volume (PCV). The lysate was cleared by centrifugation for 10 min at 16000 g, 4 °C. Samples were run on 4–12 % Bis-Tris-HCl (NuPAGE) gels. After blotting, the membrane (Immobilon PVDF, 0.2 uM) was blocked in 5 % low fat dry milk in TBS (TBS with 0.1 % Tween 20). The primary antibodies, CHK2-P (Thr68) (Cell signaling, 21975), CHK2 (Cell signaling, 3340), MCM2-P (S139) (Cell signaling, 8861), beta actin (Abcam, 8226), γH2AX (pSer319) (Biolegend), SHPRH (Abcam 80129), HLTF (Abcam 17984), P53-phospho (CST92845), P53 (MA5-12571) as well as the secondary antibodies IRDye 800CW (Goat Anti-Rabbit) and IRDye 700RD (Goat Anti-Mouse) Secondary Antibody (LI-COR Bioscience) were diluted in 5 % dry milk in TBS and the proteins were visualized using the Odyssey Imager.

MTT- assay (3-(4.5-Dimethylthiazol-2-yl)-2.5 diphenyl-tetrazolium bromide). Cells were seeded into 96 well plates (4000 cells/ well) and incubated for 4 hours. Cells were treated with methyl methanosulfonate (MMS) (Sigma Aldrich), mitomycin-C (MMC) (Sigma-Aldrich), Cisplatin (Hospira) or UVB (Vilber Lourmat, Bio Spectra V5, 312 nm, cells exposed in 100 μl medium, additional 100 μl added after UVB-exposure). The drugs were added on day 0, and cells were harvested 24, 48 and 72 hours after UVB-treatment and 24, 72 and 96 hours after MMC, MMS and Cisplatin treatment. OD was measured at 565 nm, and the average from at least 6 wells was used to calculate cell survival.
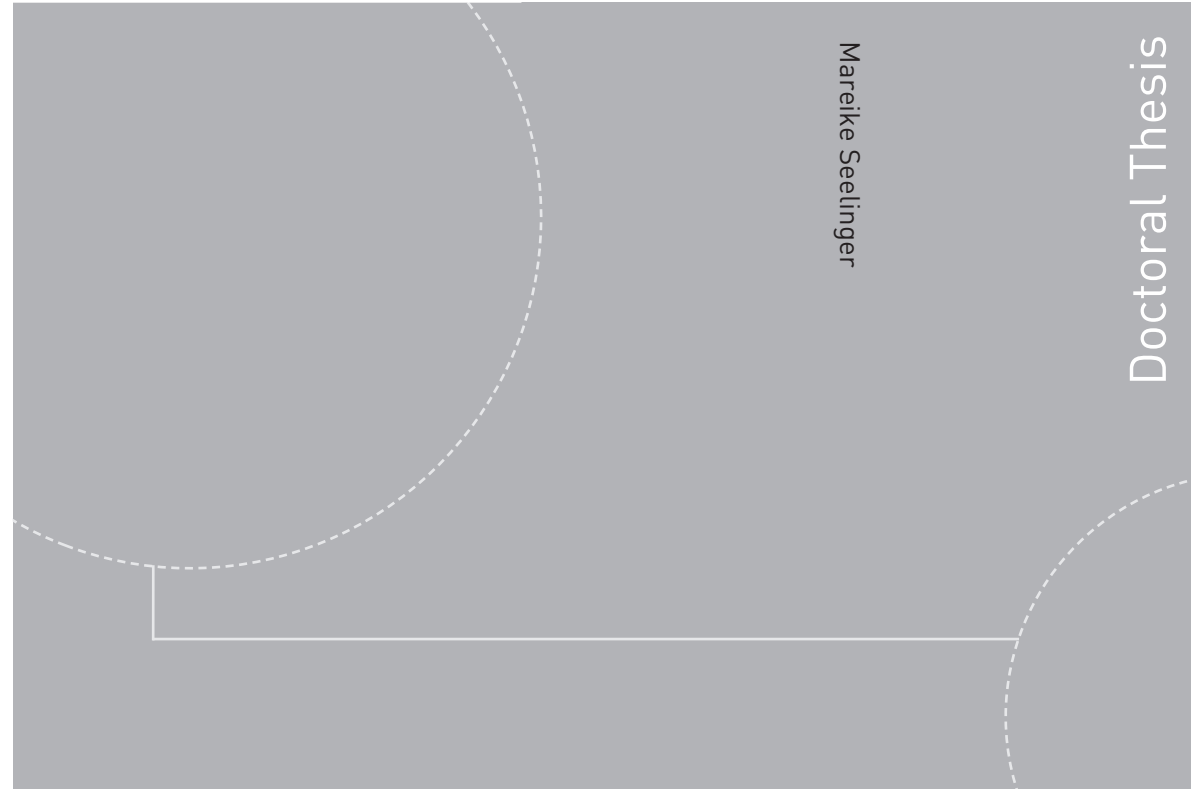
Acknowledgments

Literature

1.   Niraj, J., A. Farkkila, and A.D. D'Andrea, *The Fanconi Anemia Pathway in Cancer.* Annu Rev Cancer Biol, 2019. **3**: p. 457-478.

2.   Rothblum-Oviatt, C., et al., *Ataxia telangiectasia: a review.* Orphanet J Rare Dis, 2016. **11**(1): p. 159.

3.   Lehmann, A.R., D. McGibbon, and M. Stefanini, *Xeroderma pigmentosum.* Orphanet J Rare Dis, 2011. **6**: p. 70.

4.   Branzei, D. and I. Psakhye, *DNA damage tolerance.* Curr Opin Cell Biol, 2016. **40**: p. 137-144.

5.   Chatterjee, N. and G.C. Walker, *Mechanisms of DNA damage, repair, and mutagenesis.* Environ Mol Mutagen, 2017. **58**(5): p. 235-263.

6.   Chang, D.J. and K.A. Cimprich, *DNA damage tolerance: when it's OK to make mistakes.* Nat Chem Biol, 2009. **5**(2): p. 82-90.

7.   Lin, J.R., et al., *SHPRH and HLTF act in a damage-specific manner to coordinate different forms of postreplication repair and prevent mutagenesis.* Mol Cell, 2011. **42**(2): p. 237-49.

8.   Motegi, A., et al., *Polyubiquitination of proliferating cell nuclear antigen by HLTF and SHPRH prevents genomic instability from stalled replication forks.* Proceedings of the National Academy of Sciences of the United States of America, 2008. **105**(34): p. 12411-12416.

9.   Chavez, D.A., B.H. Greer, and B.F. Eichman, *The HIRAN domain of helicase-like transcription factor positions the DNA translocase motor to drive efficient DNA fork regression.* J Biol Chem, 2018. **293**(22): p. 8484-8494.

10.   Kim, J.J., et al., *Promoter methylation of helicase-like transcription factor is associated with the early stages of gastric cancer with family history.* Ann Oncol, 2006. **17**(4): p. 657-62.

11.   Capouillez, A., et al., *Expression of the helicase-like transcription factor and its variants during carcinogenesis of the uterine cervix: implications for tumour progression.* Histopathology, 2011. **58**(6): p. 984-8.

12.   Zhang, M., et al., *A novel protein encoded by the circular form of the SHPRH gene suppresses glioma tumorigenesis.* Oncogene, 2018.

13.   Moinova, H.R., et al., *HLTF gene silencing in human colon cancer.* Proc Natl Acad Sci U S A, 2002. **99**(7): p. 4562-7.

14.   Unk, I., et al., *Role of yeast Rad5 and its human orthologs, HLTF and SHPRH in DNA damage tolerance.* DNA Repair (Amst), 2010. **9**(3): p. 257-67.

15. Scharer, O.D., *DNA interstrand crosslinks: natural and drug-induced DNA adducts that induce unique cellular responses.* Chembiochem, 2005. **6**(1): p. 27-32.

16. Warren, A.J., A.E. Maccubbin, and J.W. Hamilton, *Detection of mitomycin C-DNA adducts in vivo by 32P-postlabeling: time course for formation and removal of adducts and biochemical modulation.* Cancer Res, 1998. **58**(3): p. 453-61.

17. Kartalou, M. and J.M. Essigmann, *Recognition of cisplatin adducts by cellular proteins.* Mutat Res, 2001. **478**(1-2): p. 1-21.

18. Unk, I., et al., *Human HLTF functions as a ubiquitin ligase for proliferating cell nuclear antigen polyubiquitination.* Proc Natl Acad Sci U S A, 2008. **105**(10): p. 3768-73.

19. Krijger, P.H., et al., *HLTF and SHPRH are not essential for PCNA polyubiquitination, survival and somatic hypermutation: existence of an alternative E3 ligase.* DNA Repair (Amst), 2011. **10**(4): p. 438-44.

20. Furrer, A. and B. van Loon, *Handling the 3-methylcytosine lesion by six human DNA polymerases members of the B-, X- and Y-families.* Nucleic Acids Res, 2014. **42**(1): p. 553-66.

21. Plosky, B.S., et al., *Eukaryotic Y-family polymerases bypass a 3-methyl-2'-deoxyadenosine analog in vitro and methyl methanesulfonate-induced DNA damage in vivo.* Nucleic Acids Res, 2008. **36**(7): p. 2152-62.

22. Drablos, F., et al., *Alkylation damage in DNA and RNA--repair mechanisms and medical significance.* DNA Repair (Amst), 2004. **3**(11): p. 1389-407.

23. Nay, S.L., et al., *Alkbh2 protects against lethality and mutation in primary mouse embryonic fibroblasts.* DNA Repair (Amst), 2012. **11**(5): p. 502-10.

24. Gilljam, K.M., et al., *Identification of a novel, widespread, and functionally important PCNA-binding motif.* J Cell Biol, 2009. **186**(5): p. 645-54.

25. Li, L., Y. Feng, and R. Luo, *Minichromosome Maintenance Complex is Required for Checkpoint Kinase 2 Chromatin Loading and its Phosphorylation to DNA Damage Response in SCC-4 Cells.* Protein Pept Lett, 2017. **24**(3): p. 223-228.

26. Berger, M., et al., *Mutations in proline 82 of p53 impair its activation by Pin1 and Chk2 in response to DNA damage.* Mol Cell Biol, 2005. **25**(13): p. 5380-8.

27. Zannini, L., D. Delia, and G. Buscemi, *CHK2 kinase in the DNA damage response and beyond.* J Mol Cell Biol, 2014. **6**(6): p. 442-57.

28. Toledo, L.I., et al., *ATR prohibits replication catastrophe by preventing global exhaustion of RPA.* Cell, 2013. **155**(5): p. 1088-103.

29. Iyer, D.R. and N. Rhind, *Replication fork slowing and stalling are distinct, checkpoint-independent consequences of replicating damaged DNA.* PLoS Genet, 2017. **13**(8): p. e1006958.

30. Cordon-Preciado, V., S. Ufano, and A. Bueno, *Limiting amounts of budding yeast Rad53 S-phase checkpoint activity results in increased resistance to DNA alkylation damage.* Nucleic Acids Res, 2006. **34**(20): p. 5852-62.

31. Zegerman, P. and J.F. Diffley, *Checkpoint-dependent inhibition of DNA replication initiation by Sld3 and Dbf4 phosphorylation.* Nature, 2010. **467**(7314): p. 474-8.

32. Lopes, M., M. Foiani, and J.M. Sogo, *Multiple mechanisms control chromosome integrity after replication fork uncoupling and restart at irreparable UV lesions.* Mol Cell, 2006. **21**(1): p. 15-27.

Mareike Seelinger

DNA damage tolerance in human cells mediated by the APIM-containing proteins REV3L, HLTF, and SHPRH

Doctoral Thesis

Mareike Seelinger

NTNU
Norwegian University of
Science and Technology
Faculty of Medicine and Health Sciences
Department of Clinical and Molecular Medicine

NTNU
Norwegian University of
Science and Technology

NTNU

NTNU
Norwegian University of
Science and Technology